Multimodal Separation and Multistage Mass Spectrometry of Synthetic Polymers

Cover Design: Junkan Song with the help of many people, especially Shally (Xiaolei) Luo, Duyi (Vivian) Cao and Jasmijn Visser

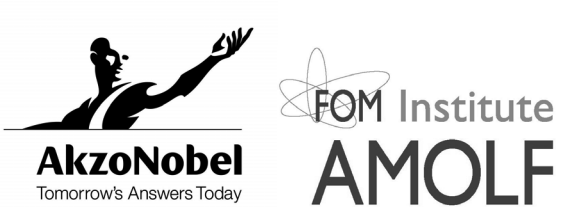

The work described in this thesis was performed at
AkzoNobel RD&I
P.O.Box 10, Deventer, 7400AA, The Netherlands
and
FOM Institute AMOLF
Science Park 104, Amsterdam, 1098XG, The Netherlands

ISBN/EAN: 978-90-77209-43-1
Multimodal separation and multistage mass spectrometry of synthetic polymers
2010, Junkan Song

Multimodal Separation and Multistage Mass Spectrometry of Synthetic Polymers

Multimodale Scheiding en Meerstaps-Massaspectrometrie
van Synthetische Polymeren
(met een samenvatting in het Nederlands)

Proefschrift

ter verkrijging van de graad van doctor aan de Universiteit Utrecht op gezag van de rector magnificus, prof.dr. J.C. Stoof, ingevolge het besluit van het college voor promoties in het openbaar te verdedigen op woensdag 19 januari 2011 des middags te 4.15 uur

door

Junkan Song

geboren op 30 janurai 1983
te *Shanghai, China*

Promoter: Prof. dr. R.M.A. Heeren

Co-promotor: Dr. O.F. van den Brink

This thesis was partly accomplished with financial support from the European Commission in the framework of the Marie Curie Early Stage Training Program POLY-MS on Multistage mass spectrometry of synthetic polymers and synthetically modified biopolymers (MEST-CT-2005-021029). Part of the work was financially supported by AkzoNobel.

博學之 審問之 愼思之 明辨之 篤行之

禮記・中庸

From Li JI, “The Classic of Rites” - Zhong Yong, “The state of equilibrium and harmony”

Sincerity is the way of Heaven. The attainment of sincerity is the way of men. He who possesses sincerity is he who, without an effort, hits what is right, and apprehends, without the exercise of thought;-he is the sage who naturally and easily embodies the right way. He who attains to sincerity is he who chooses what is good, and firmly holds it fast. To this attainment there are requisite ***the extensive study of what is good, accurate inquiry about it, careful reflection on it, the clear discrimination of it, and the earnest practice of it.***

此書獻給我的父親和母親 (to my parents)

Contents

1
Introduction

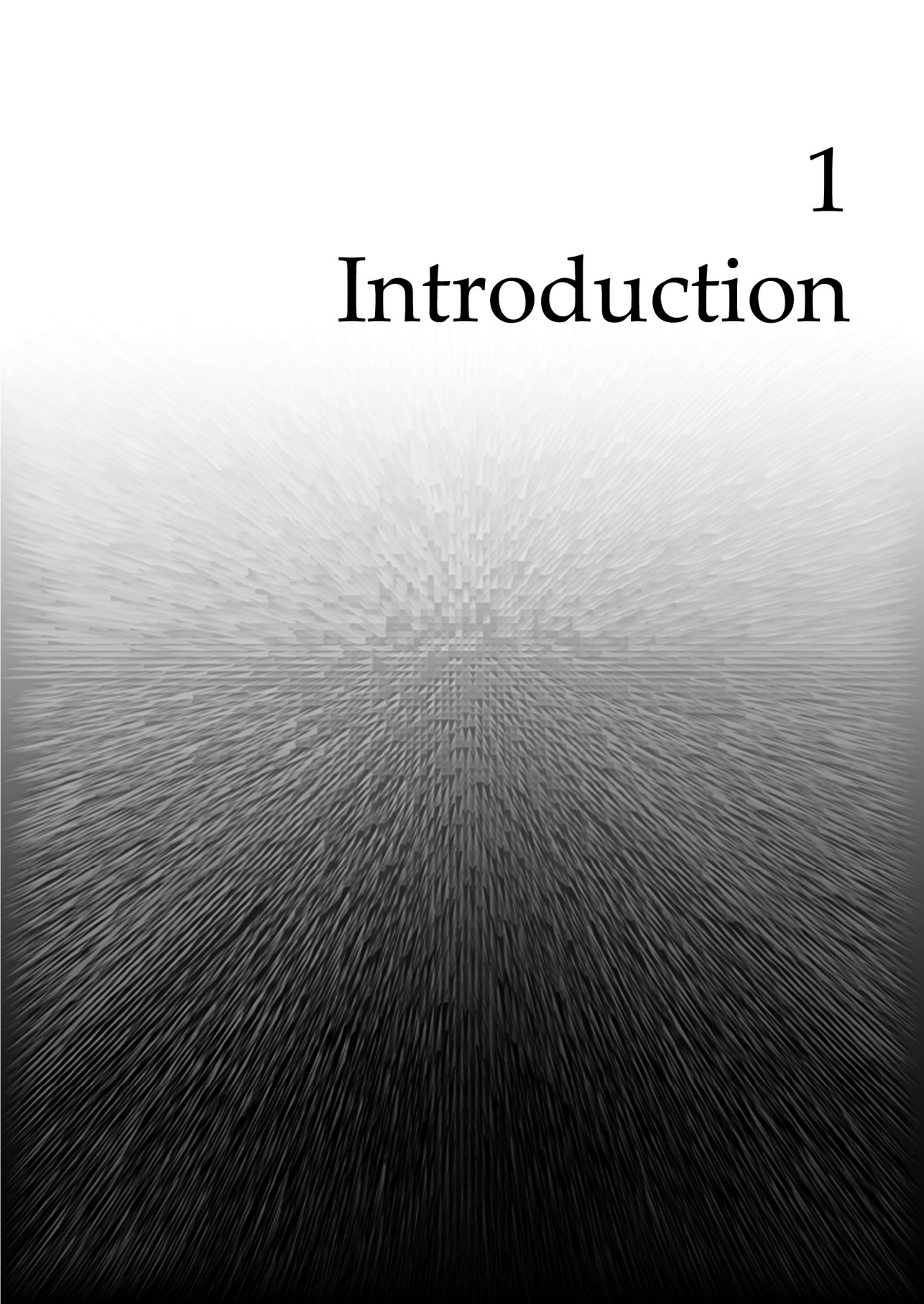

1.1 General Introduction

The history of synthetic polymers can be traced back to the nineteenth century. Henri Braconnot's pioneering work in derivative cellulose compounds starting from 1811 perhaps was the earliest important work in polymer science. In 1907-1909, Dr. Leo Baekeland created the first completely synthetic polymer, Bakelite (poly oxybenzylmethylenglycol anhydride), a thermosetting phenol formaldehyde resin. Synthetic polymers and polymer-based materials since then developed rapidly and have become essential and indispensable in agriculture, industry, life sciences, pharmaceutical and everyday household. Increasing demand on polymers with tailor-made properties, such as chemical or physical-resistance, thermo-responsiveness, biodegradability, etc., has led to an extraordinary range of new materials. Many new polymerisation techniques have been invented to produce these polymers with well-defined structures.

Numerous characterisation techniques have been developed to understand the properties of the synthetic polymer and lead to better understanding and improvement of polymerisation. The most popular polymer characterisation methods are, among others, gel-permeation chromatography (GPC), nuclear magnetic resonance (NMR), light scattering, Fourier transform infrared spectroscopy (FTIR), Raman spectroscopy and differential scanning calorimetry (DSC). These techniques provide information on polymer properties such as end group compositions, crystallinity, molecular weight and dispersity. However, most of the methods mentioned above only produce results on an average over the entire molecular weight distribution of the polymer.

Therefore, the combination of mass spectrometry (MS) with liquid chromatographic separation (LC) has particular value in synthetic polymer characterisation. LC is capable of separating relatively low molecular weight polymers (< 5,000 Da) and providing both qualitative and quantitative information. Mass spectrometry has the ability to determine the elemental composition of individual molecules in the polymer products even at very low levels of abundance. The invention of elecrospray ionisation (ESI) enables the coupling of LC with MS. The combination of LC and MS allows the study of polymer system not only over the whole distribution but also the individual polymer molecules.

Coupled with various separation techniques, such as LC and ion mobility spectrometry (IMS), mass spectrometry shows the abilities of providing detailed information of polymers such as endgroup structures, endgroup distribution, copolymer sequence and etc.

1.2 POLY-MS project

This thesis is a part of the POLY-MS project. The POLY-MS project is a European Community funded Marie Curie early stage research training programme (MEST-CT-2005-021029) for six PhD students. POLY-MS focuses on polymer characterisation using collision-induced dissociation multistage mass spectrometry. The project consortium unites researchers with background in fundamental mass spectrometry, ion physics, quantum chemistry, separation techniques and applied innovation-focused research that can give impetus to the field of polymer analysis. All four partners in the project, AkzoNobel, the FOM Institute for Atomic and Molecular Physics (AMOLF, Amsterdam, the Netherlands), the Chemical Research Centre of the Hungarian Academy of Sciences (Budapest, Hungary) and Jan Dlugosz University (Czestochowa, Poland), have extended experience in the field of mass spectrometry.

1.3 Scope of the Thesis

In this thesis the application of multistage mass spectrometry combined with multimodal separations to the characterisation of (co)polymer will be discussed. Properties such as endgroup compositions and monomer sequence were studied by using mass spectrometry with or without separation techniques.

A general introduction to polymer characterisation and the techniques used in this study is given in **Chapter 2**. Polymer properties such as molecular weight distribution, polymer

architecture and polymerisation methods will be introduced first. Following that, two of the major ionisation methods in mass spectrometry, electrospray ionisation (ESI) and matrix-assisted laser desorption / ionisation (MALDI), will be discussed. In this chapter, the instrumentation of some advanced mass spectrometers such as Orbitrap and Fourier transform ion cyclotron resonance (FTICR) MS will be also described. As mentioned earlier, LC separation is an important tool for polymer characterisation. Therefore, various LC techniques are presented in chapter 2, too.

In **Chapter 3** the cation charge effects on MS/MS of a synthetic polymer will be studied and discussed. The catalytic influence of the cation on the fragmentation processes can be clearly demonstrated by performing a simple size-dependence analysis using breakdown diagrams with (at least) two different cations. A simple procedure for determination of the effect of the cation on the fragmentation pathways (charge-catalysed or charge-independent) is described in the chapter, too. The information obtained is important for investigations by means of quantum chemical modelling. This procedure should be generally applicable to homopolymers or alternating copolymers.

C**hapter 4** demonstrates the value of coupling LC to high resolution and high accuracy MS/MS instrument for homopolymer characterisation. Issues like endgroup determination, isomer discrimination will be the main focus of this chapter. The comprehensive assignment of the peaks in the LC-MS data revealed the dominant polymerisation mechanisms in the synthesis procedure.

Copolymer structure determination is discussed in **Chapter 5**. In this chapter, the methods used in chapter 4 on homopolymer are applied in the study of copolymer. Structures with different end groups in PMMA and P(MMA-*r*-BA) were successfully assigned using both gradient elution LC-IT MS and exact mass experiments on an FTICR MS instrument. Isobaric materials in PMMA were discriminated using accurate FTICR MS^2. Isocratic LC-MS reduced the complexity of the spectra of P(MMA-*r*-BA), allowed easier attribution of peaks and shortened the experimental time.

A further and novel step in the characterisation of PMMA was made by using ion mobility spectrometry (IMS)-mass spectrometry (IMS-MS) is demonstrated in **Chapter 6**. The developments in IMS-MS show promising potential for structure elucidation of synthetic polymers. In this chapter, detailed endgroup mapping of poly(metyl methacrylate)

with complex end group combinations was achieved without the need of a preceding time-consuming LC separation. The combination of drift time and mass-to-charge separation offers an effective approach to identify individual compounds in extremely complex mixtures covering a relatively wide molecular weight distribution. The 2D and 3D visualisation of the data enhances the extraction of structural information reflecting differences in mass, size and/or conformation of the molecules.

Finally in **Chapter 7,** an example of using a combination of characterisation techniques to analyse complex polymer systems and their degradation processes will be demonstrated. Techniques including GPC, NMR and LC-MS^n were utilised to study a poly(butylene adipate-co-butylene terephthalate) copolyester and its degradation products. GPC and NMR confirmed the successful partial degradation and revealed some key structures. Cyclic structures, which were not identified by NMR, were successfully identified by switching the scan mode of the mass spectrometer. A novel elemental composition determination method, using MS^2 experiment on the first ^{13}C isotope peak that helped to confirm the elemental composition of the fragments is also introduced in this chapter.

2
Theoretical Background

2.1 Introduction

Mass spectrometry has many advantages over other characterisation methods of polymer systems. The technique measures the mass-to-charge ratio of ions and thereby allows the study of individual molecules. Coupling with LC often reduces the complexity of the mass spectra and helps to overcome problems such as ion suppression in the mixture of analytes. These abilities expand the applicability of mass spectrometry for the molecular characterisation of polymer systems. Some limitations, however, such as poor ionisation efficiency of certain polymers or relatively high molecular weight polymers remain.

Section 2.2 gives some examples of studies of polymers aiming to identify properties, such as the molecular weight distribution, the statistical information of the chains and the polymerisation methods used.

In Section 2.3, several fundamental aspects of mass spectrometry including the instrumentation used in this study will be discussed. The introduction of LC separation in studies of polymer systems and its combined use with MS will follow in Section 2.4.

2.2 Polymer Properties

Polymers have diverse functions and structures. A conventional way of polymer classification is shown in Figure 2.1.[1]

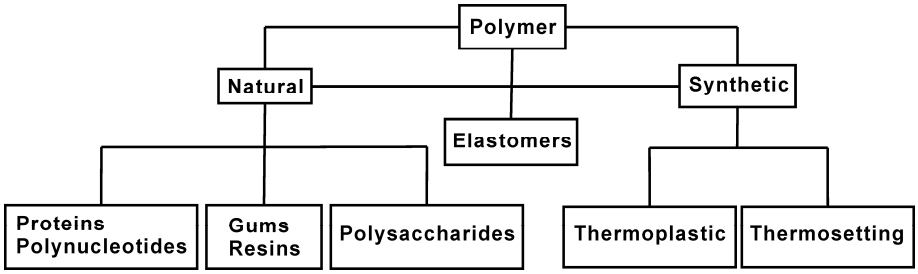

Figure 2.1. A conventional way of polymer classification.

Synthetic polymers generally have less complex structures than natural polymers or elastomers (elastic+polymer, polymers having the viscoelastic properties of natural rubber).

Modern definitions distinguish between synthetic polymers, other than the way shown in Figure 2.1, are on the basis of their polymerisation mechanisms (either step or chain polymerisation). In general, step polymerisations produce heteroatom polymer backbones and chain polymerisations produce homoatom polymer backbones. Through various polymerisation methods, synthetic polymers can be modified to exhibit specific properties. Therefore studies of synthetic polymer products have significant scientific and practical value.

2.2.1 Molecular Weight Distribution and Its Determination

A synthetic polymer does not have an exact molecular weight. This is due to the fact that the length of the chains formed in a polymerisation reaction is determined by random events. For example, in a radical polymerisation, the chain propagation and termination reactions are totally random which results in a product having a mixture of chains with a distribution of chain lengths.

Therefore, (synthetic) polymers are characterised by their molecular weight distribution and the associated average molecular weight rather than by a single molecular weight. Several parameters are commonly used to define the molecular weight distribution. These include the number average molecular weight (M_n), the weight average molecular weight (M_w), the z-average molecular weight (M_z), viscosity average molecular weight (M_v) and the dispersity ($Đ$). Their mathematical definitions are given in equations 2.1-2.5.

$$M_n = \frac{\sum M_i N_i}{\sum N_i} \qquad \text{(Eq. 2.1)}$$

$$M_w = \frac{\sum M_i^2 N_i}{\sum M_i N_i} \qquad \text{(Eq. 2.2)}$$

$$M_z = \frac{\sum M_i^3 N_i}{\sum M_i^2 N_i} \qquad \text{(Eq. 2.3)}$$

$$M_v = \left[\frac{\sum M_i^{1+\alpha} N_i}{\sum M_i N_i} \right]^{\frac{1}{\alpha}} \qquad \text{(Eq. 2.4)}$$

$$Đ = \frac{M_w}{M_n} \qquad \text{(Eq. 2.5)}$$

In Equations 2.1-2.4 N_i is the number of polymer molecules and M_i is the molecular weight. The quantity α in the expression for the viscosity average molecular weight, varies from 0.5 to 0.8 and depends on the interaction between solvent and polymer in a dilute solution.[1] Figure 2.2 shows a typical distribution curve and illustrates the difference between M_n, M_v, M_w and M_z. The average values are related to each other as follows, $M_n < M_v < M_w < M_z$, in the distribution curve.

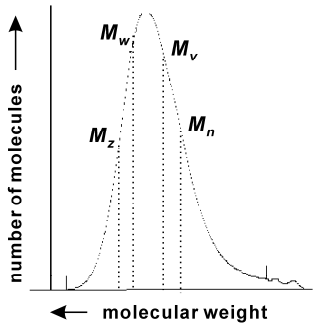

Figure 2.2. A typical molecular weight distribution curve for a synthetic polymer.

The dispersity ($Đ$) indicates how narrow a molecular weight distribution is. The molecular weight distribution of a polymer depends on factors such as chemical kinetics and synthesis procedure in the production process. Ideal step-growth polymerisation gives a polymer with dispersity of 2. Ideal living polymerisation (a chain polymerisation in which chain transfer and chain termination are absent.) results in a dispersity of 1.[1] Figure 2.3 shows a schematic illustration of polymers with different dispersities ($Đ$).

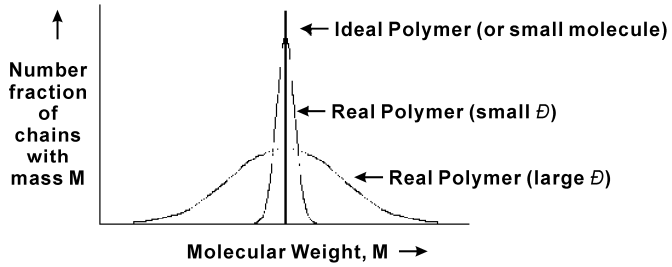

Figure 2.3. Schematic illustration of polymers with different dispersities.

Several modern polymer characterisation techniques, such as vapour pressure osmometry, light scattering and size exclusion chromatography (SEC), have been applied to study the molecular weight distribution (MWD) of polymers. Although limited by its seldom quantitative nature, mass spectrometry is still a powerful tool to obtain the information about M_n, M_w and $Đ$. Many polymer classes have been tested by mass spectrometry using different ionisation techniques.

Nielen[2] reported the use of ESI-MS hyphenated with SEC to study the characterisation of polydisperse synthetic polymers having different polarities. It was demonstrated that ESI-MS is an important tool for the characterisation of polymers and for the identification of chemical composition. A wide range of polydisperse synthetic polymers such as poly(tetrahydrofuran), poly (methyl methacrylate), polyester and poly(styrene) were characterised in terms of repeating units and end-groups. The MS data were used to compute accurate calibration curves for the SEC column used. Thus, accurate calibrations of SEC/RI can be obtained from SEC/ESI-MS, so that accurate M_n, M_z and $Đ$ values can be obtained. The MWD of synthetic polymers have also been studied with matrix-assisted laser desorption/ionisation time-of-flight (MALDI-TOF) mass spectroscopy.[3, 4]

2.2.2 End Groups and End Group Determination

The properties of polymers are largely influenced by their end groups.[5] End group identification is also crucial for understanding polymerisation mechanisms and further processing of the polymers. The number of end groups of branched polymers depends on the degree of branching. A linear polymer molecule consists of a chain with two end groups. A good example of highly branched polymers is dendrimers[6-8] which can have more than hundreds of end groups. Cyclic unbranched polymers, on the other hand, do not have end groups.

Several modern analytical methods, such as NMR, FTIR and MS, often in combination, are used for the characterisation of end groups. Since the beginning of the 1980's, mass spectrometry has become an important and conventional tool to study end groups of polymers due to the invention of new ionisation methods and their applications to polymers. Techniques such as field desorption (FD),[9-11] fast atom bombardment (FAB)[11-13] and

secondary ion mass spectrometry (SIMS)[14-16] have been applied for polymer studies. The disadvantage of these ionisation methods is the occurrence of fragmentation in the ionisation process. The introduction of MALDI[17, 18] and ESI[19, 20] minimised this effect and made them the most suitable ionisation methods for polymer analysis.

De Koster and van Rooij introduced a linear regression method[21, 22] to determine the mass of the monomer and end groups with high accuracy. By plotting the experimentally measured mass as a function of the degree of polymerisation, the combined end group mass (with cation) can be determined from the intercept of the regression line.

$$m_{exp} = m_{monomer} \times n + m_{endgroup} + m_{cation} \qquad \text{(Eq 2.6)}$$

For the accuracy of the calculation, the mass of an electron has to be subtracted from the neutral atom since the ion is charged by a cation. This method has been successfully applied to many polymer systems including linear polymers, hyperbranched polymers and polymer mixtures.[22-25] It is also used through **Chapter 4** to **Chapter 6** in this thesis.

Multistage MS/MS has also been demonstrated to obtain end group information of synthetic polymers in addition to MS study.[26-28] The fragment ions produced in an MS/MS experiment are often generated by a cleavage of the backbone and therefore are useful for end group determination.

2.2.3 Polymer Architecture and Its Analysis

The intramolecular arrangement of the monomers, the polymer architecture, is an important microstructural feature that determines a polymer's properties. The simplest polymer architecture is a linear chain with a single backbone with no branching. A branched polymer is composed of a main chain with branches consisting of monomers of the same type as the main chain and a graft polymer has branches consisting of a different monomer than the backbone. Many special types of branched polymers have been developed in recent years, such as star polymers,[29] comb polymers[30] and dendrimers.[31] Figure 2.4 illustrates these structures.

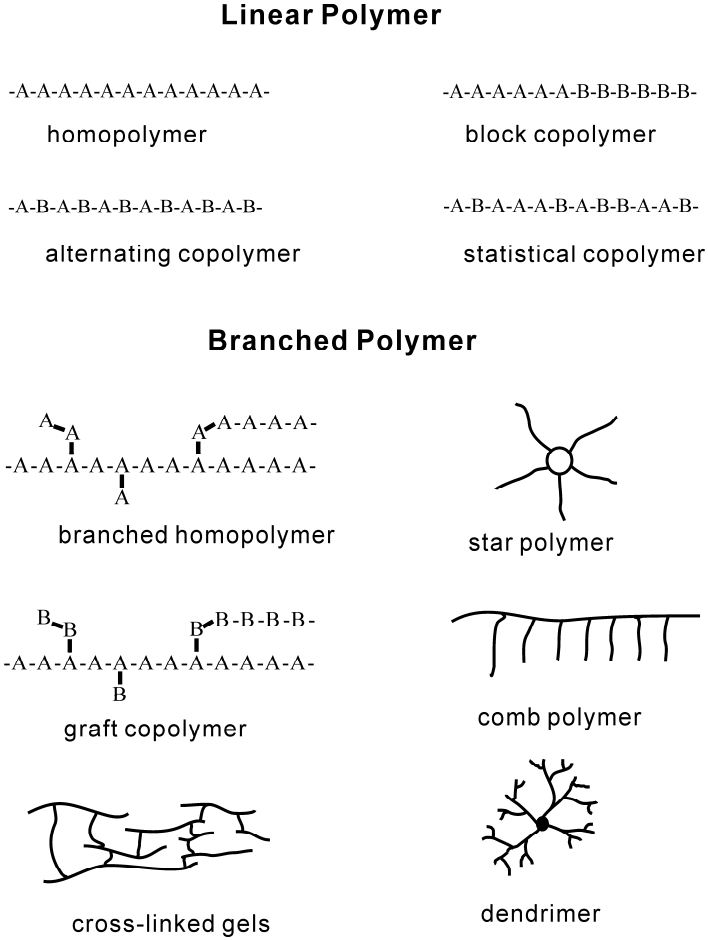

Figure 2.4. Various polymer architectures. A and B denote different monomers.

Modern analytical techniques, such as NMR, IR, SAXS (small-angle X-ray scattering) and Raman spectroscopy, are often used to obtain information, such as branching, cross-linking and copolymer sequencing, of polymer architectures.

Mass spectrometry has also been applied to characterise the architectures of the polymers using aspects such as monomer sequence,[32, 33] block length [34] and dendrimer or hyperbranching structure.[23, 35-38]

2.2.4 Polymerisation methods

The variety of polymerisation methods nowadays is so diverse that is very difficult to categorise them. However, in general there are two types of polymerisation, *viz.* step polymerisation and chain polymerisation.

Step polymerisation is often referred to as condensation polymerisation because of the release of small molecules such as water during the formation of polymer. The polymer chain grows in a step-wise fashion; the initial stage of the reaction involves the bi-functional or multifunctional monomers to form dimers, then trimers and longer oligomers and finally polymers. Large quantities of higher molecular weight material are only formed near the completion of the reaction. Polymers such as polyesters, polyamides, polycarbonates and polyurethanes are normally produced by step polymerisation.[39-44]

In chain polymerisation, unsaturated monomer molecules add on to a growing polymer chain. The chain reaction is initiated by an external source (radiation, initiator or catalyst) and involves monomer addition to an active centre (which may be a radical, an ion or a polymer-catalyst bond). Chain polymerisations are very fast reactions and can form high molecular weight polymer molecules at once. Longer reaction times won't increase the molecular weight, but give higher reaction yields. The most conventional chain polymerisations are free radical, anionic and cationic polymerisations.

Free radical polymerisation is the most applicable method to polymerise a large range of (functional) vinyl monomers.[45, 46] It works well in a wide range of operating conditions such as in water,[47] with or without solvent,[48] etc. But the selectivity of free radical polymerisation is not optimal since the radicals are very active. Three general stages are involved in a free radical polymerisation: initiation, propagation and termination. Figure 2.5 illustrates these stages. Polymer chains may be terminated by either combination or disproportionation. Mass spectrometry is an ideal tool to determine the occurrence of the latter reaction, disproportionation, because of the formation of a chain with an unsaturated end group. The mass of this chain is 2 Da less than the mass of the chain terminated by combination.[25]

- **Initiation**

  $I \rightarrow 2R^*$

  $R^* + M \rightarrow RM^*$

- **Propagation**

  $RM^* + M \rightarrow RM_2^*$

  ……

  $RM_n^* + M \rightarrow RM_{n+1}^*$

- **Termination**

  $RM_x^* + RM_y^* \rightarrow RM_{(x+y)}R$ Combination

  $RM_x^* + RM_y^* \rightarrow (RM_x\text{-}H) + (RM_y + H)$ Disproportionation

Figure 2.5. Initiation, propagation and termination of a free radical polymerisation

Various side reactions such as polymer radical transfer to solvent and to monomer may occur to terminate the polymer chain in the process of free radical polymerisation.[25, 49, 50] The addition of a chain transfer agent, however, results in the destruction of one radical and the creation of another radical. It is often used to control the molecular weight, reduce side reactions and produce polymers with special end group functionality.[49, 51, 52] Examples of free radical polymerisation mechanisms will be explained and studied in Chapter 4 to Chapter 6.

Many new polymerisation methods, especially controlled/living radical polymerisation such as atom transfer radical polymerisation (ATRP)[53] and reversible addition-fragmentation chain transfer polymerisation (RAFT)[54] have been developed to overcome the disadvantage of free radical polymerisation. But most of them have not been applied to industrial production yet.

2.3 Mass Spectrometry

The unequalled sensitivity and detection limits of mass spectrometry allowed it to become an outstanding analytical method. It has applications in many fields such as atomic physics, reaction kinetics and all kinds of chemical or biochemical analysis.

The rapid development of mass spectrometry has led to the invention of new ionisation methods and fragmentation methods. Many instruments have been built by a great variety

of manufacturers. Figure 2.6 shows the very basic setup of a mass spectrometer. There are five essential parts for a modern-day mass spectrometer.

1) Inlet: a device to introduce the sample.

2) Ion source: section that produces gas-phase ions from the sample.

3) Ion analyser: one or several analysers to separate ions according to their mass-to-charge ratio and in some cases perform fragmentation.

4) Detector: counts the ions from the analysers. Ion analyser and detector are combined in some cases such as ICR and Orbitrap.

5) Controlling computer: control the system and process the data (mass spectra).

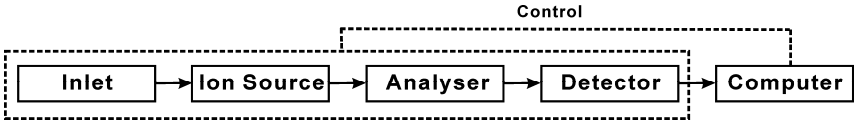

Figure 2.6. Schematic of the basic setup of a mass spectrometer.

2.3.1 Ionisation Methods

The first and very crucial step of mass spectrometry is ionisation, which is the production of gas-phase ions from the analyte molecules. As mentioned earlier in this chapter, the application of many techniques such as FD, FAB and SIMS has been demonstrated in polymer studies. However, it was not until the invention of 'soft' ionisation methods, such as electrospray ionisation (ESI) and matrix-assisted laser desorption/ionisation (MALDI), that mass spectrometry really started to take the centre stage in polymer analysis.

2.3.1.1 Electrospray Ionisation

Electrospray ionisation was invented by John Fenn[19, 20] and awarded him a Nobel prize in 2002. (Although as early as in the 1960's, the early model of ESI-MS was already tested by Dole and co-workers on polystyrene molecules.[55]) In electrospray ionisation, a sample solution is pushed through a very small charged, usually metal, capillary. To produce the sample solution the analyte is dissolved in a large amount of relatively volatile solvent such

as water or methanol. Volatile acids, bases or buffers, are often added to the solution as well to facilitate the formation of adduct ions. The analyte exists as an ion in solution either in a protonated form, as an anion or as a cation if additional salt is added. The combination of the presence of an electric field and the fact that like charges repel causes the liquid to leave from the capillary producing a Taylor-cone[56] shaped charged spray that consists of a mist or an aerosol of small droplets about 10μm across. Heated nitrogen gas is sometimes used to help nebulise the liquid and to help evaporate the neutral solvent in the small droplets. As the small droplets evaporate, suspended in the air, the charged analyte molecules are forced closer together. The drops become unstable as the similarly charged ions come closer together and the droplets once again break up, which can be theoretically described by the Rayleigh stability limit.[57] This process repeats itself until the analyte is free of solvent and becomes a lone ion. The lone ion then continues along to the mass analyser of a mass spectrometer. See Figure 2.7 for this ionisation process.

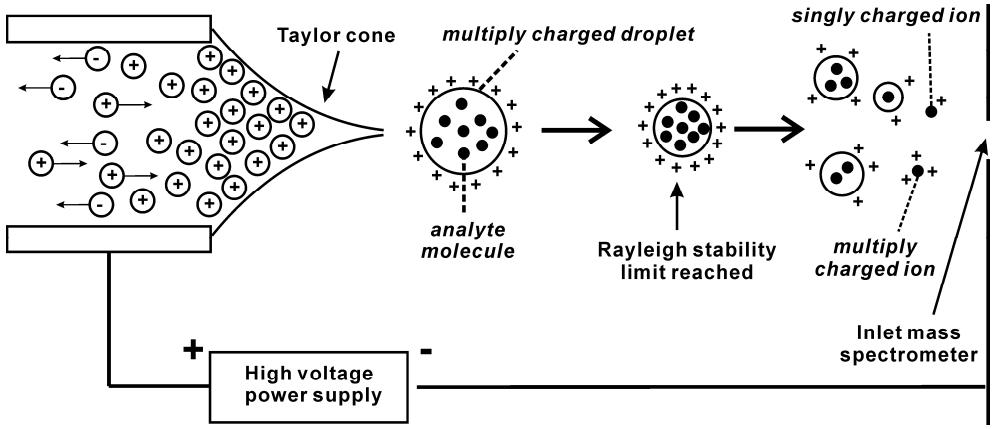

Figure 2.7. Illustration of the ESI process.

In electrospray processes the ions observed are quasimolecular ions that are ionised by the addition of a proton to give $[M+H]^+$ (M = analyte molecule, H = hydrogen ion), or other cation such as sodium ion, producing $[M+Na]^+$. Alternatively when negation ion electrospray is perfomed, a (labile) proton may be removed from the analyte producing a $[M-H]^-$ ion. In electrospray multiply charged ions such as $[M+2H]^{2+}$ are often observed. For large macromolecules there will often be a distribution of many charge states. Electrons

themselves have neither been added nor removed as with some other ionisation methods. The formation of ions in electrospray is somewhat analogous to acid-base reactions.

ESI has many advantages such as the ease to interface with chromatographic methods and the ability to produce multiply charged ions. It has significantly changed the field of mass spectrometry. Many publications discussed the application of ESI-MS to synthetic polymer characterisation such as polymerisation mechanism study,[58] end group analysis,[25, 59-61] polymer degradation,[62] sequence confirmation,[32, 63] quantitative study[25, 50] and copolymer distribution.[28, 64, 65]

2.3.1.2 Matrix-assisted Laser Desorption/Ionisation

Since its introduction by the laboratories of Tanaka[66] and of Hillenkamp,[17, 18] MALDI has rapidly grown in applications ranging from sequencing peptides to measuring the average molecular weights of complex synthetic polymer materials.

In MALDI, a dilute solution of the analyte is mixed with a more concentrated matrix solution. Typical MALDI matrices are aromatic organic acids. A small aliquot of the mixture is applied to the MALDI target and left to crystallise as the solvent evaporates. After the target is placed in the source of the mass spectrometer, a laser irradiates the target, vaporising the matrix and desorbing polymer oligomers into the gas phase. Neutral gas-phase oligomers are cationised by protons or metal cations present in the desorption plume. The ions are extracted into the mass spectrometer, mass analysed and then detected.

MALDI is one of the most prolific ionisation method in the characterisation of synthetic polymers. MALDI-MS is used to determine repeat units, end groups and molecular weight distributions.[4, 67] It has also been applied to generate valuable information on reaction mechanisms, kinetics, and degradation.[4, 60]

2.3.2 Mass Analysis

Mass analysis can be achieved in either single or multiple stages (combined with collision). Multiple stages of mass analysis in a single experiment have been used to determine the chemical structure of polymers for many years. In the "classical" ionisation

methods for mass spectrometry, like electron impact (EI), spectra usually contain a good amount of fragment ions that can be used to help confirm or elucidate chemical structures. In the more modern methods of ionisation, like ESI or MALDI, spectra often only contain the ionised molecule with very little fragmentation and consequently the spectra are of little use for structural characterisation. Therefore, tandem mass spectrometry is required to obtain structure info.

In an MS/MS experiment, the first stage of mass analysis is used to select a specific mass range for examination in a second stage of mass analysis. Between the two stages, additional energy is added to the system to fragment the ions selected in the first stage. These fragment ions are mass analysed in the second stage. In addition, MS/MS can be performed either 'in space' or 'in time' depends on the instrument used. Quadrupole Time-of-Flight (Q-TOF) is an example of the instruments that perform MS/MS in space. Multiple stages of MS (or MS^n) 'in time' are possible on ion trap and FTMS instruments.

The development of collision-induced dissociation (CID) and post-source decay (PSD) to achieve MS/MS increased the value of tandem MS for the study of polymer systems. Collision-induced dissociation (CID), also known as collision-activated dissociation (CAD), is a mechanism by which to fragment molecular ions in the gas phase.[68] In a CID process, the precursor ions are usually accelerated by some electrical potential to high kinetic energy in the vacuum of a mass spectrometer to then collide with neutral gas molecules (often helium, nitrogen or argon) in a collision cell which is integrated in the case of trapped ion instruments. The repeated collisions with the collision gas build up internal energy in the molecule by converting some of the kinetic energy. Eventually the fragmentation threshold is reached which results in bond breakage and the formation of product ions.

CID experiments can be achieved using instruments such as tandem sector and time-of-flight type instruments at relatively high (keV range) energies. It can also be achieved at relatively low (eV range) energies by using ion trapping type MS such as quadrupole ion trap MS and FTICR MS instruments. CID can be performed using either single or multiple collisions with a selected gas and each of these factors influences the distribution of internal energy that the activated ion will obtain. Single collision needs high energy to effect fragmentation, while multiple collision can (also and preferably) be done at low

energies. Partial or complete structural determination can be realised by studying the fragment ions produced in CID. It is especially useful for the investigation of isobaric and/or isomeric materials.[25]

Other fragmentation methods for special purposes have also been designed. Notable methods include electron-capture dissociation (ECD),[37] electron-transfer dissociation (ETD)[69] and infrared multiphoton dissociation (IRMPD).[70] But the application of these methods in synthetic polymer analysis is limited or has not yet been explored.

2.3.3 Instrumentation

Mass spectrometers used for the studies in this thesis are quadrupole ion trap (Bruker Esquire 3000plus ion trap), Orbitrap (Thermo Scientific LTQ Orbitrap XL), FTICR (Thermo Scientific LTQ FT Ultra Hybrid) and IMS-MS (Waters Synapt G2 HDMS mass spectrometer). The fundamental aspects and/or setup of these instruments will be described in the following parts.

2.3.3.1 Quadrupole Ion Trap

A quadrupole ion trap (Paul trap) instrument[71, 72] is the three dimensional analogue of a linear quadrupole mass filter. Wolfgang Paul, the inventor of the quadrupole ion trap, shared Nobel Prize in Physics for his contribution to the development of the ion trap instrument.[73] Ions are firstly generated outside the trap by an external source (e.g. ESI) and then introduced to the trap. Ions in the trap experience the forces applied by a radio frequency (RF) field in three dimensions. The trap system consists of three electrodes, a ring electrode between two end-cap electrodes, as shown in Figure 2.8. The internal surface shape of these three electrodes follows a three dimensional nearly hyperbolic profile. Holes at the centre of the end-cap electrodes allow ions to enter and exit the trap. A high voltage RF potential is applied to the ring electrode and the end-cap electrodes are held at ground. The oscillating potential difference established between the ring and end-cap electrodes forms a substantially quadrupolar field. The field can trap ions of a particular mass range depending on the RF voltage level. An auxiliary voltage is fed to the exit end-cap electrode.

This additional voltage is used for various purposes during the precursor ion isolation, fragmentation, and mass analysis phases of the scan sequence. The range of ion masses that can be trapped simultaneously is described by the stability diagram derived from the Mathieu equation.[74, 75] A detailed description of the ion motions and stability in the quadrupole ion trap can be found elsewhere.[76, 77]

Because the ions are introduced into the trap from an external source, a collision gas is present in the trap to reduce the energy of the incoming ion beam and facilitate retention of at least a certain portion of the ions that are injected into the ion trap. The quadrupole ion trap is also a storage device so that it is possible to accumulate weak signals over an extended period of time[78] (practically from 10 μs to 200 ms depending on the experimental conditions). By varying the accumulation time, the dynamic range of the instrument is greatly extended.

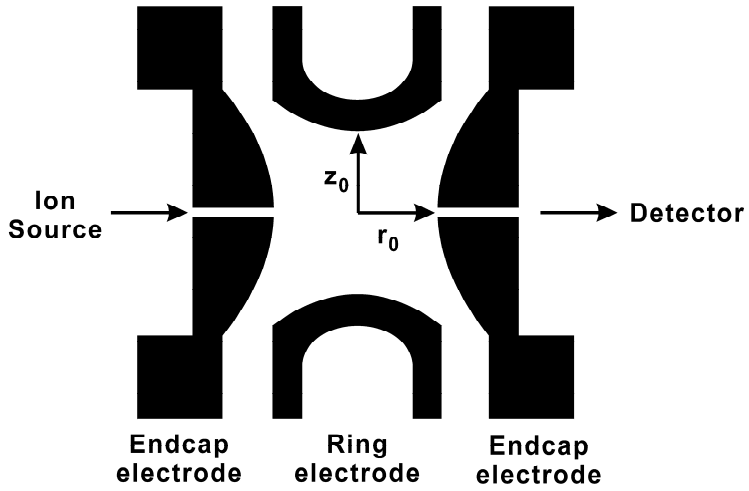

Figure 2.8. Illustration of a quadrupole ion trap consisting of three electrodes.

Quadrupole ion trap instruments have many advantages in chemical analysis such as high sensitivity, multistage mass spectrometry (MS^n) possibility and high resolution (which is accessible through slow scans although the mass accuracy is relatively poor in that case).

In a Bruker Esquire 3000 Plus quadrupole ion trap, MS/MS can be achieved in two extra steps, *viz.* isolation and fragmentation. Multistage MS (MS^n) is made possible by repeating the isolation and fragmentation cycle for several times.

In a quadrupole ion trap each particular mass has its own specific resonance. In the isolation process, all ions except the precursor ion can be ejected by the generation of a broadband frequency spectrum with all resonating frequencies present except for the frequency corresponding to the resonance of the precursor ion.

In the fragmentation process, the energy of the precursor ion selected is increased by resonance excitation using the dipole field. The resonance excitation waveform applies excitation in a small frequency band around the precise resonance frequency to increase the stability of the excitation. The resonating precursor ions quickly take up energy from the dipolar field and collide with the background gas (helium in this case) which causes them to dissociate to create product ions.

A schematic illustration of a typical MS/MS scan as operated on the Esquire 3000plus is presented in Figure 2.9.

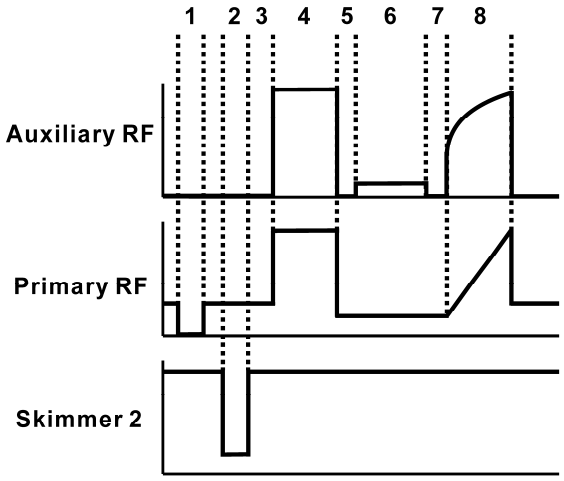

Figure 2.9. A typical MS/MS scan process on Bruker Esquire 3000plus qIT. The segments are 1) clearing the trap 2) accumulation of ions 3) isolation delay 4) precursor ion isolation 5) fragmentation delay 6) fragmentation 7) scan delay and 8) mass scan and analysis.

2.3.3.2 Orbitrap

The orbitrap is a relatively new type of mass analyser, invented by Makarov[79]. The orbital trapping idea was first implemented as early as in the 1920's by Kingdon.[80] The Kingdon trap has also been realised in many variations[81, 82] and is used in experiments studying the spectroscopy of ions.[82, 83]

An orbitrap employs trapping in an electrostatic field with potential distribution.[82, 84] See Eq 2.7 for the mathematical calculation of the field.

$$U(r,z) = \frac{k}{2}(z^2 - \frac{r^2}{2}) + \frac{k}{2}(R_m)^2 \ln[\frac{r}{R_m}] + C \qquad \text{(Eq 2.7)}$$

in which r and z are cylindrical coordinates (z is 0 being the plane of the symmetry of the field), k is the expression of the field curvature, R_m is the characteristic radius and C is a constant. This quadro-logarithmic field can be represented as a combination of quadrupole and logarithmic potentials. Figure 2.10 shows a schematic illustration of an orbitap

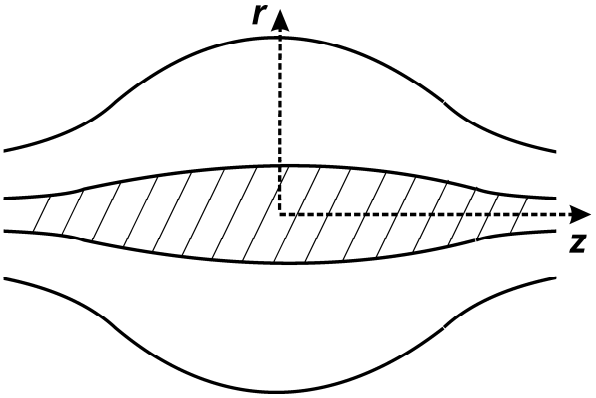

Figure 2.10. Schematic of an orbitrap with the quadro-logarithmic field.

Ion stability in an orbitrap is achieved only due to ions orbiting around an axial electrode due to the absence of any magnetic or RF fields. Orbiting ions perform harmonic oscillations along the electrode with a frequency proportional to $(m/z)^{-1/2}$. See Eq. 2.8 for this calculation. A detailed description of the equation can be found elsewhere.[79]

$$\omega = \sqrt{(z/m) \times k} \qquad \text{(Eq 2.8)}$$

The oscillations are detected using image current detection and are transformed into mass spectra using fast FT which is similar to FTICR.

An orbitrap instrument is capable of measuring at high mass resolution (up to 100,000 – 200,000) due to the high accuracy in definition of the electrostatic field. It also has high mass accuracy, dynamic range (around 5000) and upper mass limit (at least *m/z* 6000).[85] Because of the high performance of the orbitrap, it has been applied to many chemical systems in various research areas.[86-89] The use of orbitrap mass spectrometry to study polymer systems has been demonstrated for determination of polymer composition,[90] fast and accurate determination of average molecular weight,[91] end group analysis and isomer discrimination.[25, 92]

The orbitrap used in the work reported in this thesis is Thermo Scientific LTQ Orbitrap XL, which is a hybrid system combining a linear ion trap and an orbitrap.

2.3.3.3 FTICR

Fourier transform ion cyclotron resonance mass spectrometry (FTICR-MS) is a mass analysis technique that combines electric and magnetic fields to simultaneously measure ion *m/z* values in the mass analyser. The cyclotron motion of ions in a magnetic field was introduced as early as in 1932. It was used for proton acceleration to high kinetic energies for nuclear physics experiments.[93] Fourier transformation algorithms for image charge detection of the cyclotron motion of the ions were only introduced some four decades later.[94, 95] This resulted in FTICR-MS, a new mass analysis technique which offers unequalled mass resolution (>750,000, even many times higher than that of an Orbitrap) and mass accuracy (ppb level). This advantage allows accurate mass analysis of a complex mixture which benefits polymer study.

The core of a FTICR-MS instrument is the ICR cell, which is a Penning trap. It is located in the centre of a super-conducting magnet. Many ICR cell designs including rectangular,[96] cubic,[97] cylindrical,[98] 'infinity' trap[99] and open-ended cell[100, 101] have been reported in the literature. The open-ended cell design minimised the loss of ions as well as improved the trapping of ions.

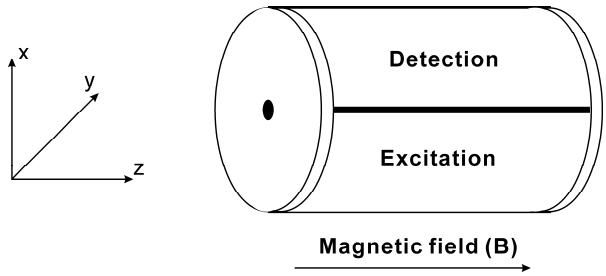

Figure 2.11. Schematic of a closed cylindrical cell. The cell contains two trapping plates, two pairs of opposite electrodes for excitation and two others for detection.

Figure 2.11 shows a schematic of a typical FTICR analyser. Ions entering the ICR cell follow a cyclotron motion in the x-y direction due to the presence of the magnetic field (parallel to the z-axis). The 'unperturbed' cyclotron (rotational) frequency, ω_c, to describe an ion of mass m and charge q moving in a spatially uniform magnetic field B and rotating around the magnetic field direction is expressed in Eq 2.9.[102]

$$\text{a) } \omega_c = \frac{qB}{m} \text{ and b) } \upsilon_c = \frac{\omega_c}{2\pi} = \frac{1.535611 \times 10^7 B}{m/z} \qquad \text{(Eq 2.9)}$$

in which υ_c is in hertz (Hz), B in tesla (T), m in microgram and z in multiples of elementary charge. According to this equation, all ions of a given mass-to-charge ratio m/q (or m/z) rotate at the same ICR frequency, is independent of velocity. This property makes ICR especially amenable to mass spectrometry since the ion frequency is relatively insensitive to the kinetic energy, so that translational energy 'focusing' is not essential for precise determination of m/z.

The detection in FT-ICR is typically preceded by excitation produced by applying a spatially uniform electric field of amplitude, E_0, directed perpendicular to the magnetic field direction, and rotating at the cyclotron frequency of ions of a particular m/z value. During the excitation process, the dimensions of the initial ion packet remain the same and the packet accelerates along a spiral trajectory. Following resonant irradiation of duration t_{excite} the ion packet's cyclotron radius r can be explained by Eq 2.10.

$$r = \frac{E_0 t_{excite}}{2B} \qquad \text{(Eq 2.10)}$$

The coherent motion of the ions is detected with the detection electrodes after kinetic excitation of the ions to an orbit with a radius smaller than the diameter of the cell. Working under very low pressure (10^{-9} to 10^{-10} mbars) is required to achieve this coherent motion. An alternating image current is induced by the ions repeatedly passing the detection electrodes. The frequency of the alternating current matches the cyclotron frequency of the ions. It is amplified and converted into an alternative voltage, the time domain voltage signal *f(t)*. (See Eq 2.11.)

$$f(t) = \sum_{i=1}^{M} N_i e^{-t/\tau_i} \cos(\omega_i t + \varphi_i) \qquad \text{(Eq 2.11)}$$

where t is the length (seconds) of transient, N_i is the number of the ions i, τ_i is the damping contant, ω_i is the cyclotron frequency of the ions i and φ_i is the phase of the ions. A mass spectrum is then be obtained by applying Fourier transformation to the time domain signal *f(t)* followed by conversion to *m/z* .

As mentioned earlier in this chapter, CID can be performed in FTICR MS. The precursor ion in an FTICR instrument is often kinetically excited with an RF pulse, using on-resonance excitation[103] or sustained-off resonance irradiation (SORI).[103, 104]

2.3.3.4 Ion Mobility Spectrometry-Mass Spectrometry--a Hybrid Instrument

Ion mobility spectrometry (IMS) was developed by Earl McDaniel in the 1950's to separate charged particles on a millisecond scale.[105] When coupled with MS, IMS offers another dimension of separation based on drift time in addition to the mass-to-charge separation. Isomers, isobars, size and/or conformation information can be obtained from the IMS-MS data.

In an IMS drift tube (cell), the incoming ions are driven by a homogeneous electric field. A carrier buffer gas is applied to oppose the incoming ion motion. The drift time of an ion moving through the tube depends on the mass, charge, size and shape of the ion. The area of an ion that the carrier buffer gas molecules strike is the cross-section of the ion. An ion with a larger cross-section will need longer time to migrate through the drift tube since more area is available for the buffer gas to collide and delay the drift of the ion. In a drift

cell with the length of L, the ion mobility (K) of an ion is determined by its drift time (t_D) and the potential difference U of a homogeneous electric field . Eq 2.12 shows the calculation of K.

$$K = \frac{L^2}{t_D U} \qquad \text{(Eq 2.12)}$$

In principle, IMS can be combined with all types of MS instruments.[106, 107] The one used for the experiments described in this thesis is a Waters Synapt G2 HDMS mass spectrometer. The layout of the instrument is very similar to the one of a Q-TOF instrument but with an IMS drift cell added after the quadrupole and before the TOF analyser. IMS-MS, IMS-MS/MS and MS/MS-IMS experiments can be performed on this instrument.

IMS-MS has been widely used in the analysis of biomolecules,[105, 108, 109] but its use in synthetic polymer systems is still very limited.[110-114] A study of a complex synthetic polymer system using IMS-MS is reported in Chapter 6.

2.4 Liquid Chromatography of Polymers and Its Use with Mass Spectrometry

2.4.1 Separation Modes in the Liquid Chromatography of Polymers

In liquid chromatography porous column packings are generally used as the stationary phase. Solutes with higher molecular weight, dependent on their size, partly penetrate into the pores of the column packing and undergo interactions with the active stationary phase located inside the pores. Two main process, steric exclusion and enthalpic interactions (also called 'adsorption'), can therefore be found in LC.

The retention volume of LC, V_{ret} is defined in Eq 2.13

$$V_{ret} = V_i + K_{\text{sec}} V_p + K_{ads} V_s \qquad \text{(Eq 2.13)}$$

where V_i is the interstitial volume, V_p is the pore volume, V_s is the stationary phase, K_{sec} and K_{ads} are the chromatographic distribution coefficients for exclusion and for adsorption, respectively. K_D can be calculated using Eq 2.14,

$$K_D = \frac{c_s}{c_m} = \exp^{(\frac{-\Delta\mu_0}{RT})} \qquad \text{(Eq. 2.14)}$$

where c_s is the concentration of a solute in the stationary phase and c_m is its concentration in the mobile phase. $\Delta\mu_0$ is the standard chemical potential difference for solute in both phases.

In size exclusion chromatography (SEC), a thermodynamically good solvent for the polymer is used as mobile phase. It effectively suppresses enthalpic interactions with the stationary phase. In this case, K_{ads}=0 and the retention is dominated by exclusion effects. K_{sec} varies from 0 for larger molecules ('total exclusion' from the pores) to 1 for small molecules ('total permeation' to the pores). Therefore, retention decreases with increasing molecular weight. A decrease in thermodynamic quality of the solvent (by changing temperature or adding a poor solvent) will result in an increase in K_{ads}. When K_{ads} is large enough to make $K_{sec}V_p+K_{ads}V_s>V_p$, the retention will be dominated by adsorption (LAC, liquid adsorption chromatography). The retention increases with increasing molecular weight in this condition. In the case when entropic exclusion effects and enthalpic adsorption effects are (nearly) balanced ($K_{sec}V_p+K_{ads}V_s=V_p$), the retention is (nearly) molecular-weight independent. This condition is called liquid chromatography at critical condition (LCCC, also known as liquid adsorption chromatography at critical condition, LACCC). A schematic illustration of the relation between V_{ret} and molecular weight in the three LC modes introduced above is presented in Figure 2.12.

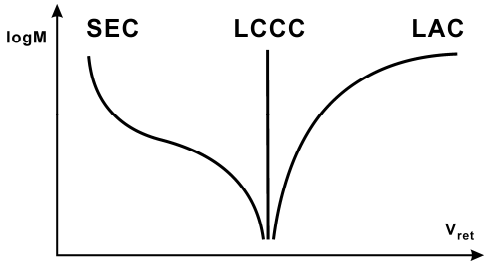

Figure 2.12. Dependence of retention volume on molecular weight for the three modes of liquid chromatography.

2.4.2 LC-MS

LC coupled online to MS mostly employs ionisation at atmospheric pressure. Most of the applications of LC-MS utilise ESI as this ionisation techniques brings about relatively high ionisation efficiencies and is able to ionise a large variety of analytes. Multiply-charged ions can easily be formed in ESI making it possible to analyse large molecules such as proteins,[115] nucleic acids[116] and polymers.[25, 65, 117] Small to medium polar analytes are also ionisable with ESI which makes it very useful in drug,[118] metabolite[119] and environmental studies.[120] In synthetic polymer analysis, LC separation prior to MS can mitigate or decrease the effects of ion suppression that may occur when direct infusion analysis is used.[25] The additional separation also produces less complex spectra allowing easier interpretation.[34, 65] Figure 2.13 shows an online coupled LC-MS scheme.

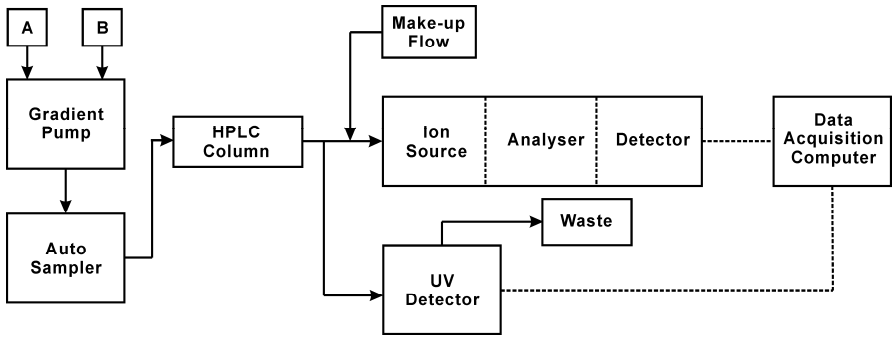

Figure 2.13. Schematic of a typical LC-MS setting.

In developing a LC-MS experiment, parameters influencing the LC separation and ionisation efficiency should both be considered. Table 2.1. lists several parameters that may influence the performance of a LC-MS experiment. LC-MS methods are most often optimised by varying one of the parameters mentioned in Table 2.1. A detailed development strategy can be found elsewhere.[121]

Table 2.1. Parameters which may influence the performance of an LC-MS analysis.

Part of the analysis	Parameters
LC (separation)	Type of column (packing materials, dimension), flow rate, organic solvent type and concentration, type of gradient, temperature and buffer type, pH and concentration
ESI (ionisation efficiency)	Flow rate, organic solvent type and concentration, buffer type, pH and concentration, applied voltage and nebuliser gas flow and temperature.

References

(1) Cowie, J. M. G., *Polymers: Chemistry & Physics of Modern Materials, Second Edition*. CRC Press Inc: 1991; p 450.
(2) Nielen, M. W. F. *Rapid Commun. Mass Spectrom.* **1996,** *10*, 1652-1660.
(3) Nielen, M. W. F. *Mass Spectrom. Rev.* **1999,** *18*, 309-344.
(4) Montaudo, G.; Samperi, F.; Montaudo, M. S. *Prog. Polym. Sci.* **2006,** *31*, 277-357.
(5) Jackson, A. T.; Bunn, A.; Hutchings, L. R.; Kiff, F. T.; Richards, R. W.; Williams, J.; Green, M. R.; Bateman, R. H. *Polymer* **2000,** *41*, 7437-7450.
(6) Hirao, A.; Matsuo, A.; Watanabe, T. *Macromolecules* **2005,** *38*, 8701-8711.
(7) Hirao, A.; Sugiyama, K.; Tsunoda, Y.; Matsuo, A.; Watanabe, T. *J. Polym. Sci., Part A: Polym. Chem.* **2006,** *44*, 6659-6687.
(8) Hirao, A.; Watanabe, T.; Ishizu, K.; Ree, M.; Jin, S.; Jin, K. S.; Deffieux, A.; Schappacher, M.; Carlotti, S. p. *Macromolecules* **2009,** *42*, 682-693.
(9) Grey Craig, A.; Cullis, P. G.; Derrick, P. J. *International Journal of Mass Spectrometry and Ion Physics* **1981,** *38*, 297-304.
(10) Lattimer, R. P.; Schulten, H. R. *International Journal of Mass Spectrometry and Ion Physics* **1983,** *52*, 105-116.
(11) Doerr, M.; Luederwald, I.; Schulten, H.-R. *J. Anal. Appl. Pyrolysis* **1985,** *8*, 109-121.
(12) Montaudo, G.; Scamporrino, E.; Vitalini, D. *Polymer* **1989,** *30*, 297-303.
(13) Vitalini, D.; Scamporrino, E. *Polymer* **1992,** *33*, 4597-4604.
(14) Campana, J. E.; Rose, S. L. *International Journal of Mass Spectrometry and Ion Physics* **1983,** *46*, 483-486.
(15) Ward, A. J.; Short, R. D. *Polymer* **1993,** *34*, 4179-4185.
(16) Li, L.; Chan, C.-M.; Ng, K.-M.; Lei, Y.; Weng, L.-T. *Polymer* **2001,** *42*, 6841-6849.
(17) Karas, M.; Bachmann, D.; Bahr, U.; Hillenkamp, F. *Int. J. Mass Spectrom. Ion Processes* **1987,** *78*, 53-68.
(18) Karas, M.; Hillenkamp, F. *Anal. Chem.* **1988,** *60*, 2299-2301.
(19) Whitehouse, C. M.; Dreyer, R. N.; Yamashita, M.; Fenn, J. B. *Anal. Chem.* **1985,** *57*, 675-679.
(20) Fenn, J. B.; Mann, M.; Meng, C. K.; Wong, S. F.; Whitehouse, C. M. *Science* **1989,** *246*, 64-71.
(21) de Koster, C. G.; Duursma, M. C.; van Rooij, G. J.; Heeren, R. M. A.; Boon, J. J. *Rapid Commun. Mass Spectrom.* **1995,** *9*, 957-962.
(22) van Rooij, G. J.; Duursma, M. C.; Heeren, R. M. A.; Boon, J. J.; de Koster, C. G. *J. Am. Soc. Mass Spectrom.* **1996,** *7*, 449-457.
(23) Muscat, D.; Henderickx, H.; Kwakkenbos, G.; van Benthem, R.; de Koster, C. G.; Fokkens, R.; Nibbering, N. M. M. *J. Am. Soc. Mass Spectrom.* **2000,** *11*, 218-227.
(24) Meyer, T.; Kunkel, M.; Frahm, A. W.; Waidelich, D. *J. Am. Soc. Mass Spectrom.* **2001,** *12*, 911-925.
(25) Song, J.; van Velde, J. W.; Vertommen, L. L. T.; van der Ven, L. G. J.; Heeren, R. M. A.; van den Brink, O. F. *Macromolecules* **2010,** *43*, 7082-7089.
(26) Jackson, A. T.; Slade, S. E.; Scrivens, J. H. *Int. J. Mass Spectrom.* **2004,** *238*, 265-277.
(27) Jackson, A. T.; Slade, S. E.; Thalassinos, K.; Scrivens, J. H. *Anal. Bioanal. Chem.* **2008,** *392*, 643-650.
(28) Crecelius, A. C.; Baumgaertel, A.; Schubert, U. S. *J. Mass Spectrom.* **2009,** *44*, 1277-1286.
(29) Boschmann, D.; Vana, P. *Macromolecules* **2007,** *40*, 2683-2693.
(30) Pensec, S.; Nouvel, N.; Guilleman, A.; Creton, C.; Boueì , F. o.; Bouteiller, L. *Macromolecules 43*, 2529-2534.
(31) Albertazzi, L.; Serresi, M.; Albanese, A.; Beltram, F. *Mol. Pharm. 7*, 680-688.

(32) Adamus, G.; Sikorska, W.; Kowalczuk, M.; Montaudo, M.; Scandola, M. *Macromolecules* **2000,** *33*, 5797-5802.
(33) Marten, E.; Müller, R. J.; Deckwer, W. D. *Polym. Degrad. Stab.* **2005,** *88*, 371-381.
(34) Falkenhagen, J.; Much, H.; Stauf, W.; Muller, A. H. E. *Macromolecules* **2000,** *33*, 3687-3693.
(35) Koster, S.; de Koster, C. G.; van Benthem, R. A. T. M.; Duursma, M. C.; Boon, J. J.; Heerena, R. M. A. *Int. J. Mass Spectrom.* **2001,** *210-211*, 591-602.
(36) Adhiya, A.; Wesdemiotis, C. *Int. J. Mass Spectrom.* **2002,** *214*, 75-88.
(37) Koster, S.; Duursma, M. C.; Boon, J. J.; Heeren, R. M. A.; Ingemann, S.; van Benthem, R. A. T. M.; de Koster, C. G. *J. Am. Soc. Mass Spectrom.* **2003,** *14*, 332-341.
(38) Chikh, L.; Tessier, M.; Fradet, A. *Polymer* **2007,** *48*, 1884-1892.
(39) Stille, J. K. *J. Chem. Educ.* **1981,** *58*, 862.
(40) Wagener, K. B.; Wanigatunga, S., Chain-Propagation and Step-Propagation Polymerization. In *Chemical Reactions on Polymers*, American Chemical Society: 1988; Vol. 364, pp 153-164.
(41) Spindler, R.; Frechet, J. M. J. *Macromolecules* **1993,** *26*, 4809-4813.
(42) Sano, M.; Sandberg, M. O.; Yamada, N.; Yoshimura, S. *Macromolecules* **1995,** *28*, 1925-1937.
(43) Labadie Jeff, W.; Hedrick James, L.; Ueda, M., A Survey of Some Recent Advances in Step-Growth Polymerization. In *Step-Growth Polymers for High-Performance Materials*, American Chemical Society: 1996; Vol. 624, pp 294-305.
(44) Ye, Y.; Choi, K. Y. *Ind. Eng. Chem. Res.* **2009,** *48*, 4274-4282.
(45) Ham George, E., New Developments and Trends in Free-Radical Polymerization. In *Applied Polymer Science*, American Chemical Society: 1985; Vol. 285, pp 151-158.
(46) Kalra, B.; Gross, R. A., Peroxidase-Mediated Free Radical Polymerization of Vinyl Monomers. In *Biocatalysis in Polymer Science*, American Chemical Society: 2002; Vol. 840, pp 297-308.
(47) Guerrero-Sanchez, C.; Wiesbrock, F.; Schubert Ulrich, S., Polymer Synthesis in Ionic Liquids: Free Radical Polymerization in Water-Soluble Systems. In *Ionic Liquids in Polymer Systems*, American Chemical Society: 2005; Vol. 913, pp 37-49.
(48) Odell Peter, G.; Listigovers Nancy, A.; Quinlan Marion, H.; Georges Michael, K., Solvent-Free Stable Free Radical Polymerization: Understanding and Applications. In *Solvent-Free Polymerizations and Processes*, American Chemical Society: 1999; Vol. 713, pp 80-95.
(49) Junkers, T.; Koo, S. P. S.; Davis, T. P.; Stenzel, M. H.; Barner-Kowollik, C. *Macromolecules* **2007,** *40*, 8906-8912.
(50) Koo, S. P. S.; Junkers, T.; Barner-Kowollik, C. *Macromolecules* **2009,** *42*, 62-69.
(51) Ahmad, N. M.; Heatley, F.; Lovell, P. A. *Macromolecules* **1998,** *31*, 2822-2827.
(52) Junkers, T.; Barner-Kowollik, C. *J. Polym. Sci., Part A: Polym. Chem.* **2008,** *46*, 7585-7605.
(53) Matyjaszewski, K.; Xia, J. *Chem. Rev.* **2001,** *101*, 2921-2990.
(54) Moad, G.; Rizzardo, E.; Thang, S. H. *Polymer* **2008,** *49*, 1079-1131.
(55) Dole, M.; Mack, L. L.; Hines, R. L.; Mobley, R. C.; Ferguson, L. D.; Alice, M. B. *J. Chem. Phys.* **1968,** *49*, 2240-2249.
(56) Taylor, G. *Proceedings of the Royal Society of London. Series A. Mathematical and Physical Sciences* **1964,** *280*, 383-397.
(57) Rayleigh, L. *Philos. Mag.* **1882,** *5*, 184-186.
(58) Buback, M.; Frauendorf, H.; Gunzler, F.; Vana, P. *J. Polym. Sci., Part A: Polym. Chem.* **2007,** *45*, 2453-2467.
(59) Jiang, X.; Schoenmakers, P. J.; Lou, X.; Lima, V.; van Dongen, J. L. J.; Brokken-Zijp, J. *J. Chromatogr., A* **2004,** *1055*, 123-133.
(60) Chaicharoen, K.; Polce, M.; Singh, A.; Pugh, C.; Wesdemiotis, C. *Anal. Bioanal. Chem.* **2008,** *392*, 595-607.
(61) Gruendling, T.; Guilhaus, M.; Barner-Kowollik, C. *Macromolecules* **2009,** *42*, 6366-6374.
(62) Rychter, P.; Biczak, R.; Herman, B.; Smylla, A.; Kurcok, P.; Adamus, G.; Kowalczuk, M. *Biomacromolecules* **2006,** *7*, 3125-3131.
(63) Zagar, E.; Krzan, A.; Adamus, G.; Kowalczuk, M. *Biomacromolecules* **2006,** *7*, 2210-2216.

(64) Adamus, G. *Macromolecules* **2009,** *42*, 4547-4557.
(65) Falkenhagen, J.; Weidner, S. *Anal. Chem.* **2008,** *81*, 282-287.
(66) Tanaka, K.; Waki, H.; Ido, Y.; Akita, S.; Yoshida, Y.; Yoshida, T.; Matsuo, T. *Rapid Commun. Mass Spectrom.* **1988,** *2*, 151-153.
(67) Montaudo, G.; Montaudo, M. S.; Puglisi, C.; Samperi, F. *Macromolecules* **1995,** *28*, 4562-4569.
(68) Sleno, L.; Volmer, D. A. *J. Mass Spectrom.* **2004,** *39*, 1091-1112.
(69) Mikesh, L. M.; Ueberheide, B.; Chi, A.; Coon, J. J.; Syka, J. E. P.; Shabanowitz, J.; Hunt, D. F. *Biochimica et Biophysica Acta (BBA) - Proteins & Proteomics* **2006,** *1764*, 1811-1822.
(70) Little, D. P.; Speir, J. P.; Senko, M. W.; O'Connor, P. B.; McLafferty, F. W. *Anal. Chem.* **1994,** *66*, 2809-2815.
(71) Paul, W.; Steinwedel, H. *Zeitschrift für Naturforschung A* **1953,** *8*, 448-450.
(72) Paul, W.; Steinwedel, H. Verfahren zur Trennung bzw. zum getrennten Nachweis von Ionen verschiedener spezifischer Ladung DE Patent 944900 1956.
(73) Paul, W. *Angewandte Chemie International Edition in English* **1990,** *29*, 739-748.
(74) Julian, R. K.; Reiser, H.-P.; Graham Cooks, R. *Int. J. Mass Spectrom. Ion Processes* **1993,** *123*, 85-96.
(75) Reiser, H.-P.; Julian, R. K.; Cooks, R. G. *Int. J. Mass Spectrom. Ion Processes* **1992,** *121*, 49-63.
(76) March, R. E. *Int. J. Mass Spectrom.* **2000,** *200*, 285-312.
(77) March, R. E. *J. Mass Spectrom.* **1997,** *32*, 351-369.
(78) Kuribayashi, S.; Yamakoshi, H.; Danno, M.; Sakai, S.; Tsuruga, S.; Futami, H.; Morii, S. *Anal. Chem.* **2005,** *77*, 1007-1012.
(79) Makarov, A. *Anal. Chem.* **2000,** *72*, 1156-1162.
(80) Kingdon, K. H. *Physical Review* **1923,** *21*, 408.
(81) McIlraith, A. H. *Nature* **1966,** *212*, 1422-1424.
(82) Knight, R. D. *Appl. Phys. Lett.* **1983,** *38*, 221-223.
(83) Lewis, R. R. *J. Appl. Phys.* **1982,** *53*, 3975-3980.
(84) Gillig, K. J.; Bluhm, B. K.; Russell, D. H. *Int. J. Mass Spectrom. Ion Processes* **1996,** *157-158*, 129-147.
(85) Makarov, A.; Denisov, E.; Lange, O.; Horning, S. *J. Am. Soc. Mass Spectrom.* **2006,** *17*, 977-982.
(86) Nielen, M. W. F.; van Engelen, M. C.; Zuiderent, R.; Ramaker, R. *Anal. Chim. Acta* **2007,** *586*, 122-129.
(87) Dunn, W. B.; Broadhurst, D.; Brown, M.; Baker, P. N.; Redman, C. W. G.; Kenny, L. C.; Kell, D. B. *Journal of Chromatography B* **2008,** *871*, 288-298.
(88) Hogenboom, A. C.; van Leerdam, J. A.; de Voogt, P. *Journal of Chromatography A* **2009,** *1216*, 510-519.
(89) Makarov, A.; Denisov, E. *J. Am. Soc. Mass Spectrom.* **2009,** *20*, 1486-1495.
(90) Dopico-García, M. S.; López-Vilariño, J. M.; Fernández-Martínez, G.; González-Rodríguez, M. V. *Anal. Chim. Acta 667*, 123-129.
(91) Gruendling, T.; Guilhaus, M.; Barner-Kowollik, C. *Macromolecules* **2009,** *42*, 6366-6374.
(92) Khanna, K.; Varshney, S.; Kakkar, A. *Macromolecules 43*, 5688-5698.
(93) Lawrence, E. O.; Livingston, M. S. *Physical Review* **1932,** *40*, 19.
(94) Comisarow, M. B.; Marshall, A. G. *Chem. Phys. Lett.* **1974,** *25*, 282-283.
(95) Comisarow, M. B.; Marshall, A. G. *Chem. Phys. Lett.* **1974,** *26*, 489-490.
(96) McIver, J. R. T. *Rev. Sci. Instrum.* **1970,** *41*, 555-558.
(97) Comisarow, M. B. *Adv. Mass. Spectrom.* **1981,** *8*, 1698-1706.
(98) Comisarow, M. B. Fourier transform ion cyclotron resonance spectroscopy method and apparatus. USA Patent No. 3937955, 1976.
(99) Caravatti, P.; Allemann, M. *Org. Mass Spectrom.* **1991,** *26*, 514-518.
(100) Gabrielse, G.; Haarsma, L.; Rolston, S. L. *Int. J. Mass Spectrom. Ion Processes* **1989,** *88*, 319-332.
(101) Beu, S. C.; Laude Jr, D. A. *Int. J. Mass Spectrom. Ion Processes* **1992,** *112*, 215-230.

(102) Marshall, A. G.; Hendrickson, C. L.; Jackson, G. S. *Mass Spectrom. Rev.* **1998,** *17*, 1-35.
(103) Senko, M. W.; Speir, J. P.; McLafferty, F. W. *Anal. Chem.* **1994,** *66*, 2801-2808.
(104) Gauthier, J. W.; Trautman, T. R.; Jacobson, D. B. *Anal. Chim. Acta* **1991,** *246*, 211-225.
(105) Kanu, A. B.; Dwivedi, P.; Tam, M.; Matz, L.; Hill, H. H. *J. Mass Spectrom.* **2008,** *43*, 1-22.
(106) Cohen, M. J.; Carroll, D. I.; Wernlund, R. F.; Kilpatrick, W. D. Apparatus and methods for detecting and identifying trace gases. US Patent 3621240, 1971.
(107) Hoaglund, C. S.; Valentine, S. J.; Sporleder, C. R.; Reilly, J. P.; Clemmer, D. E. *Anal. Chem.* **1998,** *70*, 2236-2242.
(108) Bohrer, B. C.; Merenbloom, S. I.; Koeniger, S. L.; Hilderbrand, A. E.; Clemmer, D. E. *Annu. Rev. Anal. Chem.* **2008,** *1*, 293-327.
(109) Fenn, L. S.; McLean, J. A. *Anal. Bioanal. Chem.* **2008,** *391*, 905-909.
(110) Trimpin, S.; Plasencia, M.; Isailovic, D.; Clemmer, D. E. *Anal. Chem.* **2007,** *79*, 7965-7974.
(111) Bagal, D.; Zhang, H.; Schnier, P. D. *Anal. Chem.* **2008,** *80*, 2408-2418.
(112) Trimpin, S.; Clemmer, D. E. *Anal. Chem.* **2008,** *80*, 9073-9083.
(113) Hilton, G. R.; Jackson, A. T.; Thalassinos, K.; Scrivens, J. H. *Anal. Chem.* **2008,** *80*, 9720-9725.
(114) Chan, Y.-T.; Li, X.; Soler, M.; Wang, J.-L.; Wesdemiotis, C.; Newkome, G. R. *J. Am. Chem. Soc.* **2009,** *131*, 16395-16397.
(115) Le Bihan, T.; Pinto, D.; Figeys, D. *Anal. Chem.* **2001,** *73*, 1307-1315.
(116) Barry, C. G.; Day, C. S.; Bierbach, U. *J. Am. Chem. Soc.* **2005,** *127*, 1160-1169.
(117) Nielen, M. W. F.; Buijtenhuijs, F. A. *Anal. Chem.* **1999,** *71*, 1809-1814.
(118) Zhang, N.; Fountain, S. T.; Bi, H.; Rossi, D. T. *Anal. Chem.* **2000,** *72*, 800-806.
(119) Onorato, J. M.; Henion, J. D.; Lefebvre, P. M.; Kiplinger, J. P. *Anal. Chem.* **2000,** *73*, 119-125.
(120) Ciminiello, P.; Dell'Aversano, C.; Fattorusso, E.; Forino, M.; Magno, S.; Poletti, R. *Chem. Res. Toxicol.* **2002,** *15*, 979-984.
(121) Moberg, M. Liquid Chromatography Coupled to Mass Spectrometry. PhD. thesis, Uppsala Universitet, 2006.

3

Discrimination between Charge-Catalysed and Charge-Independent Fragmentation Processes of Cationised Poly (*n*-Butyl Acrylate)

This chapter is based on, Junkan Song, Antony Memboeuf, Ron M.A. Heeren, Károly Vékey and Oscar F. van den Brink, *Rapid Communications in Mass Spectrometry* **2010**, *24*, 3214-3216.

By performing a simple size-dependence analysis using breakdown diagrams with (at least) two different cations, the catalytic influence of the cation on the fragmentation processes can be clearly demonstrated. A simple procedure for determination of the effect of the cation on the fragmentation pathways (charge-catalysed or charge-independent) is described in the chapter. The information obtained is important for investigations by means of quantum chemical modelling. Although the MS/MS spectra for PBA generated on ion trap instrument are rather simple (only two major fragment ion peaks are observed), this procedure should be generally applicable to homopolymers or alternating copolymers.

3.1 Introduction

When performing structural investigation of macromolecular systems using tandem mass spectrometry, an important matter is the choice of the cation and how that does affect the tandem mass spectra. Moreover, when studying mechanistic aspects, the role of the adduct ions in the mechanism of the fragmentation processes is often discussed: Is the process charge-induced (more accurately described as charge-catalysed) or charge-remote (more accurately described as charge-independent). The catalytic effect of lithium has been studied in cationised poly(ethylene glycols) (PEGs).[1] The activation energy of the main fragmentation process for the trimer was shown, by means of Density Functional Theory calculations, to decrease by as much as 0.3 eV in the presence of lithium (in comparison with the protonated trimer).

In this chapter, the role of cation adducts on the fragmentation of even electron ions will be discussed based on the results obtained on the fragmentation of poly (*n*-butyl acrylate), PBA, with different alkali ions and various degrees of polymerisation. A method to clarify the role of the charge on the fragmentation processes will be presented.

3.2 Experimental Section

3.2.1 Sample Information

The PBA sample was obtained from AkzoNobel Car Refinishes, Sassenheim, The Netherlands. It was prepared by radical polymerisation using tert-butyl peroxy-3,5,5-trimethylhexanoate as initiator at 140 ^{o}C in xylene. The number average molecular weight is 2,800 and the weight average molecular weight is 5,510. These values were measured by gel permeation chromatography (GPC) calibrated with polystyrene standards. The structure of PBA selected for the experiments is shown in Scheme 3.1.

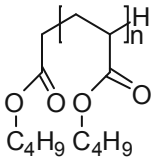

Scheme 3.1. The PBA selected for the present study.

3.2.2 Mass Spectrometry

The experiments were performed on a Bruker Esquire 3000plus ion trap mass spectrometer with PBA from 4 up to 12 monomeric units (polymerisation degree varies with different cations). Analysis was executed using direct infusion (using a Cole-Parmer 74900 series syringe pump at 0.6 ml/h) with samples dissolved in methanol (Fluka) at an approximate concentration of 20 μM. Various alkali salts (Li, Na, K and Cs) were added to the samples with equimolar concentration. The capillary voltage was set to 3 kV, the drying gas was operated at 300 °C, the average pressure of the ion trap was 9.8×10^{-6} mbar (uncorrected gauge, although the real pressure in the source is known to be 2-3orders of magnitude higher20), and the collision gas was Helium. The number of ions trapped in the cell was approximately10 000 (fixed using the ion charge control optionsICC) and was kept constant through the complete set of measurements. The parent ions were isolated with a 1 Th window (1 m/z unit), and a delay of 50 ms was applied before the excitation starts. The excitation stage lasted 60 ms using an excitation width of 6 Th.

PBA oligomers with positively charged alkali ion adducts including Li^+, Na^+, K^+ or Cs^+ were studied in the system. The main fragmentation processes observed are the loss of 56 Da and 130 Da in the cases of lithium and sodium adducts. Using high resolution and high accuracy mass spectrometry, the elemental compositions of these losses were identified to be C_4H_8 and $C_8H_{16}O$[2]. Backbone cleavage was not observed for PBA; all neutral losses originate from side chain cleavages[3]. The PBA used here (i.e. with a butylmethyl carboxylate and a hydrogen end group, see Scheme 3.1) was specifically selected for this work in order to avoid any end group fragmentation.

3.3 Results and Discussion

When potassium and caesium were used for adduct formation, no significant fragmentation was observed. This is most probably due to cation detachment, which was shown, e.g. in the case of cationised PEGs, to become preferential as the size of the cation increases[3]. This observation supports previous reports claiming the value of low mass cations for structural investigation of oligomers using tandem MS: stable complexes are formed with Li^+ and Na^+ cations that enable the macromolecule to dissociate into various fragments carrying specific structural information.

To study the energetics of polymer fragmentation, the survival yield (SY)[4-8] is a convenient quantitative measure. It is defined according to Eq 3.1:

$$SY = \frac{I_M}{I_M + \sum I_F} \qquad \text{(Eq 3.1)}$$

in which I_M is the intensity of the cationised molecule and ΣI_F is the sum of all product ion intensities. The survival yield curve is typically of the sigmoid-type (continuously decreasing from 1, at low energy, to 0 at high energy). Similarly the intensity of the individual product ions can be used as numerator in Eq1 and the corresponding curves can then be plotted. This way, a breakdown diagram is obtained. These diagrams were plotted in the case of lithium and sodium cationised PBA with 10 monomeric units and are shown in Figure 3.1.

Only two of the most intense fragmentation processes (i.e. neutral loss of 56 and loss of 130 Da) are shown here for the sake of clarity and as they represent altogether between 80-90% of the product ions observed.

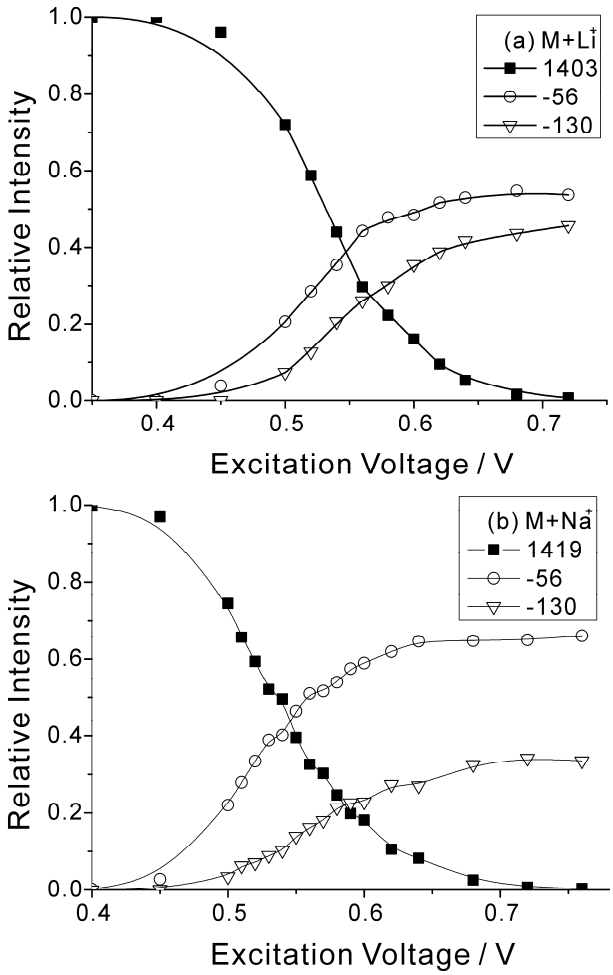

Figure 3.1. Breakdown diagrams of (a) lithium and (b) sodium cationised poly (*n*-butyl acrylate) with 10 monomeric units.

Two examples of tandem MS/MS spectra underlying the data presented in Figure 3.1 are shown in Figure 3.2 and Figure 3.3.

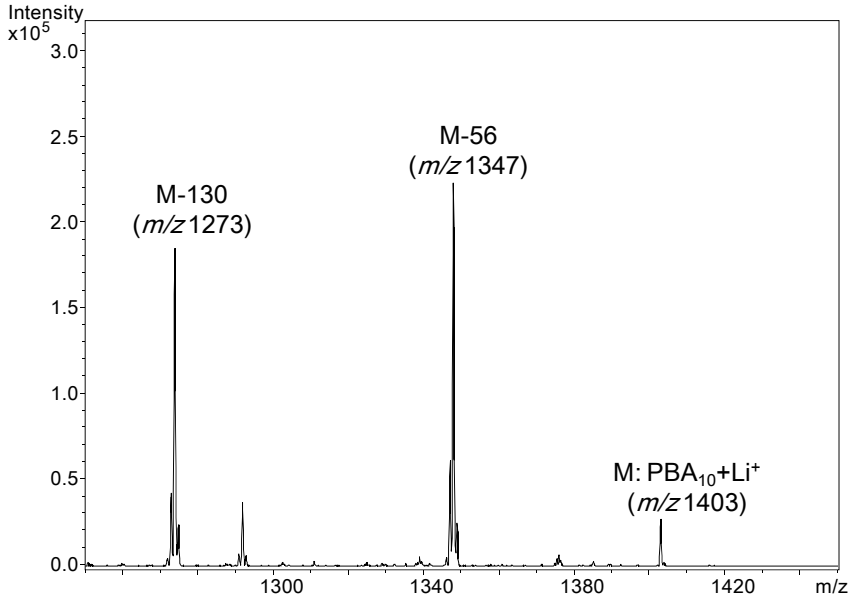

Figure 3.2. MS/MS spectrum of *m/z* 1403 ($PBA_{10}+Li^+$) at excitation voltage of 0.64 V

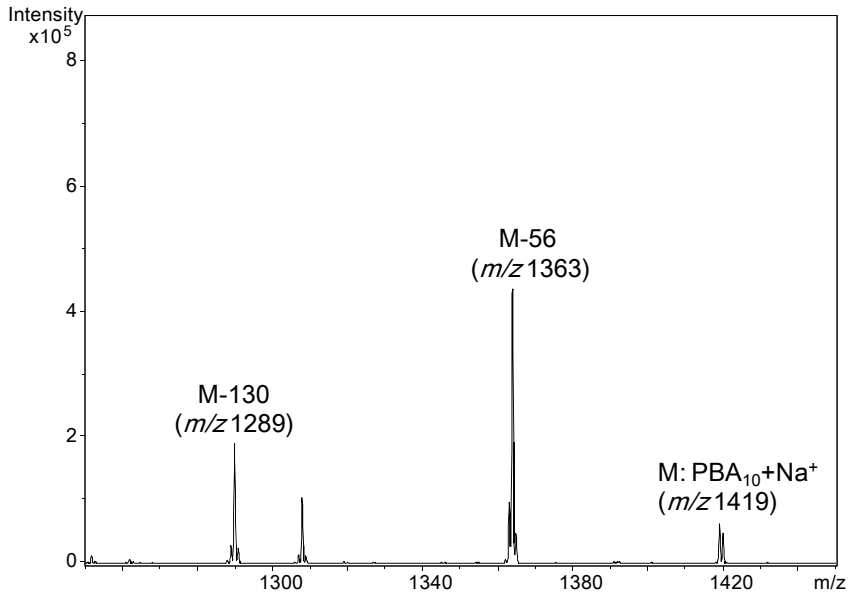

Figure 3.3. MS/MS spectrum of *m/z* 1419 ($PBA_{10}+Na^+$) at excitation voltage of 0.64 V

In the case of the lithium adduct, the distance between the two curves of the product ions is smaller and curves are more parallel to each other, while they are much more separated in the case of the sodium adduct. This observation is not influenced by varying the degree of polymerisation. Breakdown diagrams of cationised PBA with a different degree of polymerisation are presented in Figure 3.4. Hence, the relative importance of the respective fragmentation pathways (loss of 56 and 130Da) changes significantly with the adduct cations.[9]

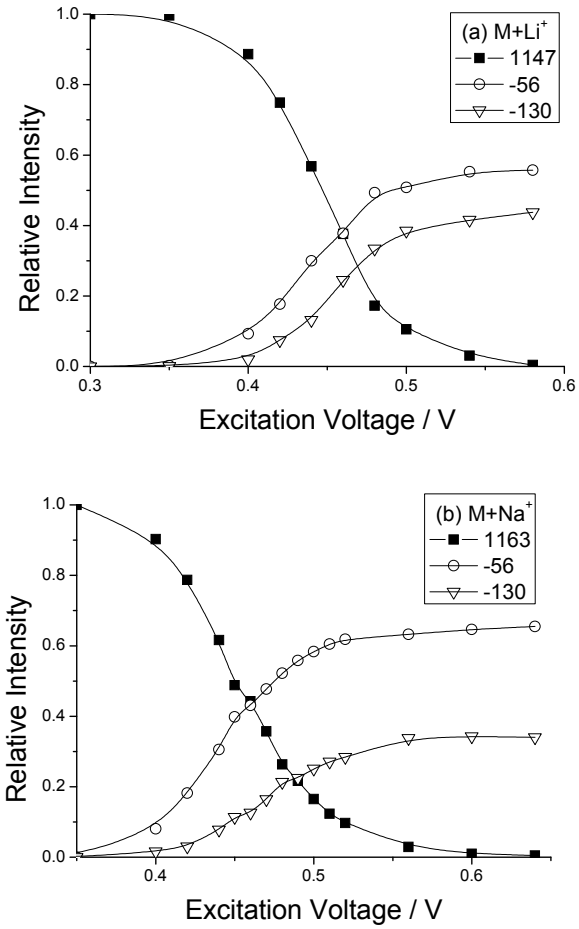

Figure 3.4. Breakdown diagrams of (a) lithium and (b) sodium cationised poly (*n*-butyl acrylate) with 8 monomeric units.

To further investigate this effect, the relative intensities of the two reaction channels were compared as a function of polymer size. For a given oligomer the ratio changes significantly with collision energy, as shown in Figure 3.1. At high energy the abundance ratio of the two fragmentation process becomes fairly constant; so this was measured corresponding to ca. 95% fragmentation (SY=0.05). The abundance ratio measured for the two processes, -56/-130, was measured as a function of molecular size, and this is shown in Figure 3.5; both for lithium and sodium cationised polymers.

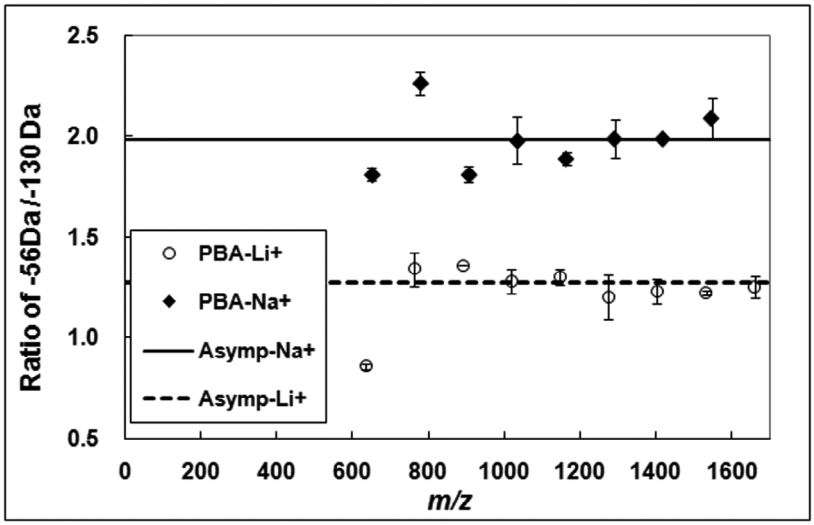

Figure 3.5. Ratios of signal intensities for the two main fragmentation processes (losses of 56 Da / 130 Da) observed at 95-100% fragmentation of the precursor ion, plotted versus *m/z* for lithium and sodium cationised PBAs. Full lines are asymptotic values obtained after averaging the last 8 values for Li^+ and the last 6 values for Na^+.

The figure shows that the relative intensities of the two main fragmentation processes are approximately independent of the degree of polymerisation; especially for hexamers and above. The asymptotic values calculated are 1.27±0.11 for PBA oligomers with Li^+ adduct and 1.99±0.12 with Na^+ adduct. The error bar value *s* presented in Figure 3.5 is the standard deviation of the ratio of the -56 and -130 product ion peaks. It is calculated according to Eq. 3.2.

$$s = \frac{\overline{I(-56)}}{\overline{I(-130)}} \sqrt{\left(\frac{s_{I(-56)}}{\overline{I(-56)}}\right)^2 + \left(\frac{s_{I(-130)}}{\overline{I(-130)}}\right)^2} \qquad \text{(Eq. 3.2.)}$$

where $\overline{I(-x)}$ is the mean value of the intensities of the product ion peak (-x), $s_{I(-x)}$ corresponds to the standard deviation of the ion peak (-x) intensities.

Figure 3.1 shows that the breakdown curve changes when the cation is changed from Li^+ to Na^+. This clearly suggests that at least one of the two (major) fragmentation processes is charge-catalysed. There are two possibilities; only one of the processes is charge-catalysed (and the other is charge independent) or both processes are charge-catalysed. As mentioned above, both fragmentation channels involve side chain losses. If the process is charge-catalysed, there is only one possible reaction channel in the cationised molecule (i.e. that close to the charged site). If the process is independent of the charge; the number of possible reaction channels will increase with the degree of polymerisation (possibly linearly with polymerisation degree). As a consequence, the abundance of charge independent processes should increase with molecular size. The abundance of a charge-catalysed process, however, will not be affected by varying the molecular size. Therefore, under conditions of similar degrees of fragmentation, a combination of a charge-catalysed and a charge-independent process will lead to a change in the intensity ratio of product ions when the mass of the precursor ions is changed. If both processes are charge-catalysed the intensity ratio will not be affected on change of the precursor ion's mass. Figure 3.5 clearly demonstrates that the ratio of the two processes reaches a constant value at n=6. Therefore, both of the fragmentation processes, *viz.* the loss of 56 Da and the loss of 130 Da, are charge-catalysed.

The flow chart shown in Scheme 3.2 can be used to formalise the above reasoning in a procedure for determining whether processes are charge-catalysed or charge-independent. The validity of this procedure is, at this stage, limited to polymers with a periodic structural pattern that show two (main) fragmentation products. There are two critical steps in the procedure: The first one is drawing breakdown diagrams with different cations, which reveals whether there is at least one charge-catalysed fragmentation process. The second

one is performing a size-dependence analysis, which provides information about the similarity of the nature of the fragmentation processes.

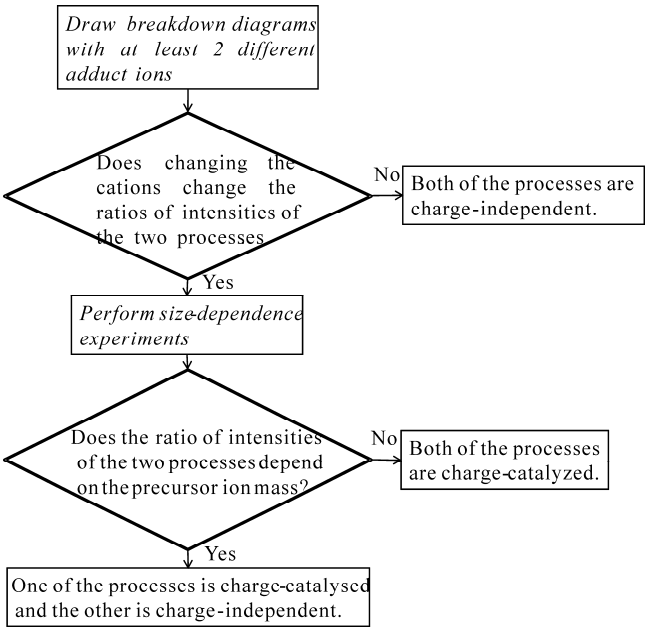

Scheme 3.2. Determination of the cation influence on two fragmentation processes (charge-catalysed/independent).

3.4 Conclusions

In this chapter, it is demonstrated that changing the size of the adduct ions can be used to increase the degree of fragmentation of polymers in tandem mass spectrometry. In fact similar to the case of PEG oligomers,[3] tandem MS spectra of PBA oligomers ionised with Li^+ and Na^+ provide more structural information than those of PBA oligomers ionised with larger cations. Although the cation doesn't qualitatively change the fragmentation pattern (the same product ions are observed), the nature of the cation changes the relative

abundance of the respective fragmentation processes. This illustrates well the catalytic effect the cation can exert on the fragmentation processes observed[10]. Moreover, it have also been shown that performing a simple size-dependence analysis using breakdown diagrams with at least two different cations, the catalytic influence of the cation on the fragmentation processes observed can be clearly demonstrated. A simple procedure for determination on the presence of an effect of the cation on the fragmentation (charge-catalysed or charge-independent) have also been delineated. This is important information for investigations by means of quantum chemical modelling. Although the MS/MS spectra obtained for PBA on ion trap instrument are rather simple (only two product ion peaks are observed), this procedure should also be generally applicable to homopolymers (or alternating copolymers). The limitation is however that there should be more than one product ion. The applicability of the method to tandem MS experiments that produce more than two different product ions should be investigated. A particularly interesting subject of research would be fragmentations in which the backbone of the polymer is cleaved in two ways, producing a multitude of product ions that can be grouped as two types.

References

(1) Memboeuf, A.; Drahos, L.; Vékey, K.; Lendvay, G. *Rapid Commun. Mass Spectrom.* **2010,** *24*, 2471-2473.
(2) Song, J.; van Velde, J. W.; Vertommen, L. L. T.; van der Ven, L. G. J.; Heeren, R. M. A.; van den Brink, O. F. *Macromolecules* **2010,** *43*, 7082-7089.
(3) Memboeuf, A.; Vekey, K.; Lendvay, G. *Eur. J. Mass Spectrom.* **2010**, Submitted.
(4) Derwa, F.; Pauw, E. d.; Natalis, P. *Org. Mass Spectrom.* **1991,** *26*, 117-118.
(5) Heeren, R. M. A.; Vékey, K. *Rapid Commun. Mass Spectrom.* **1998,** *12*, 1175-1181.
(6) Memboeuf, A.; Nasioudis, A.; Indelicato, S.; Pollreisz, F.; Kuki, A.; Keki, S.; van den Brink, O. F.; Vekey, K.; Drahos, L. *Anal. Chem.* **2010,** *82*, 2294-2302.
(7) Collette, C.; Drahos, L.; Pauw, E. D.; Vekey, K. *Rapid Commun. Mass Spectrom.* **1998,** *12*, 1673-1678.
(8) Guo, X.; Duursma, M. C.; Kistemaker, P. G.; Nibbering, N. M. M.; Vekey, K.; Drahos, L.; Heeren, R. M. A. *J. Mass Spectrom.* **2003,** *38*, 597-606.
(9) Cooks, R. G.; Patrick, J. S.; Kotiaho, T.; McLuckey, S. A. *Mass Spectrom. Rev.* **1994,** *13*, 287-339.
(10) Naray-Szabo, G.; Ferenczy, G. G. *Chem. Rev.* **1995,** *95*, 829-847.

4

Investigation of Polymerisation Mechanisms of Poly (*n*-Butyl Acrylate)s Generated in Different Solvents by LC-ESI-MS/MS

This chapter is based on, Junkan Song, Jan W. van Velde, Luc L.T. Vertommen, Leo G.J. van der Ven, Ron M.A. Heeren and Oscar F. van den Brink, *Macromolecules* **2010**, *43*, 7082-7089.

Liquid chromatography-electrospray ionisation-tandem mass spectrometry (LC-ESI-MS^2) was employed for the characterisation of three poly (*n*-butyl acrylate)s. These polymers were produced at high temperature using the same initiator, tert-butyl peroxy-3,5,5-trimethylhexanoate, but in different solvents, *viz.* pentyl propionate, xylene and butyl acetate. Exact mass experiments performed on these polymers in an Orbitrap instrument supplied valuable information on the end group structures. Study of the data allowed identification of many reactions during the polymerisation such as β-scission and chain transfer to solvent or radical transfer to solvent from the initiator. Different fragmentation pathways were observed from the same precursor mass on MS^2 experiments, indicating the presence of isomers. The comprehensive assignment of the peaks in the LC-MS data allowed description of the end group distribution in a semi-quantitative way. The results clearly show that the solvent used for polymerisation has strong influences on the polymer compositions.

4.1 Introduction

Acrylic polymers serve a huge global market. Noted for their transparency and resistance to breakage, they have been widely used in coatings, in medical and recently also in pharmaceutical areas.[1-3] Radical polymerisation using peroxide initiators offers control of molecular weight and dispersity.[4] Recent developments on controlled/living radical polymerisations, such as ATRP, offer much better control of these variables.[5] However, only very limited number of commercially available products are produced in such way. Radical polymerisation is still used as a major industrial method to develop acrylic polymer products.

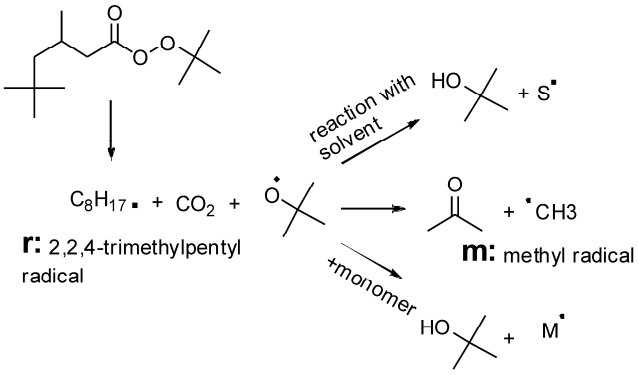

Scheme 4.1. Initiation mechanism for Trigonox 42S initiator.

The mechanism of radical polymerisation has been well-studied for many years. Three stages are involved in the polymerisation: initiation, chain propagation and chain termination. Scheme 4.1 shows the possible initiation species by the peroxide initiator (Trigonox 42S) which was used in this study. The many possibilities of initiation species will result in different end groups.[6] An octyl radical (C_8H_{17}•, r) is the major initiation species for this peroxide under the condition used here. The other part of the initiator, the butyloxyl radical, can undergo several possible reaction routes. One is to produce acetone and methyl radicals (CH_3•, m) that also start initiation. Second initiation route is to react with the solvent used in the polymerisation and transfer the radical to the solvent; the

solvent radical formed will then start the polymerisation. Another possible initiation route is to transfer the radical to monomer.

Radical polymerisation of alkyl acrylate at relatively high temperature introduces some specific initiation and termination mechanisms. An intramolecular chain transfer reaction, namely intramolecular backbiting, observed in many cases,[7-10] will increase the complexity of the end group distribution. The backbiting reaction forms a tertiary carbon-centered radical by hydrogen abstraction to a secondary carbon at the chain end or a tertiary carbon on the main chain. The carbon-centered radical formed undergoes β-scission to generate a β-scission radical and a terminally unsaturated chain. This mechanism is shown in Scheme 4.2. The chain that undergoes β-scission will therefore generate four oligomers through four pathways, namely β1a, β1b, β2a and β2b, which can be terminated in many different ways. The chain from pathway β1a is identical to the normal radical propagation species and could be terminated by hydrogen abstraction, combination or disproportionation. The other end of the chain, X as shown in Scheme 4.2, could be from the initiator radical or the solvent radical. Pathway β1b will generate a chain terminated by an unsaturated end group formed by β-scission at one side of the chain. Similarly, β2a will also form a terminally unsaturated chain but with the other side of chain with end group formed by either the initiator radical or the solvent radical. The last oligomer formed by β-scission pathway β2b can be terminated by hydrogen abstraction, as well as by combination or disproportionation. As stated in Scheme 4.2, these four routes will all form different end groups and result in different masses. The unique mass features are so distinctive that MS is a very suitable tool to recognise them. However, when the secondary carbon on the main chain is terminated by branching to form a 3-arm or a 4-arm star, the products formed in this pathway have identical mass to the linear structure and therefore cannot be distinguished by MS. Information on branching level could be obtained by ^{13}C NMR spectroscopy.[11] Furthermore, all the oligomer formed by β-scission could undergo further backbiting, β-scission or branching. The possibility however is very low in the low molecular weight fraction of the polymer. There is also evidence that chain transfer may not occur to the backbone but to the side chains.[12]

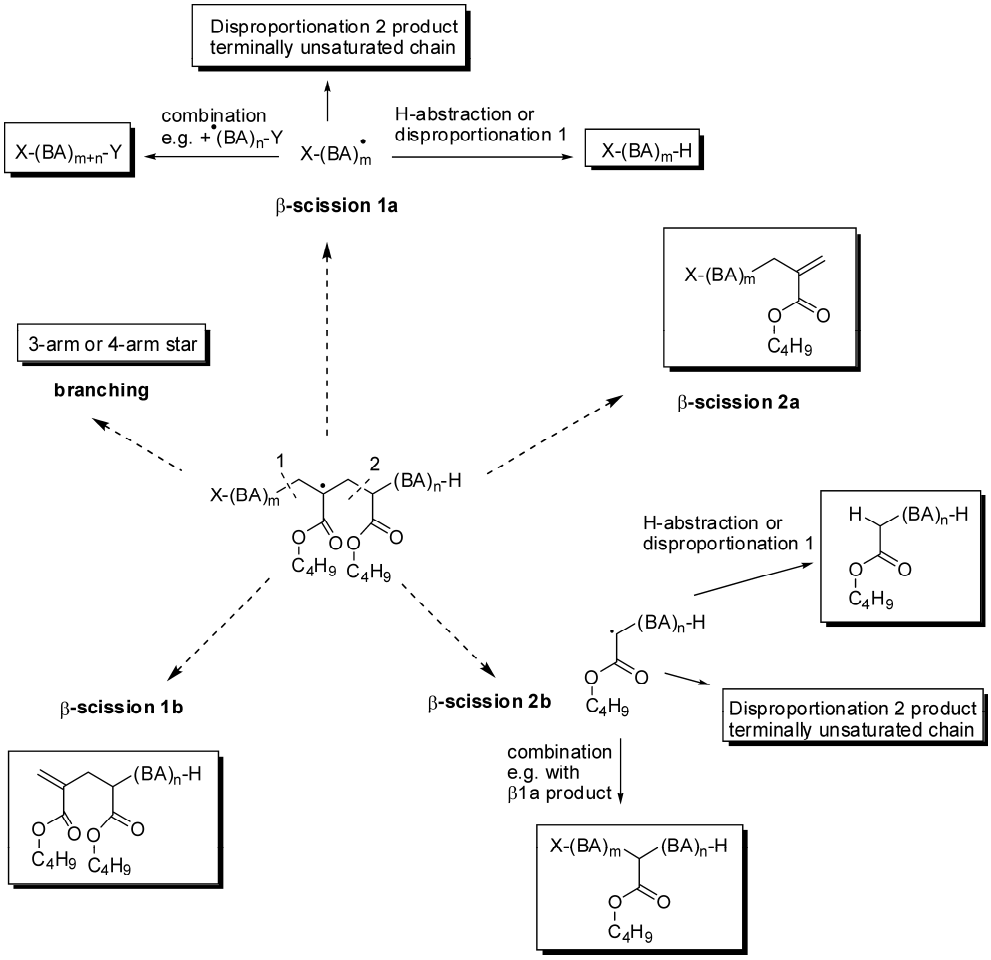

Scheme 4.2. β-scission of alkyl acrylate radical polymerisation at relatively high temperature.

In addition, chain transfer to solvent is also reported as a common reaction in radical polymerisation. The solvent effect was observed and investigated in several previous studies.[13-15] Scheme 4.3 shows the reactions of chain transfer to solvent in the cases investigated in this study. The solvent radicals shown in the scheme are the most likely structures formed under these conditions.

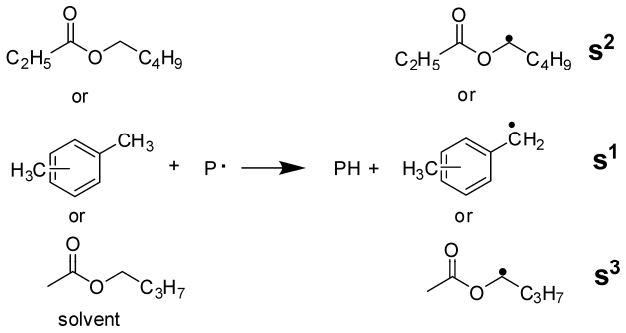

Scheme 4.3. Chain transfer to solvent in the cases of pentyl propionate, xylene and butyl acetate (P· = propagating chain).

Understanding the structure and quantity of the end groups is important information to have for polymer structure design and to control the physical or chemical properties. A great variety of techniques has been developed to determine the structural properties of polymers since their invention. The conventional technique to obtain the molecular weight and dispersity of polymers is gel-permeation chromatography (GPC),[16] Fourier-transform infrared (FTIR) spectroscopy and nuclear magnetic resonance spectroscopy (NMR) spectroscopy[17] are used to give structural information, while differential scanning calorimetry (DSC)[18] is used to determine the crystalline structure of polymers.

Over the last decade, the development of 'soft' ionisation methods such as electrospray ionisation (ESI) and matrix-assisted laser desorption/ionisation (MALDI)[19-28] allowed mass spectrometry to become an important tool for the characterisation of synthetic polymers. Characterisation of synthetic polymers of relatively high molecular weight can be achieved due to the formation of multiply charged ions generated by electrospray ionisation.[29] Information such as average molecular weight (in some cases) and polymer structures may be obtained.[30-33]

Furthermore, tandem mass spectrometry (MS/MS) has been employed to many synthetic polymer systems for structural studies. The very first MS/MS studies used magnetic sector instrumentation and date back to 1985.[34, 35] Many instruments for multistage mass spectrometry have been developed which perform MS/MS. Tandem MS/MS studies on synthetic polymers are commonly performed on tandem quadrupole-time-of-flight[36-38] and

ion trap[39-43] mass spectrometers. Collision-induced dissociation (CID)[36, 44] is the method used in most cases to fragment the selected precursor ions. The precursor ions are accelerated by electrical potential to high kinetic energy in the vacuum and then collide with neutral gas molecules. Part of the kinetic energy is converted into internal energy in the collision. This results in bond breakage and the fragmentation of the precursor ions. The fragment ions produced are used for partial or complete structural determination.

Junkers et al.[11] demonstrated using ESI-MS for detailed mapping of the product spectrum in acrylate polymerisation in order to obtain mechanistic information. In addition, research was performed on acrylic polymers synthesised by free radical polymerisation in the presence of chain transfer agent which used ESI-MS for quantification.[45] In this chapter, we went a step further to characterise three poly(n-butyl acrylate)s synthesised by free radical polymerisation using high resolution and high accuracy LC-ESI-MS^n. The PBAs were polymerised under high temperatures but in different solvents. The combined mass of the end groups of a polymer may be calculated from the high accuracy and resolution mass spectrometric data. MS^n spectra show different fragmentation patterns for the same nominal mass and thus allow discrimination between isomers deriving from different end groups. We utilised these different fragmentation patterns in an attempt to aid quantification of the different initiation and termination reactions during free radical polymerisation of PBA in the relatively lower molecular weight region of the spectra.

4.2 Experimental Section

4.2.1 Polymer Synthesis

All PBA samples were obtained from AkzoNobel Car Refinishes, Sassenheim, the Netherlands. They were prepared by radical polymerisation using the same initiator, tert-butyl peroxy-3,5,5-trimethylhexanoate, but different temperatures and solvents, viz. pentylpropionate (A), xylene (B) and butyl acetate (C). The molecular weight averages of the resultant PBA samples were measured by GPC calibrated with polystyrene standards.

Table 4.1 lists the composition, the process and the results obtained by GPC characterisation of the samples.

Table 4.1 Polymerisation Information of the Three PBAs[a]

Sample Code	A	B	C
Solvent	pentyl propionate	xylene	butyl acetate
M_n (g/mol)	2467	2800	3761
M_w (g/mol)	4757	5510	10186
Polymerisation Temperature (°C)	168	140	140

[a]Monomer used was butyl acrylate in all samples. Initiator used was tert-butyl peroxy-3 ,5, 5 trimethylhexanoate (Trigonox 42S).

4.2.2 Mass Spectrometry

Mass spectra were acquired by liquid chromatography-ESI-MS (LC-ESI-MS). A Thermo Scientific LTQ Orbitrap XL mass spectrometer was used in this study. The LC system was an Agilent 1100 series LC binary pump with DAD detector. The LC column in the LC-ESI-MS setup was an Alltech Kromasil C18 (150 mm * 4.6 mm). During analysis, the column temperature was thermostatised at 30 °C. A gradient of tetrahydrofuran (THF) (Sigma-Aldrich) / H_2O (from Millipore Direct-Q) was used as mobile phase. Formic acid (FA) (Fluka) at a level of 0.1% was added to both mobile phases. Samples with a concentration of 2 mg/ml in methanol were prepared. Data were processed and analysed using Thermo Scientific Xcalibur 2.0 data systems.

4.3 Results and Discussion

4.3.1 End Group Determination and Structure Assignment

LC separation was used prior to and online with MS. A wide range of gradients was tested to optimise the LC separation. The best separation of the PBA samples was achieved using gradient from 50% THF / 50 % H_2O to 100% THF in 30 minutes. All oligomers were

ionised by sodium ions, forming $[M+Na]^+$ species, presumably from residual sodium salts in the solvents. Figure 4.1 shows the summation mass spectra (1-18 minutes) of all three PBA samples from the ESI-Orbitrap LC-MS experiments. The combination of LC separation and summation over the separated peaks serves the purpose of mitigating or decreasing the effects of ion suppression that may occur when infusion analysis is used.

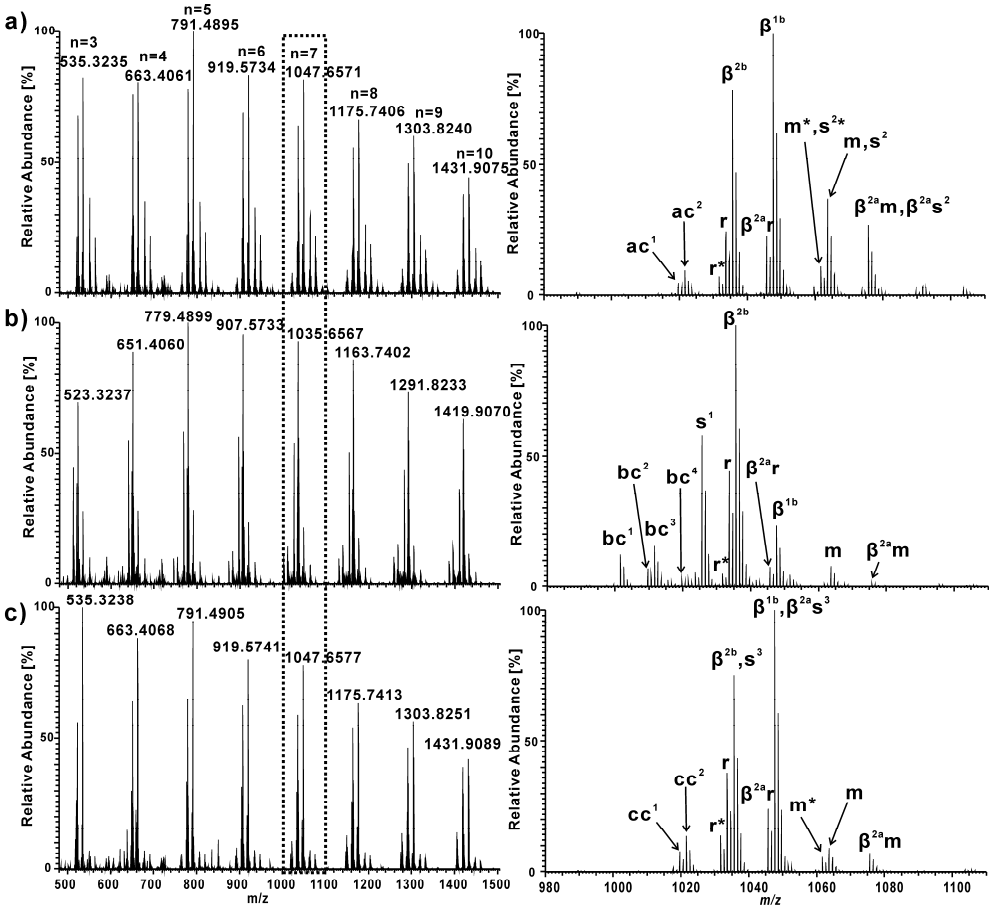

Figure 4.1. Left: Summation mass spectra (1'-18') of all three PBA samples on LC/ESI-Orbitrap MS; Right: Expanded spectra (*m/z* 980-1110) of the corresponding samples. The solvents used in the polymerisation were a) pentylpropionate, b) xylene and c) butyl acetate.

Based on the GPC data mentioned previously, the mass spectral data is only from a low molecular weight fraction of the full distribution. Several series of peaks start at *m/z* 513

continuing to greater than *m/z* 1448 with a separation of 128 Da between each group (the acquisition range of the MS was *m/z* 500 to 1500). The 128 Da separation between peaks is, clearly, attributed to the mass of BA, of which the molecular formula is $C_7H_{12}O_2$ and the theoretical exact mass is 128.0837 Da. Multiply charged peaks were observed with very low intensity and therefore not taken into consideration here. The summed LC-MS spectrum alone, however, was not sufficient to identify the different structures in the complicated product systems.

The many possible initiation and termination mechanisms yield a great number of potential combinations. In the spectra of all three PBA samples, one of the most intense and common set of peaks are those from series β^{2b}, *m/z* 523 + (n-3)*128, irrespective of the solvent used in polymerisation. The mass-to-charge ratios of eight peaks from this series in all three PBAs were plotted against the number of BA units, as shown in Figure 4.2 (only for PBA (C)).[46]

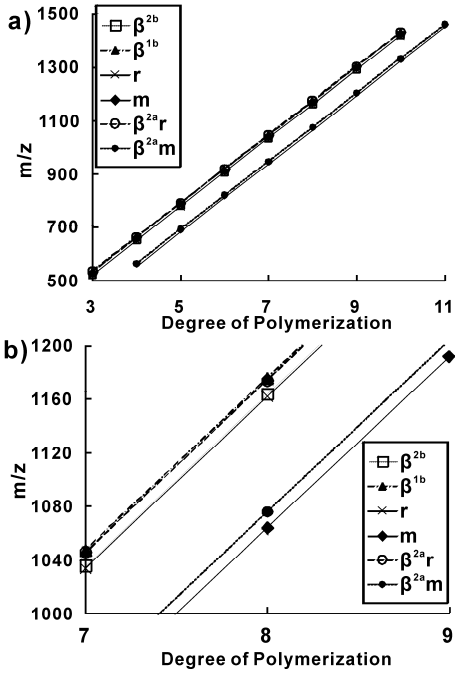

Figure 4.2. a) Linear regression of *m/z* peaks of several series from PBA (C). (m/z 500 – 1500, degree of polymerisation 3-11) b) Expanded area of a) (m/z 1000 – 1200, degree of polymerisation 7-9).

The residual masses were 139.0731 Da for PBA (A), 139.0734 Da for PBA (B) and 139.0733 Da for PBA (C), as calculated using linear regression. The monomer masses calculated were 128.0834 (Δ=2.34 ppm) for all three PBAs and the standard deviations were 0.56 ppm (A), 0.57 ppm (B) and 0.39 ppm (C). The chemical composition of the combined mass of the end groups is $[C_6H_{12}O_2]Na^+$. (Δ=0.72 ppm (A), 2.88 ppm (B) and 2.16 ppm (C)). It agrees well with the end group structure formed by an initiating β-scission radical (pathway β2b) and terminated by hydrogen abstraction or disproportionation. The structure of the chains in this series is shown in Scheme 4.4.

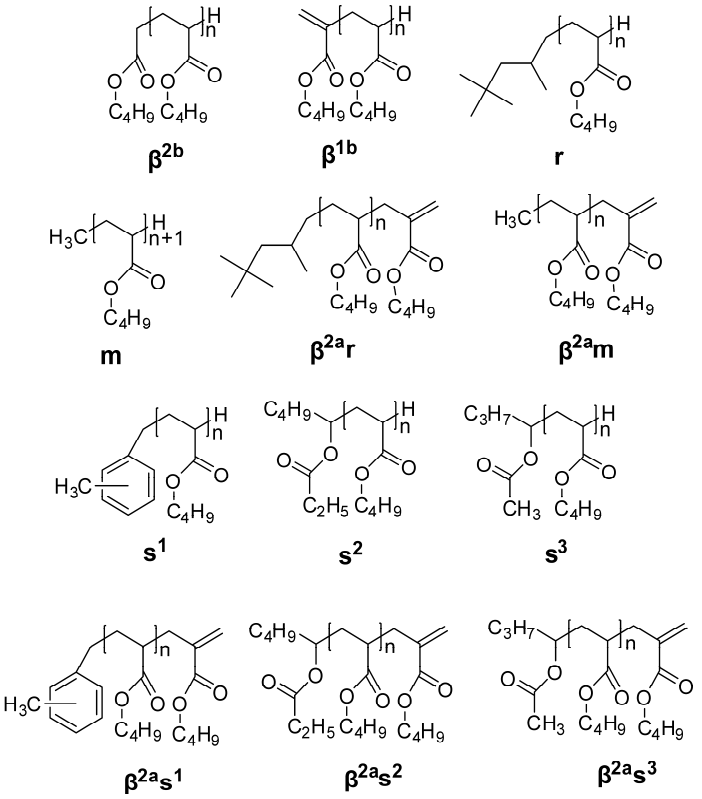

Scheme 4.4. Proposed structures of the end group combination series in polymers PBA (A-C).

Another very intense series of peaks in all three spectra is series β^{1b}, *m/z* 535+(n-3)*128. The same identification process as used for series β^{2b} was applied for this series. A residual

mass of 151.0724 Da was calculated using linear regression for all three PBAs. The elemental composition of this mass is proposed to be $[C_7H_{12}O_2]Na^+$ (Δ=4.0 ppm). The end group structure attributed to this series is the result of β1b, β-scission forming an unsaturated chain end. The proposed structure is given in Scheme 4.4. In this case, the errors of the experimental and theoretical BA mass are 0.78 ppm for PBA (A), (B) and 1.56 ppm for (C). The standard deviations are 0.34 ppm (A), 0.59 ppm (B) and 0.46 ppm (C).

Using this identification process, another end group combination was identified in all three PBAs resulting from 1) the radical initiator and terminated by either hydrogen abstraction or disproportionation; 2) β-scission pathway β1a and then terminated by either hydrogen abstraction or disproportionation. The two different pathways were indistinguishable because they result in identical elemental composition and structure. The series r, showing peaks at *m/z* 521+(n-3)*128 was found to have a residual mass of 137.1303 Da from PBA(A), 137.1297 Da from PBA(B) and 137.1303 Da from PBA(C). This mass is attributed to the combined end groups having elemental composition $[C_8H_{18}]Na^+$ (Δ=1.46 ppm for PBA(A) and (C), 2.92 ppm for PBA(B)). It indicates that the chain has an octyl end group from the peroxide initiator, formed as described in Scheme 4.1, and a hydrogen at the other end. The differences between the experimental and theoretical BA mass within the series are 1.56 ppm (A) and 0.78 ppm (B and C). The standard deviations were 0.25 ppm (A), 0.27 ppm (B) and 0.24 ppm (C). In a similar way, series m, *m/z* 551+(n-4)*128 with residual mass of 39.0211 Da from PBA (A), 39.0200 Da from PBA (B) and 39.0211 Da from PBA (C) was found to have $[CH_4]Na^+$ as end group composition (Δ=15.4 ppm (for A and C), 12.8 ppm (for B)). The molecules in this series are proposed to originate from initiation by a methyl radical from the peroxide initiator and termination by hydrogen abstraction or disproportionation; or from a methyl radical initiated chain undergoing β1a followed by termination through hydrogen abstraction or disproportionation (see Scheme 4.1 for the mechanism of methyl radical formation from the initiator). The differences between the experimental and theoretical BA mass are 0.78 ppm (A), 0.51 ppm (B) and 2.34 ppm (C). The standard deviations were 0.22 ppm (A), 0.34 ppm (B) and 0.41 ppm (C).

Two more series that are observed in all three PBA spectra are β^{2a}r and β^{2a}m. Both of the series result from β-scission pathway β2a, forming an unsaturated end group. The

difference between the two is that series β^{2a}r was octyl radical initiated and series β^{2a}m was methyl radical initiated. Both the octyl radical and the methyl radical were formed from the peroxide initiator (see Scheme 4.1). A comparison of the experimental data with the theoretical data for selected oligomers from PBA (C) is presented in Table 4.2.

Table 4.2. Comparison of experimental and theoretical mass for several peak series from PBA (C).

Monomeric Unit	3	4	5	6	7	8	9	10
β^{2b}	Standard deviation is 0.39 ppm							
$Mass_{exp}$(Da)	523.3238	651.4069	779.4905	907.5739	1035.6573	1163.7406	1291.8242	1419.9078
$Mass_{theo}$(Da)	523.3241	651.4079	779.4916	907.5753	1035.6591	1163.7428	1291.8265	1419.9102
Δ (ppm)	0.65	1.49	1.41	1.57	1.70	1.88	1.79	1.72
β^{1b}	Standard deviation is 0.34 ppm							
$Mass_{exp}$(Da)	535.3238	663.4068	791.4905	919.5739	1047.6577	1175.7416	1303.8251	1431.9092
$Mass_{theo}$(Da)	535.3241	663.4079	791.4916	919.5753	1047.6591	1175.7428	1303.8265	1431.9102
Δ (ppm)	0.63	1.61	1.39	1.34	1.30	1.01	1.09	0.73
r	Standard deviation is 0.25 ppm							
$Mass_{exp}$(Da)	521.3807	649.4645	777.5482	905.6317	1033.7152	1161.7988	1289.8826	1417.9653
$Mass_{theo}$(Da)	521.3813	649.4650	777.5487	905.6324	1033.7162	1161.7999	1289.8836	1417.9674
Δ (ppm)	1.08	0.75	0.67	0.83	0.95	0.95	0.80	1.46
m	Standard deviation is 0.22 ppm							
$Mass_{exp}$(Da)	-	551.3553	679.4391	807.5227	935.6063	1063.6899	1191.7736	1319.8573
$Mass_{theo}$(Da)	-	551.3554	679.4392	807.5229	935.6066	1063.6904	1191.7741	1319.8578
Δ (ppm)	-	0.25	0.10	0.25	0.35	0.43	0.41	0.39
β^{2a}r	Standard deviation is 0.53 ppm							
$Mass_{exp}$(Da)	533.3810	661.4647	789.5485	917.6326	1045.7162	1173.8002	1301.8842	1429.9689
$Mass_{theo}$(Da)	533.3813	661.4650	789.5487	917.6324	1045.7162	1173.7999	1301.8836	1429.9674
Δ (ppm)	0.56	0.45	0.25	-0.22	0	-0.26	-0.46	-1.05
β^{2a}m	Standard deviation is 0.06 ppm							
$Mass_{exp}$(Da)	-	563.3554	691.4392	819.5229	947.6067	1075.6906	1203.7747	1331.8586
$Mass_{theo}$(Da)	-	563.3554	691.4392	819.5229	947.6067	1075.6906	1203.7741	1331.8578
Δ (ppm)	-	0	0	0	0	0	-0.08	-0.15

There is a unique series, s^1, *m/z* 513+(n-3)*128, that is only observed in the spectrum of PBA(B), where xylene was used as the solvent. The residual mass calculated using linear regression is 129.0678 Da. The elemental composition of the residual mass is $[C_8H_{10}]Na^+$ (Δ=2.32 ppm). It is assigned as arising from chain transfer to solvent or radical transfer from initiator to solvent. A xylol radical is formed when a growing polymer chain abstracts hydrogen from a methyl group in the xylene solvent (Scheme 4.3). As mentioned in the introduction, another mechanism for the formation of a xylol radical could be the abstraction of a hydrogen by an initiator radical. The structural formula of the ion noted from the data is $[C_8H_9\text{-}(BA)_n\text{-}H]Na^+$. The difference between the experimental and theoretical BA mass is 1.56 ppm and the standard deviation of the experimental mass is 0.52 ppm.

4.3.2 LC-MS^2 of Isomer Discrimination

Since all three PBA samples were polymerised under similar conditions, it is expected that chain transfer to solvent or solvent radical initiation has taken place in each of the polymerisations, especially as the solvents used there are prone to this phenomenon. Calculation of the masses of PBA oligomers with end groups resulting from solvent radical formation by initiator radical transfer to solvent or chain transfer to solvent, and then terminated by either hydrogen abstraction or disproportionation indicated that they would overlap with series m and series β^{2b}, in PBA(A) (from pentyl propionate) and PBA(C) (from butyl acetate) respectively, as they have the same elemental composition.

LC coupled with multistage mass spectrometry, when set up properly, can discriminate between isomers with exact same mass by producing different fragments. Therefore, LC-MS^2 experiments were performed to obtain fragmentation information and thus investigate the presence of structural isomers with different end group structures.

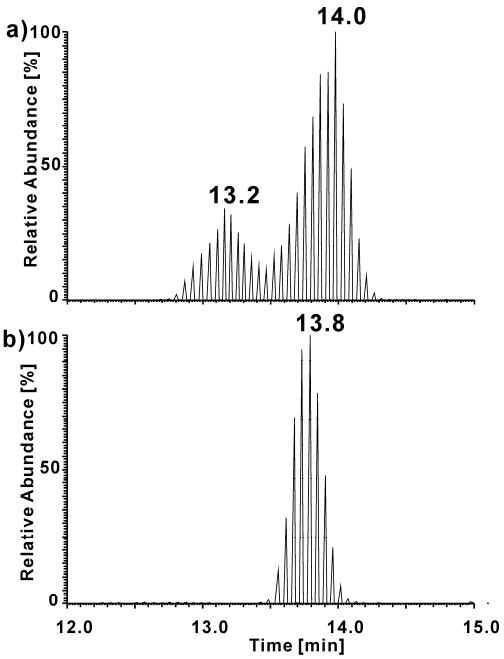

Figure 4.3. Partial (12' – 15') EIC traces for *m/z* 935.6 for a) PBA (A) (polymerised in pentyl propionate) and b) PBA (B) (polymerised in xylene) on LC-Orbitrap MS.

Figure 4.3 shows the LC traces (extracted ion count chromatogram, EIC) of *m/z* 935.61 for PBA(A) (polymerised in pentyl propionate) and PBA(B) (polymerised in xylene). Automatic MS^2 was engaged throughout the whole separation. This procedure performs MS/MS of every base peak in the individual MS spectra throughout the entire LC experiment. Only one LC elution peak was observed for PBA(B). Figure 4.4 shows the partial LC-MS^2 spectra of *m/z* 935.6100 (PBA(A) and PBA(B)) obtained in the Orbitrap instrument.

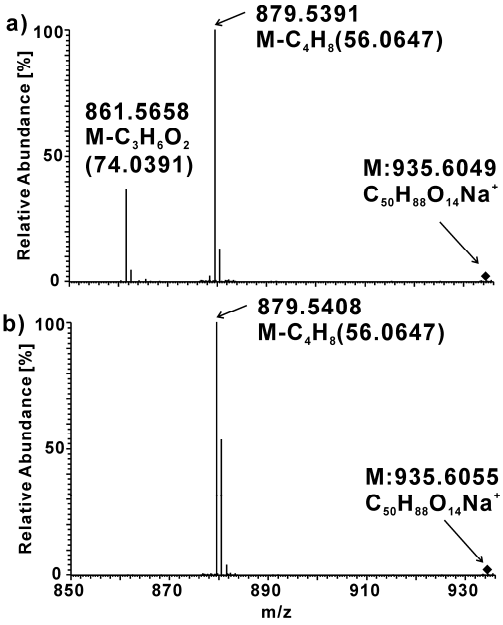

Figure 4.4. Partial LC – MS^2 spectrum of a) *m/z* 935.6049 (PBA(A)) and b) 935.6055 (PBA(B)) obtained on Orbitrap instrument.

A single fragmentation pathway was observed producing a peak at *m/z* 879.54 in the LC-MS^2 spectrum of PBA(B). The pathway involves a loss of *m/z* 56 (C_4H_8) from the side chain of the PBA, indicating that no backbone cleavage happened during the fragmentation process. But from the chromatogram of PBA(A), two LC peaks were observed at 13.2 minutes and 14.0 minutes. A loss of *m/z* 74 in addition to the *m/z* 56 loss was observed in the combined spectra summed across the whole LC chromatogram. Judging from the corresponding elution time, we propose this additional loss is from the polymer eluting at

13.2 minutes. The elemental composition of *m/z* 74 could either be $C_4H_{10}O$ or $C_3H_6O_2$. The LC-MS/MS data from the Orbitrap analysis showed that the accurate mass of this loss is *m/z* 74.0391 which agrees well with the exact mass of $C_3H_6O_2$ (*m/z* 74.0368) rather than $C_4H_{10}O$ (*m/z* 74.0732). In the spectra of PBA(A), the two different fragmentation pathways as well as the two LC peaks in the EIC of *m/z* 935.6100 prove that two isomers exist at this identical exact mass. Series s^2, which exclusively displays the loss of *m/z* 74, therefore results from chain transfer to the pentyl propionate solvent (or the pathway β1a). In this case, the molecular formula for *m/z* 935.6100 is $[C_8H_{15}O_2\text{-}(BA)_3\text{-}H]Na^+$. Scheme 4.5 plots the proposed fragmentation pathway, involving the loss of propanoic acid from the end of the polymer chain (from the initiation of the chain by the radical originating from the pentyl propionate solvent) that gives rise to the peak at *m/z* 861.5658. The same fragmentation pathway was observed in the spectra from Series $\beta^{2a}s^2$ resulting from β-scission pathway β2a.

Two similar cases, series s^3 and $\beta^{2a}s^3$, were identified as overlapping with series β^{2b} and series β^{1b} respectively in PBA(C) using LC-MS/MS. In both series (s^3 and $\beta^{2a}s^3$) a loss of *m/z* 60 (acetic acid) from the end of the polymer chain (resulting from the initiation by the butyl acetate solvent radical) was observed in MS/MS in addition to the *m/z* 56 side chain loss. The fragmentation mechanism is analogous to the one described in Scheme 4.5. The difference between series s^3 and series $\beta^{2a}s^3$ is that the former resulted from pathway β1a (or chain transfer to solvent) and the latter from the pathway β2a. An alternative to the high mass resolution approach described in this paper would be the use of ion mobility spectroscopy (IMS)/MS to separate the different structural isomers in the gas phase[47, 48]. This could also help differentiate between linear and branched oligomers of PBA.

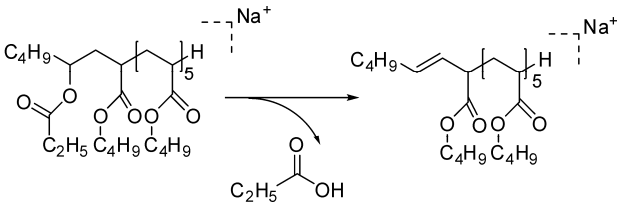

Scheme 4.5. Proposed fragmentation of $[C_8H_{15}O_2\text{-}(BA)_6\text{-}H+Na]^+$ (*m/z* 935) from PBA(A).

Unsaturated terminated species formed by disproportionation were observed in the spectra of all three PBAs with relatively low intensities. For example, for series r*, *m/z* 519+(n-3)*128, the residual mass calculated is 135.1138. Hence, the elemental composition is $[C_8H_{16}]Na^+$ (Δ = 4.44 ppm). The difference between the experimental and theoretical BA mass is 1.56 ppm and the standard deviation is 0.35 ppm. The disproportionation termination resulted in an unsaturated end group at one side of the polymer while the original initiation species sit on the other side. In the spectra, we could easily notice the mass difference of *m/z* 2.0157 (two hydrogens) with respect to the normal terminated chain. This mass difference is consistent for series r and r* (The average error is 0.7 mDa and the standard deviation is 0.5 mDa). Similar cases found in the spectra were, for example, series m* and β^{2a}r*.

4.3.3 Isobaric Materials Discrimination

The high accuracy and resolution data from the Orbitrap instrument also allow us to observe some less intense series of peaks that have *m/z* very close to the more intense series of peaks already discussed, which normally cannot be discriminated using mass spectrometers with relatively low accuracy and resolution (such as standard ion trap instruments). Figure 4.5 shows two peaks with 0.072 Da difference in PBA(B), generally pointing at exchange of O_2 against C_2H_8 in elemental composition.

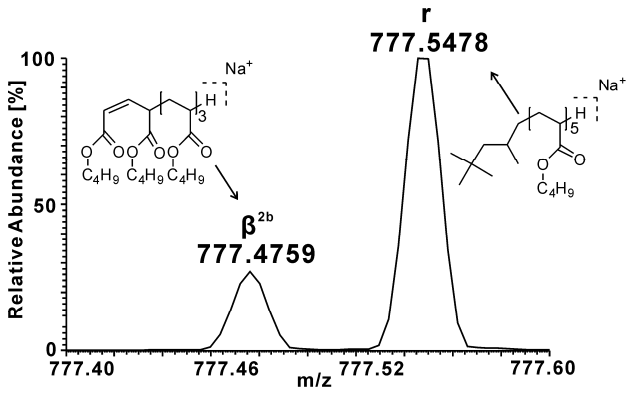

Figure 4.5. Expanded Orbitrap MS summation spectrum for PBA(B) (777.4000-777.6000)

The second peak with a mass of *m/z* 777.5478 is from series r (Δ = 1.29 ppm). Through calculation, the elemental composition of the ion at *m/z* 777.4759 is assigned to $C_{41}H_{70}O_{12}$ (Δ = 0.03 ppm). The structure of this oligomer is proposed to result from the β-scission pathway β2b combined with termination by disproportionation. The resulting structure is shown in Figure 4.5. The series is labeled as β^{2b}*. This lower intensity peak would not be observed with low resolution mass spectrometry since the peak would merge with the very intense neighboring peak. The high accuracy and resolution mass spectrometry allowed its detection.

Similarly, another series with low abundance was located in PBA(B), labeled as series $\beta^{2a}s^1$. We propose it to result from xylol radical initiated chain and terminated by β-scission pathway β2a. The theoretical combined end group mass of the series is *m/z* 141.0675 which is isobaric with the second isotopic peak (with two ^{13}C atoms) of series β^{2b} (141.0797). Unfortunately, only the first two peaks (trimer and tetramer) in the series were resolved. The peak observed at *m/z* 781.4913 in the spectra, where the pentamer would be expected, has a broader peak shape and does not allow the identification of the pentamer from series $\beta^{2a}s^1$. The required resolution at the pentamer (*m/z* 781.4861 $\beta^{2a}s^1$ and *m/z* 781.4983 β^{2b}) to distinguish these two peaks would be 64,000, which would require an instrument with even higher resolving power than the Orbitrap, such as FT-ICR MS. Moreover, the intensity of the second isotopic peak is also higher than the normal isotope pattern from series β^{2b} in PBA(A) and PBA(C).

4.3.4 Insight to Polymerisation Mechanisms

Evidence of the polymer chain terminated by combination was observed in the relatively low molecular weight region only at very low intensity. However, the intensity of the peaks of the same series increases when the degree of polymerisation increases in all three PBAs. It is expected that termination by combination has a higher possibility to generate a longer chain rather than a short oligomer. In the expanded spectra of Figure 4.1, the peaks labeled with ac^1 and ac^2 in PBA(A), bc^1-bc^4 in PBA(B) and cc^1 and cc^2 in PBA(C) are all terminated by combination. As shown in Scheme 4.2, two types of combinations could

happen in this polymerisation system, 1) two chains both undergoing β1a and/or from standard initiation or chain transfer from solvent (as the structure is the same for these two species) and 2) one chain undergoing β1a and/or standard initiated or chain transfer to solvent initiated chain and the other undergoing β2b. Moreover, the resulting products from combination may have a large variety of combined end groups from the two initiator radicals and the solvent radicals. However, not every combination was observed in the spectra. For example, in the case of PBA(B), peaks in series bc^1 and bc^2 were formed by the combination of two chains both undergoing β1a and/or from standard initiation or chain transfer from solvent (bc^1: xylol endgroup at both ends; bc^2: xylol endgroup at one end and octyl endgroup at the other). Those in series bc^3 and bc^4 were formed by the combination of one chain undergoing β1a and/or from standard initiation or chain transfer from solvent and the other undergoing β2b (bc^4: xylol endgroup at both ends; bc^4: xylol endgroup at one end and octyl endgroup at the other). In PBA(A) and (C), some of these combinations resulted in peaks that have mass-to-charge ratios too close to the most intense peaks and hence not all of them are resolved. No combination with methyl or butyloxyl end-capped chains was observed in the spectra of any of the three PBAs.

Scheme 4.4 shows the proposed structures (without the cation adduct) for all major peak series identified in the ESI-MS spectra of PBA(A), PBA(B) and PBA(C). The corresponding series from disproportionation or combination are not presented. Table 4.3 lists the combinations of initiation and termination mechanisms of these series and their corresponding combined end group masses. (Structural illustrations are presented in Appendix 1.)

Butyloxyl radical initiated chains were not observed in the spectra. This is attributed to this radical mainly contributing to the formation of methyl radicals and/or to radical transfer to solvent. The radical itself is also not large enough[6] to undergo a 1,5-H-shift reaction and then start an intramolecular chain-transfer reaction.

Table 4.3. Possible initiation and termination mechanisms in the radical polymerisation of PBA(A-C) and their resulting combined end group masses. The corresponding mass in the termination column includes a sodium adduct. Observed series are listed in parentheses in the corresponding position.

Initiation (or chain transfer to solvent) / Termination (except combination)	Initiator			Solvent			Resulting from β-scission
	Octyl radical	Butyloxyl radical	Methyl radical	Pentyl propionat eradical	Xylene radical	Butyl acetate radical	
	113.1330	73.0653	15.0235	143.1072	105.0704	115.0759	
H-abstraction or disproportionation 1, β1a then H-abstraction or disproportionation 1 (23.9970)	137.1301 (r)	97.0624	39.0205 (m)	167.1043 (s^2)	129.0675 (s^1)	139.0730 (s^3)	-
Disproportionation to form unsaturated chain (21.9814)	135.1144 (r*)	95.0467	37.0049 (m*)	165.0886 (s^2*)	127.0518 (s^1*)	137.0573 (s^3*)	-
β2a (35.9970)	149.1301 (β^{2a}r)	109.0624	51.0205 (β^{2a}m)	179.1043 (β^{2a} s^2)	141.0675 β^{2a} s^1)	151.0730 $\beta^{2a}s^3$	-
β1b (151.0730)	-	-	-	-	-	-	151.0730 (β^{1b})
β2b then H-abstraction (139.0730)	-	-	-	-	-	-	139.0730 (β^{2b})
β2b then disproportionation (137.0573)	-	-	-	-	-	-	137.0573 (β^{2b}*)

4.3.5 Semi-quantitative Study

ESI-MS is not a fully quantitative method. It can still be used in a semi-quantitative way to address the amount of polymer initiated or terminated by different mechanisms, especially at higher degrees of polymerisation[45] (this is because any differences in end group structures should play a smaller role in the ionisation mechanism, presuming that the cation used binds with the oxygens in the ester of the main chain predominantly, as may be indicated by previous results from other acrylic polymers[49]).

The graph in Figure 4.6 was derived from the LC-ESI-MS data by summation of the peak intensities of the respective end group combinations in PBA(B) (from xylene). Series $\beta^{2a}s^1$ was not taken into consideration because the oligomers in this series that are larger than the tetramer could not be resolved from the second isotopic peaks in series β^{2b}. The calculation in Figure 4.6 was derived from the LC-ESI-MS data by summation of the peak intensities of the respective end group combinations in PBA(B) (from xylene).

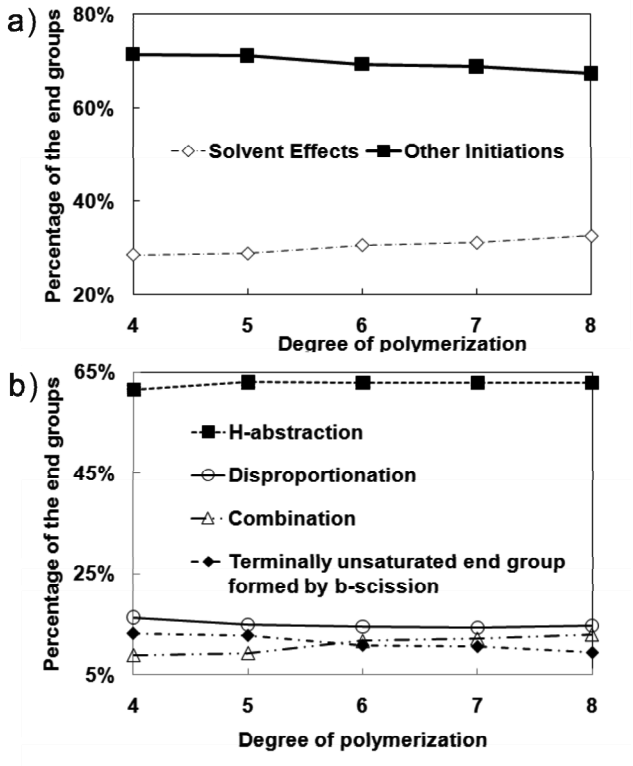

Figure 4.6. Comparison of the percentages (relative intensity) of PBA(B) with end groups formed from different a) initiation and b) termination mechanisms. Data derived from summing the respective peak intensities in LC-ESI-Orbitrap data.

Table 4.4 shows the intensities of the respective end groups for the tetramer. In the first column, 'H' means H-abstraction; 'D1' means disproportionation to form an identical end group as H-abstraction; 'D2' denotes disproportionation to form an unsaturated end group; 'C' denotes combination.

The total intensity of the peaks observed can be obtained by summing all the intensities in Table 4.4 minus table coordinates (X4,Y1). The peak is double counted in (X4,Y1) and (X3,Y3) because they are the same products. The percentage of end group influenced by solvent effects and other initiations were calculated through the equations shown on next page.

Table 4.4.The intensities of the respective end groups for a tetramer in PBA(B).

	Y1 octyl radical	Y2 methyl radical	Y3 xylene radical	Y4
X1 β1a then H or D1	196947.8	44941.2	248577.4	-
X2 β1a then D2	19804.2	4831.5	19155.1	-
X3 β1a then C (end group=octyl)	-	-	20023.2	-
X4 β1a then C (end group=methyl)	20023.2	-	43641.2	-
X5 β1b	-	-	-	127294.6
X6 β2a	33921.3	7930	-	-
X7 β2b then H or D1	-	-	-	405298.9
X8 β2b then D2	-	-	-	61145.6
X9 β2b then C (with chain from β1a then C)	4895.2	-	45576.2	-

$$\text{Solvent effects} = \frac{(X1,Y3)+(X2,Y3)+(X3,Y3)+(X4,Y3)+(X9,Y3)}{Total\ Intensity}\times 100\% \qquad \text{(Eq. 4.1)}$$

Other initiations = 1-Solvent effects (Eq. 4.2)

The percentages of endgroup terminated by H-abstraction, disproportionation, combination and (β1b+β2a) were calculated through the following equations:

$$\text{Disproportionation} = \frac{((X2,Y1)+(X2,Y2)+(X2,Y3)+(X8,Y4))\times 2}{Total\ Intensity}\times 100\% \qquad \text{(Eq. 4.3)}$$

$$\text{H-abstraction} = \frac{(X1,Y1)+(X1,Y2)+(X1,Y3)+(X7,Y4)-Disproportionation/2}{Total\ Intensity}\times 100\% \qquad \text{(Eq. 4.4)}$$

$$\text{Combination} = [(\frac{(X4,Y1)+(X4,Y3)+(X9,Y1)+(X9,Y3)}{Total\ Intensity}\times 100\% \qquad \text{(Eq. 4.5)}$$

Terminally unsaturated endgroup formed by (β1b+β2a)

$$= \frac{(X4,Y1)+(X4,Y3)+(X9,Y1)+(X9,Y3)}{Total\ Intensity}\times 100\% \qquad \text{(Eq. 4.6)}$$

As suggested earlier, the data generally shows an increasing amount of end groups formed by combination of chains when the degree of polymerisation increases. In the case of the radical polymerisation of PBA in xylene, these data indicate that more than 30% of the chains were formed by the influence of solvent, either from initiator radical transfer to

xylene or chain transfer to xylene. Hydrogen-abstraction is the main termination contributing 60% to the end group formed. Disproportionation is less frequently observed than hydrogen-abstraction and only contributes a modest 15% to the polymerisation. Combination contributed 9% to the end group in the case of tetramer and the influence increased to 13% in octamer. The amount of chains with terminally unsaturated end group formed by two different β-scission pathways β1b and β2a is 13% for tetramer and decreases with the degree of polymerisation, dropping to 9% for octamer. In the cases of PBA (A) and (C), the existence of isomers originating from different initiation and termination mechanisms makes the quantitative study rather difficult to perform.

The β-scission reaction is theoretically not favored to happen to one specific side[11]. Therefore, the ratio of the products generated through β1b and β2a should be 1:1. However, it's difficult to calculate from the data we have since the intensity of peaks in series $\beta^{2a}s^1$ cannot be taken in consideration. The peaks in this series are not resolved as mentioned previously. Without the data from series $\beta^{2a}s^1$ (peaks in the series were generated from β2a), pathway β1b shows a relatively higher influence than β2a. The cause of this proposed difference in abundance is unclear, from the proposed mechanism (Scheme 4.2).

4.4 Conclusions

LC-ESI MS^2 of the three PBA samples identified many initiation and termination reactions during the polymerisation, including peroxide initiator initiation, solvent radical initiation or chain transfer to solvent, four different β-scission pathways, H-abstraction, disproportionation and combination. The combination of these mechanisms generated a great variety of end groups for these polymers which were all identified by using high resolution LC-MS, although some of the series were not resolved at higher degrees of polymerisation. Multistage MS showed different fragmentations for peaks that had identical exact mass but different elution times. Isomers were observed that originated from different initiation mechanisms. The high accuracy and resolution MS spectra obtained

using the Orbitrap allowed discrimination of two isobars with 0.072 Da mass difference which could easily be overlooked in normal low mass accuracy and resolution MS. The comprehensive attribution of the peaks in the LC-MS data allowed us to address the end group distribution in a semi-quantitative way for one of the polymers studied. Although the data do not allow semi-quantitative comparison of the various initiation and termination mechanisms in all three PBAs, the results clearly show that the solvent used for polymerisation strongly influences the polymer compositions.

References

(1) Drin, A. P.; Efanova, V. V.; Shut, N. I. *Journal of Engineering Physics and Thermophysics* **1994,** *66*, 164-171.
(2) Okor, R. S. *J. Controlled Release* **1990,** *12*, 195-200.
(3) Chen, R. G.; Wu, S. H. Process for the preparation of crylic polymers for pharmaceutical coatings. US Patent 5380790, 1995.
(4) Capek, I.; Potisk, P. *Eur. Polym. J.* **1995,** *31*, 1269-1277.
(5) Matyjaszewski, K.; Xia, J. *Chem. Rev.* **2001,** *101*, 2921-2990.
(6) Buback, M.; Frauendorf, H.; Gunzler, F.; Vana, P. *J. Polym. Sci., Part A: Polym. Chem.* **2007,** *45*, 2453-2467.
(7) van Herk, A. M. *Macromol. Rapid Commun.* **2001,** *22*, 687-689.
(8) Subrahmanyam, B.; Baruah, S. D.; Rahman, M.; Baruah, J. N.; Dass, N. N. *J. Polym. Sci., Part A: Polym. Chem.* **1992,** *30*, 2531-2549.
(9) Quan, C.; Soroush, M.; Grady, M. C.; Hansen, J. E.; Simonsick, W. J. *Macromolecules* **2005,** *38*, 7619-7628.
(10) Junkers, T.; Barner-Kowollik, C. *J. Polym. Sci., Part A: Polym. Chem.* **2008,** *46*, 7585-7605.
(11) Junkers, T.; Koo, S. P. S.; Davis, T. P.; Stenzel, M. H.; Barner-Kowollik, C. *Macromolecules* **2007,** *40*, 8906-8912.
(12) Pugh, C.; Fan, G.; Kasko, A. M. *Macromolecules* **2005,** *38*, 8071-8077.
(13) Jovanovic, R.; Dubé, M. A. *J. Appl. Polym. Sci.* **2001,** *82*, 2958-2977.
(14) Jovanovic, R.; Dubé, M. A. *J. Appl. Polym. Sci.* **2004,** *94*, 871-876.
(15) Mckenna, T. F.; Villanueva, A.; Santos, A. M. *J. Polym. Sci., Part A: Polym. Chem.* **1999,** *37*, 571-588.
(16) Hammond, J. M.; Hooper, J. F.; Stutchbury, J. E. *Journal of Polymer Science: Polymer Symposia* **1975,** *49*, 117-125.
(17) Cheng, H. N.; Early, T. A. *Macromol. Symp.* **1994,** *86*, 1-14.
(18) Taniguchi, S.-i.; Takeshita, H.; Arimoto, M.; Miya, M.; Takenaka, K.; Shiomi, T. *Polymer* **2008,** *49*, 4889-4898.
(19) Whitehouse, C. M.; Dreyer, R. N.; Yamashita, M.; Fenn, J. B. *Anal. Chem.* **1985,** *57*, 675-679.
(20) Fenn, J. B.; Mann, M.; Meng, C. K.; Wong, S. F.; Whitehouse, C. M. *Science* **1989,** *246*, 64-71.

(21) Karas, M.; Bachmann, D.; Bahr, U.; Hillenkamp, F. *Int. J. Mass Spectrom. Ion Processes* **1987,** *78*, 53-68.
(22) Karas, M.; Hillenkamp, F. *Anal. Chem.* **1988,** *60*, 2299-2301.
(23) Nielen, M. W. F. *Mass Spectrom. Rev.* **1999,** *18*, 309-344.
(24) Peacock, P. M.; McEwen, C. N. *Anal. Chem.* **2004,** *76*, 3417-3428.
(25) Hanton, S. D. *Chem. Rev.* **2001,** *101*, 527-570.
(26) Scrivens, J. H.; Jackson, A. T. *Int. J. Mass Spectrom.* **2000,** *200*, 261-276.
(27) McEwen, C. N.; Peacock, P. M. *Anal. Chem.* **2002,** *74*, 2743-2748.
(28) van Rooij, G. J.; Duursma, M. C.; Heeren, R. M. A.; Boon, J. J.; de Koster, C. G. *J. Am. Soc. Mass Spectrom.* **1996,** *7*, 449-457.
(29) Kallos, G. J.; Tomalia, D. A.; Hedstrand, D. M.; Lewis, S.; Zhou, J. *Rapid Commun. Mass Spectrom.* **1991,** *5*, 383-386.
(30) Montaudo, G.; Montaudo, M. S.; Puglisi, C.; Samperi, F. *Macromolecules* **1995,** *28*, 4562-4569.
(31) Schriemer, D. C.; Li, L. *Anal. Chem.* **1997,** *69*, 4169-4175.
(32) Schriemer, D. C.; Li, L. *Anal. Chem.* **1997,** *69*, 4176-4183.
(33) Gruendling, T.; Guilhaus, M.; Barner-Kowollik, C. *Macromolecules* **2009,** *42*, 6366-6374.
(34) Craig, A. G.; Derrick, P. J. *J. Am. Chem. Soc.* **1985,** *107*, 6707-6708.
(35) Craig, A. G.; Derrick, P. J. *Journal of the Chemical Society. Chemical Communications* **1985,** *13*, 891.
(36) Jackson, A. T.; Scrivens, J. H.; Williams, J. P.; Baker, E. S.; Gidden, J.; Bowers, M. T. *Int. J. Mass Spectrom.* **2004,** *238*, 287-297.
(37) Jackson, A. T.; Slade, S. E.; Scrivens, J. H. *Int. J. Mass Spectrom.* **2004,** *238*, 265-277.
(38) Jackson, A. T.; Slade, S. E.; Thalassinos, K.; Scrivens, J. H. *Anal. Bioanal. Chem.* **2008,** *392*, 643-650.
(39) Chen, R.; Li, L. *J. Am. Soc. Mass Spectrom.* **2001,** *12*, 832-839.
(40) Chen, R.; Yu, X.; Li, L. *J. Am. Soc. Mass Spectrom.* **2002,** *13*, 888-897.
(41) Arnould, M. A.; Wesdemiotis, C.; Geiger, R. J.; Park, M. E.; Buehner, R. W.; Vanderorst, D. *Prog. Org. Coat.* **2002,** *45*, 305-312.
(42) Wollyung, K. M.; Wesdemiotis, C.; Nagy, A.; Kennedy, J. P. *J. Polym. Sci., Part A: Polym. Chem.* **2005,** *43*, 946-958.
(43) Cerda, B. A.; Horn, D. M.; Breuker, K.; McLafferty, F. W. *J. Am. Chem. Soc.* **2002,** *124*, 9287-9291.
(44) Chaicharoen, K.; Polce, M.; Singh, A.; Pugh, C.; Wesdemiotis, C. *Anal. Bioanal. Chem.* **2008,** *392*, 595-607.
(45) Koo, S. P. S.; Junkers, T.; Barner-Kowollik, C. *Macromolecules* **2008,** *42*, 62-69.
(46) Koster, S.; Duursma, M. C.; Boon, J. J.; Heeren, R. M. A. *J. Am. Soc. Mass Spectrom.* **2000,** *11*, 536-543.
(47) Baker, E. S.; Gidden, J.; Anderson, S. E.; Haddad, T. S.; Bowers, M. T. *Nano Lett.* **2004,** *4*, 779-785.
(48) Trimpin, S.; Clemmer, D. E. *Anal. Chem.* **2008,** *80*, 9073-9083.
(49) Gidden, J.; Jackson, A. T.; Scrivens, J. H.; Bowers, M. T. *Int. J. Mass Spectrom.* **1999,** *188*, 121-130.

5

End-group Analysis of Acrylic (co)Polymers by LC-ESI-MS/MS

This chapter is based on, Junkan Song, Jan W. van Velde, Luc L.T. Vertommen, Donald F. Smith, Ron M.A. Heeren and Oscar F. van den Brink, **Submitted.**

End-group analysis was achieved on poly(methyl methacrylate) and poly(methyl metacrylate-*r*-butyl acrylate) by liquid chromatography-electrospray ionization-ion trap mass spectrometry (LC-ESI-IT MS) and electrospray ionization-fourier transform ion cyclotron resonance tandem mass spectrometry (ESI-FTICR MS^2). The two polymers were produced by radical polymerization in butyl acetate at relatively high temperature using the same initiator, tert-butyl peroxy-3,5,5-trimethylhexanoate. In both polymers, structures with different end groups were successfully assigned using gradient elution LC-IT MS, with the aid of exact mass experiments on an FTICR MS instrument. Isobaric materials in PMMA were discriminated using accurate mass FTICR MS^2. Isocratic LC-MS reduced the complexity of the spectra of P(MMA-*r*-BA), facilitated easier attribution of peaks and shortened the experimental time.

5.1 Introduction

The demand of copolymeric materials in daily life has been growing in the past decades. Many new copolymers have been developed to meet the consumer and industry needs.[1-3] Numbers of new polymerization techniques have been invented to serve the purpose of synthesizing polymers with more complicated and targeted structures. Controlled/living radical polymerization[4] such as stable free radical polymerization (SFRP),[5] atom transfer radical polymerization (ATRP)[6] and reversible addition-fragmentation chain transfer polymerization (RAFT)[7] are the best examples of the newly developed polymerization methods.

Amongst all polymerization methods, free radical polymerization is one of the very often used methods to synthesize polymers in industry. Peroxide initiation has been intensively studied using various methods in the past.[8] Three stages are involved in the polymerization: initiation, chain propagation and chain termination. A detailed scheme of the initiation mechanism can be found in Chapter 4. Basically, for the initiator Trigonox 42S used in this study, octyl radicals (C_8H_{17}•, r), and methyl radicals (CH_3•, m) were produced to start the polymerization. Under the conditions applied, radical transfer to solvent or monomer can also occur and start the polymerization.[9] The many possibilities of initiation species will result in a variety of end groups.

High-temperature radical polymerization introduces some specific initiation and termination mechanisms. An intramolecular chain transfer reaction, namely intramolecular backbiting, observed in many cases,[10-14] will increase the complexity of the end group distribution. The backbiting reaction forms a tertiary carbon-centered radical by hydrogen abstraction to a secondary carbon at the chain end or a tertiary carbon on the main chain. The carbon-centered radical formed undergoes β-scission to generate a β-scission radical and a terminally unsaturated chain. The mechanism of β-scission of a PMMA chain is shown in Scheme 5.1. Two β-scission routes are possible that can happen on either side of the molecule and therefore generate four different structures. Route I will produce two molecules with identical structures as a normal propagating chain and a terminally unsaturated chain generated by disproportionation. Route II, on the other hand, will produce two molecules, one having a CH_2 group more in the backbone (β^1) and the other

having one CH_2 less in the backbone (β^2). A similar mechanism on a PBA chain was presented in a previous study.[9] As a consequence, four oligomers (β^{1a}, β^{1b}, β^{2a} and β^{2b}) will be generated through four pathways, which can be terminated in many different ways.

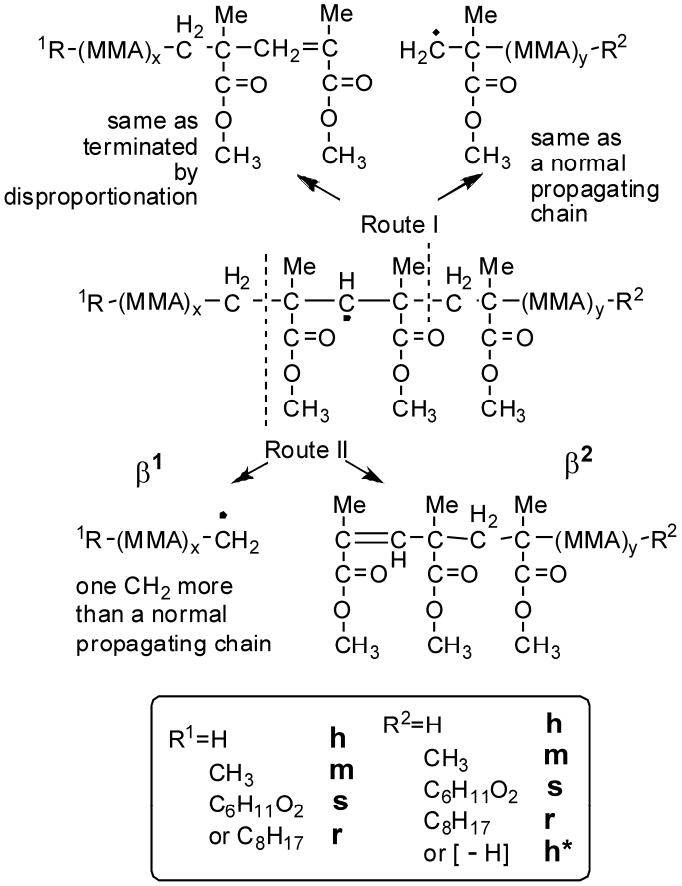

Scheme 5.1. β-scission of methyl methacrylate radical polymerization in butyl acetate as solvent under relatively high temperature.

In addition, solvent effects in radical polymerization such as chain transfer to solvent have also been observed and investigated in several studies.[9, 15-17]

For the analysis of increasingly complicated polymer structures more potent techniques are required. All polymeric materials have a molecular weight distribution, a functionality distribution such as different end groups and a composition distribution (in copolymer).

Classic methods such as size exclusion chromatography (SEC) can be applied to determine the molecular weight distribution of polymers. Gradient elution of polymers has been developed to separate polymers according to their polarity (and can therefore be used for separation based on end group and/or the heterogeneity of copolymer). Liquid chromatography at critical conditions of adsorption (LACCC) has also been studied and applied to many polymer systems.[18-20] Under the (near-)critical condition of adsorption, the elution of a polymer is independent of its molecular weight distribution but only based on its end-group functionality. This offers a possible solution to analyze a complicated copolymer system if the near-critical condition of a monomer fraction is achieved.

Electrospray-Mass Spectrometry (ESI-MS)[21, 22] alone is able to discriminate among different masses and has a remarkably high sensitivity. Furthermore, tandem MS/MS can produce fragment ions for partial or complete structural determination.[23] The use of chromatography and MS techniques has proven to be mutually complementary and powerful for polymer structural analysis. Montaudo *et al.*[24] demonstrated use of SEC-MALDI MS measurement on a P(MMA-BA) copolymer system to determine the bivariate distribution. Gruendling et al.[25] demonstrated the application of SEC-ESI MS on the determination of absolute individual molecular weight distributions from polymer mixtures (same monomer class but different end groups). The approach of LACCC-MS has been applied to poly(ethylene oxides), poly(propylene oxides) and their copolymers by Falkenhagen *et al.*.[26]

Some other attractive and recently developed methods, such as LC-NMR-MS[27] or IMS-MS,[28, 29] will also offer information on end group structures. But both techniques, however, have only had limited application in the characterization of synthetic polymer so far.

In this chapter, both gradient elution LC and isocratic elution LC are coupled to ESI MS to investigate the structures of PMMA and P(MMA-*r*-BA). The variety of combined mass of the end groups of a polymer observed by LC-IT MS is further investigated using high resolution and high accuracy FTICR MS. By gradient elution LC, a separation based on polarity (end-group functionality) and molecular weight distribution is obtained on PMMA and its copolymer. Isocratic elution, is applied to reduce the effects of MMA on elution.

5.2 Experimental Section

5.2.1 Polymer Synthesis

All the samples analyzed in this study were supplied by AkzoNobel Car Refinishes, Sassenheim, the Netherlands. They were prepared by radical polymerization in butyl acetate as solvent under relatively high temperature (160 ^{o}C) using tert-butyl peroxy-3,5,5-trimethylhexanoate [Trigonox 42S] as initiator. The molecular weight averages of samples were measured by GPC calibrated with polystyrene standards. Table 5.1 lists the the molecular weight averages obtained by GPC of the methyl methacrylate homopolymer and the methyl methacrylate butyl acrylate copolymer. The ratio of monomers used in the copolymer sample was 1:1.

Table 5.1. Polymerization Information of the PMMA and P(MMA-*r*-BA)[a]

Monomer	methyl methacrylate	methyl methacrylate and *n*-butyl acrylate
M_n (g/mol)	3340	1804
M_w (g/mol)	6214	3012

5.2.2 Mass Spectrometry

Mass spectra were acquired by direct infusion electrospray ionization-mass spectrometry (ESI-MS) and liquid chromatography-ESI-MS (LC-ESI-MS). Two mass spectrometers, *viz.* a Bruker Esquire 3000plus and a Thermo Scientific LTQ FT Ultra Hybrid were used in this study. The LC system was an Agilent 1100 series LC binary pump with DAD detector. The LC column in the LC-ESI-MS setup was an Alltech Kromasil C18 (150mm*4.6mm). During analysis, the column temperature was thermostatized at 30 °C. A gradient of tetrahydrofuran (THF) (Sigma-Aldrich) / acetonitrile (ACN) (Sigma-Aldrich) and H_2O (from Millipore Direct-Q) (55:45 v/v, premixed) was used as mobile phase. Formic acid (FA) (Fluka) at a level of 0.1% was added to both mobile phases. For analysis employing direct infusion (using a Cole-Parmer 74900 series syringe pump at 0.6 ml/h) samples were dissolved in methanol (Fluka) at an approximate concentration of 100 μg/ml. For LC-MS analysis, samples with a concentration of 2 mg/ml in THF were prepared. Data were processed and analyzed using Bruker DataAnalysis 3.3 and Thermo Scientific Excalibur 2.0 data systems respectively.

5.3 Results and Conclusions

5.3.1 Gradient Elution LC-MS of PMMA

LC separation was used prior to and online with MS. A wide range of gradients was tested to optimize the LC separation. The best separation of the PMMA samples was achieved using gradient from 5% THF / 95% ACN and H_2O (55:45 v/v, premixed) to 100% THF in 60 minutes. The selection of mobile phase is based on the solubility of PMMA in these solvents. In this gradient setting, THF is a strong solvent for PMMA, ACN is a poor solvent for PMMA and H_2O is a non-solvent[30]. All oligomers were ionized by sodium ions, forming $[M+Na]^+$ species, presumably from residual sodium salts in the solvents.

Figure 5.1a shows the partial (retention time 2-35 minutes) LC-MS data showing log abundance of the PMMA(A) molecules with sodium adduct ions (data point weight) versus *m/z* (as y-axis) versus chromatographic elution time (as x-axis). Clear distributions of the peaks with *m/z* differences of 100 along the y-axis are attributed to the mass of MMA (100 Da). The distributions along the retention time (x-axis) originate from PMMA with various end groups and molecular weight distributions. The corresponding average mass spectra of the three ranges of retention time are shown in Figure 5.1b) 6-20 minutes, c)18-28 minutes and d)30-32 minutes.

According to the gradient elution condition used, structures with higher polarity and lower molecular weight will elute earlier in the LC. The end groups potentially present in this PMMA sample includes hydrogen (H), methyl (CH_3) and octyl (C_8H_{17}) from the initiator and acetic acid ($C_6H_{11}O_2$) from the solvent. Unsaturated end groups are also possible due to β-scission (see Scheme 1) and disproportionation. Amongst all, structures with either H or CH_3 end group will have a higher polarity than those with C_8H_{17} as end group. Three elution time windows are observed: PMMA with no C_8H_{17} end group (6-20 minutes; Figure 5.1b), with C_8H_{17} end group at one end of the polymer chain (18-28 minutes; Figure 5.1c) and with C_8H_{17} end group at both ends of the polymer chain (30-32 minutes; Figure 5.1d).

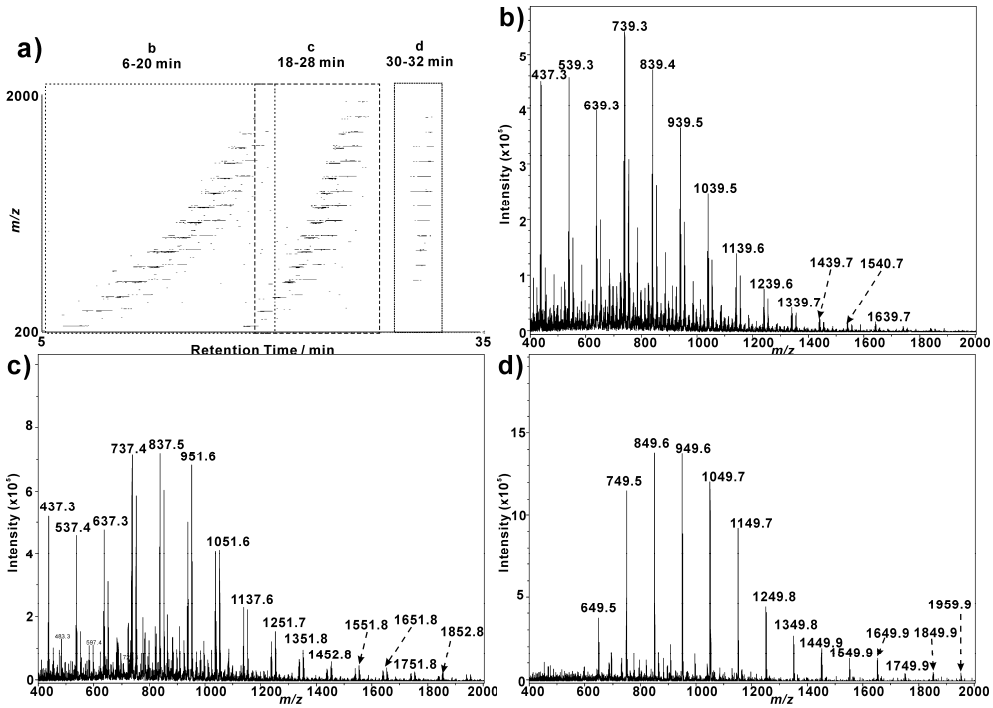

Figure 5.1 a) Gradient elution LC-MS data obtained on ITMS showing log abundance of the PMMA with sodium adduct ions (data point weight) versus *m/z* (as y-axis) versus retention time (as x-axis); The corresponding average mass spectra of PMMA in different range of retention time, b) 6-20 minutes, c) 18-28 minutes, d) 30-32 minutes.

Because ITMS does not allow confirmation of the elemental composition of the end groups due to lack of mass accuracy, the homopolymer sample was analysed by FT-ICR-MS. Figure 5.2 shows the summation spectra of ESI-FTICR MS data of PMMA. Although LC was not applied prior to the experiment and hence the polymer sample was not separation in time based on end group, the resolution and mass accuracy of the FTICR MS instrument were sufficient to discriminate and identify the majority of the peaks. Although some of the peaks have relatively lower intensity in the FTICR MS spectra than in the IT MS spectra (they might have suffered from ion suppression in the infusion experiment), the infusion FTICR MS data is still qualitatively valid for structure elucidation. Using linear regression[31], exact residual masses of every series resulting from the various initiation and termination mechanisms were obtained. The naming system used in Figure 5.2 is similar to

that used in previous reports[8, 9]. For example, series rh with m/z 335+100*(n-3) was attributed to the structures resulting from initiation by octyl radical from the peroxide initiator and termination by disproportionation to form an unsaturated end group. The calculated residual mass for the series was 139.1144 Da which is exactly the theoretical mass of $[C_8H_{16}+Na]^+$. The standard deviation of the data is 0.0001. The theoretical exact mass of an MMA monomer is 100.0524 Da while the calculated value is also exactly 100.0524 ± 0.0001Da. A more detailed description of procedure of the method can be found in the supporting information. This example shows that the unequalled high accuracy and resolution of FTICR MS instrument makes it a very powerful and suitable tool to determine the exact masses and corresponding elemental compositions even in complex synthetic polymer systems.

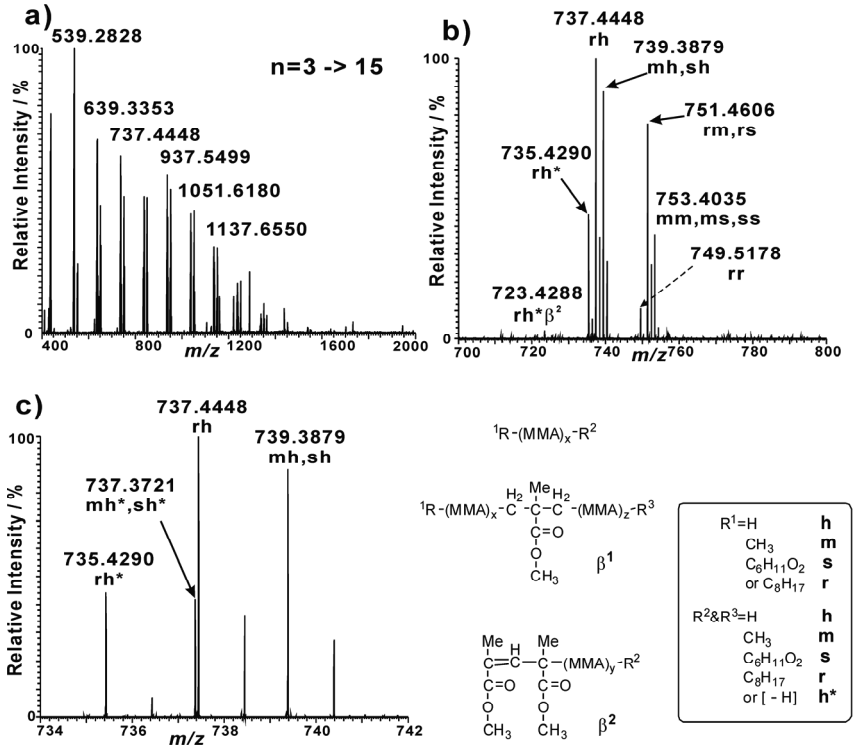

Figure 5.2 Average mass spectra of PMMA on FTICR-MS, a) the entire scan range *m/z* 400-2000, b) expanded (*m/z* 700-800) mass spectra with series assignment, c) further expanded (*m/z* 734-742) mass spectra with series assignment.

In the LC-IT MS data, the series m/z 337+100*(n-2) (nominal mass) was observed in both the retention time window 6-20 minutes and the retention time window 18-28 minutes. The results obtained on FTICR MS reveal the existence of isobaric materials at these nominal masses. In Figure 5.2c, split peaks were observed at *m/z* 737.3721 and *m/z* 737.4448 with 0.0727 Da mass differences. The elemental compositions are $C_{36}H_{58}O_{14}$ and $C_{38}H_{66}O_{12}$, calculated from the exact mass data. The end groups are assigned as $C_6H_{10}O_2$ and C_8H_{18}, respectively. The two peaks were therefore attributed to series sh* (or mh*) and rh. The theoretical mass difference of these two structures is 0.0728 Da (Δ<0.0001 Da). FTICR MS^2 further supports this attribution since different fragmentation pathways were observed. By applying a broad isolation window, both *m/z* 737.3721 and *m/z* 737.4448 were selected as precursor ion so that product ions were produced from both structures. On the other hand, application of a narrower isolation window to only include the more intense peak *m/z* 737.4448 as precursor ion was applied to generate product ions only from this structure. The product ions exclusively observed when a broad excitation window was applied could therefore be assigned to be the fragments from the peak observed at *m/z* 737.3721.

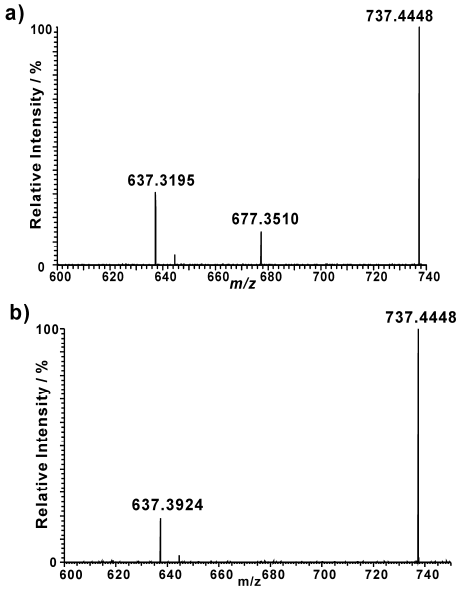

Figure 5.3 FTICR MS^2 spectra of *m/z* 737.4, a) isolation window *m/z* ± 0.2; b) isolation window *m/z* ± 0.05.

Figure 5.3 shows FTICR MS^2 spectra of *m/z* 737.4 obtained at different isolation windows. Figure 5.3a was obtained using the relatively broad isolation window (*m/z* ± 0.2) and Figure 5.3b was obtained using the very narrow isolation window (*m/z* ± 0.05). Thus, only *m/z* 737.4448 was selected as precursor ion in Figure 5.3b. Losses of 100.0524 were observed in both cases (In Figure 5.3a a peak at m/z 637.3195, calculated from m/z 737.3721, in Figure 5.3b a peak at m/z 637.3924, calculated from m/z 737.4448.). A unique loss of m/z 60.0211 was only observed in the MS^2 spectra including m/z 737.3721 as precursor ion. The loss is attributed to acetic acid ($C_2H_4O_2$) from the end of the polymer chain (resulting from the initiation by the butyl acetate solvent radical).[9] It agrees well with the theoretical mass of $C_2H_4O_2$, which is exactly 60.0211. Nominally isobaric peaks were observed up to *m/z* 1437 (resolution is 19,700). Larger molecules were not well ionized in the infusion FTICR experiment and produced peaks with low intensities. Possible cause of this is the use of methanol but not THF as initial solvent. Unfortunately, the experimental setup didn't allow the use of THF so no experiment could be carried out in this solvent.

5.3.2 Gradient Elution LC-MS of P(MMA-r-BA)

The same gradient used for LC-MS experiment of PMMA was applied to study P(MMA-*r*-BA). Figure 5.4a is the partial (retention time 2-40 minutes) gradient elution LC-MS data obtained on IT MS showing log abundance of the P(MMA-*r*-BA) the sodium adduct ions (data point weight) in a coordinate system of *m/z* (as y-axis) versus retention time (as x-axis). The average mass spectrum of P(MMA-*r*-BA) obtained on gradient elution LC-IT MS is shown in Figure 5.4b, and Figure 5.4c shows the average mass spectrum of P(MMA-*r*-BA) obtained on FTICR MS without preceding LC separation.

The LC-MS dataset of the copolymer system, as expected, is more complicated than the homopolymer system due to the addition of the BA fraction. Structures with different end groups, however, can still be observed and attributed. The FTICR MS data aided to obtain elemental compositions and thus facilitated further end group structure assignment. Table 5.2 lists all observed series assignments (end group combinations) with their retention time range and corresponding masses. Interestingly, β-scission is involved in almost all dominant end group combinations. The cause of this is the relatively high polymerization

temperature and the corresponding high probability of β-scission reaction for both monomers.

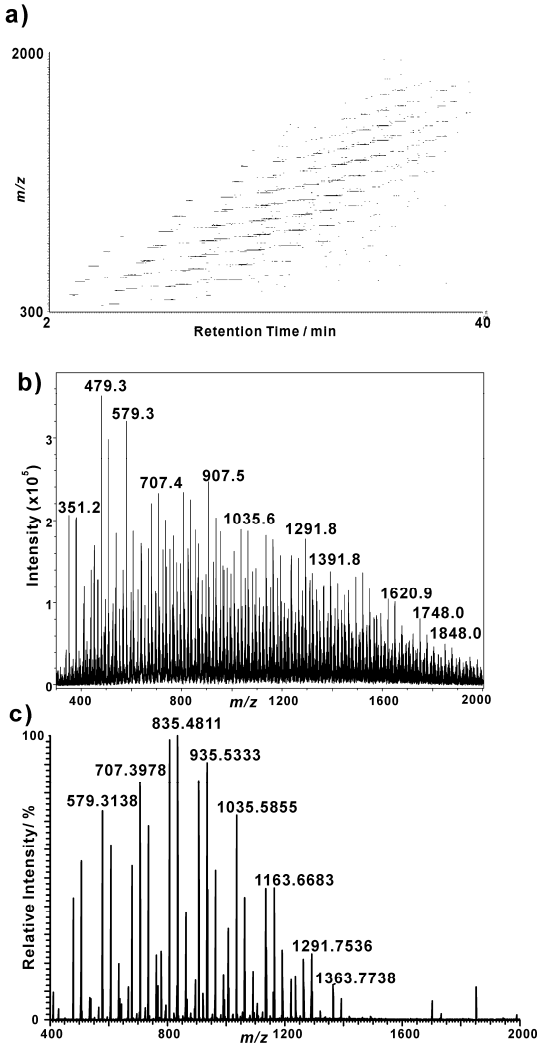

Figure 5.4 a) Gradient elution LC-IT-MS data showing log abundance of the P(MMA-*r*-BA) with sodium adduct ions (data point weight) in a coordinate system of *m/z* (as y-axis) versus retention time (as x-axis), b) average mass spectrum of P(MMA-*r*-BA) obtained on gradient elution LC-IT MS (summation range: 2-40 minutes, *m/z* 300-2000), and c) average mass spectrum of P(MMA-*r*-BA) obtained by FTICR MS. (*m/z* 400-2000)

Table 5.2. P(MMA-r-BA) series with corresponding elution time in two elution condition.*

Gradient elution time (minutes)	0-18	8-31.5	30-40
Isocratic elution time (minutes)	0-2.5	2.4-7.6	7.5-15
Series assignment	β^{1a}s	β^{1b} or β^{2a}s	β^{2a} r
Residual mass	39, 67, 95	51, 79, 07, 35, 63, 91, 19, 47	33, 61, 89, 17, 45

* Observed range of number of MMA is 0-18 and number of BA is 0-14.

The FTICR MS spectra are less complicated than the LC-IT MS spectra. Several series were not observed in the FTICR MS spectra. The possible cause of this observation is again the initial solvent used for the experiments in the infusion analysis. Some polymer structures might have very low solubility in methanol. Another possible cause is the ion suppression effects in the infusion experiment. The combination of LC separation and summation over the separated peaks, however, mitigated and decreased this effect and gives a better reflection of the composition of the sample.

5.3.3 Isocratic Elution LC-MS of PMMA and P(MMA-r-BA)

Isocratic elution LC-MS was applied to both PMMA and P(MMA-*r*-BA) samples. The mobile phase used was 50% THF / 50% ACN and H_2O (55:45 v/v, premixed). This is similar to the condition used in earlier research done by Cools *et al.*[32] and Philipsen *et al.*[33]. The aim of applying this isocratic condition is to achieve a near-critical separation on PMMA and to expand the study of P(MMA-*r*-BA). Generally, in an AB copolymer system, if critical condition is achieved on A, the elution will not be affected by A but only by B and the total end group functionality.

Figure 5.5 shows the isocratic elution LC-MS data obtained on IT MS as log abundance of the PMMA with sodium adduct ions (data point weight) in a coordinate system of *m/z* (as y-axis) versus retention time (as x-axis).

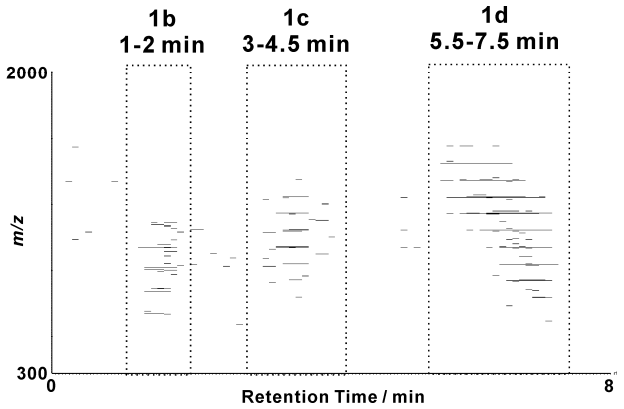

Figure 5.5 Isocratic elution LC-MS data obtained on IT MS showing log abundance of the PMMA with sodium adduct ions (data point weight) versus *m/z* (as y-axis) versus retention time (as x-axis).

Three elution time windows were observed in the data. They correspond to the three areas observed in Figure 5.1b, 1c and 1d. PMMA with the same end-group functionality eluted in the same elution time window despite its molecular weight distribution. The axes of Figure 5.5 can therefore be transformed to end-group functionality or number of octyl end groups (x-axis) and molecular weight or degree of MMA polymerization (y-axis).

Figure 5.6a shows the isocratic elution LC-MS data obtained on the copolymer using IT MS and plots log abundance of the P(MMA-*r*-BA) with sodium adduct ions (data point weight) in the coordinate system of *m/z* (as y-axis) versus retention time (as x-axis). The corresponding average mass spectra of P(MMA-*r*-BA) in different retention time windows are shown in Figure 5.6b (2.5-2.8 minutes), 5.6c (5-6 minutes) and 5.6d (10-12 minutes).

Peaks in the mass spectrum shown in Figure 5.6b all have the same end groups and number of BA units but a different number of MMA units. The structures are attributed to series β^{1a}s, which results from a solvent radical initiation chain that underwent β-scission and was terminated by hydrogen abstraction. They have no octyl end group. The number of BA units of the molecules detected in Figure 5.6b is 2. Likewise, in Figures 6c and 6d, all the peaks have the same end groups (series β^{1b} or β^{2a}s for Figure 5.6c) and series β^{2a}r for Figure 5.6d and number of BA units (both 5 for Figure 5.6c and for Figure 5.6d) but numbers of different number MMA units.

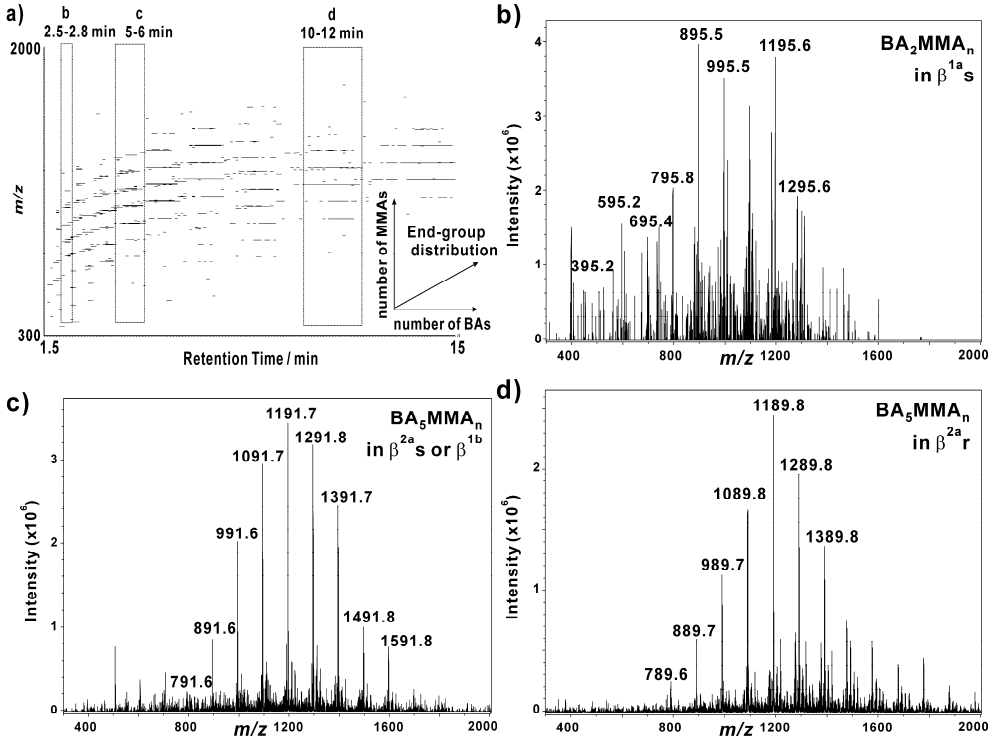

Figure 5.6 a) Isocratic elution LC-MS data obtained on IT MS showing log abundance of the P(MMA-*r*-BA) with sodium adduct ions (data point weight) versus *m/z* (as y-axis) versus retention time (as x-axis); The corresponding average mass spectra of P(MMA-*r*-BA) in different range of retention time, b) 2.5-2.8 minutes, c) 5-6 minutes (on next page) and d) 10-12 minutes.

Thus, between each consecutive pair of retention time windows, the residual masses differed by 28 Da (*viz*, the substitution of one MMA with one BA). The results confirmed this elution condition is based on the end-group functionality (polarity) and the number of BA units. The MMA effect on elution is ultimately minimized in this condition. The observed ranges of number of MMA and BA are 0-18 and 0-14, respectively. The observed range of number of MMA and BA is 0-18 and 0-14. A semiquantitative way to address the amount of BA-MMA copolymer with different number of BA and MMA from 2.4 – 7.6 minute elution time in isocratic condition has been attempted by summation of the peak intensities of the respective structures. It is presented in Figure 5.7.

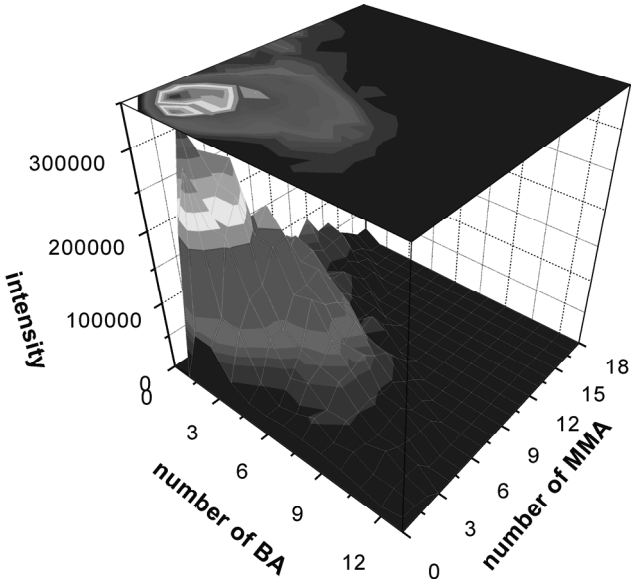

Figure 5.7. Semiquantitative study on BA-*r*-MMA copolymer from retention time window 2.4-7.6 minutes.

A different approach to analyse the copolymer system would be to find the near-critical condition for BA fraction[20]. Contrary to the condition applied in this study, a near-critical condition for BA will minimize the influence of BA on LC elution. The copolymer elution would then behave as influenced by end-group functionality and number of MMA units. This will be highly complementary to the study in this chapter.

5.4 Conclusions

Separation and detection/identification based on the end groups in the homopolymer PMMA has been achieved by the combination of gradient elution LC with MS. By using high-resolution and high-accuracy MS and MS^2, elemental compositions of the molecules were obtained. End group could therefore be determined.. Isobaric materials with subtle structure differences (end group) were easily identified by applying different isolation windows in MS^2 experiment.

The same analytical strategy was applied to the copolymer. Although the structures could still be assigned, the complex copolymer system presented more difficulties to fully analyze all the end groups of the peaks with relatively low intensity, such as peaks from series β^{1a}s.

The isocratic elution LC-MS allowed identification of copolymer with different end groups in a short analysis time. It was applied to the system to reduce the complexity of the spectra. A near critical condition was achieved on PMMA using isocratic elution LC-MS. PMMA was separated based on their end-group functionality. The molecular weight distribution of PMMA had almost no influence on the elution. When applying the same isocratic elution condition to the P(MMA-r-BA) polymer, the effect of MMA fraction on elution was minimized to almost none. The elution therefore is purely based on the molecular distribution of BA and the total end-group functionality. The MS snapshot therefore is simplified

Combining the results in both elution conditions online coupled with MS, it can be concluded that the relatively reactive solvent has influences in the compositions of PMMA and P(MMA-*r*-BA). The effect of *β*-scission during polymerization on the copolymer composition is very dominant (all four series found in the copolymer is resulted from *β*-scission). Its effect on PMMA homopolymer composition is difficult to evaluate since two of the *β*-scission products are identical to the normal propagating chains.

References

(1) Percec, V. *Chem. Rev.* **2009,** *109*, 4961-4962.
(2) Kobayashi, S.; Makino, A. *Chem. Rev.* **2009,** *109*, 5288-5353.
(3) Barbey, R.; Lavanant, L.; Paripovic, D.; Schuwer, N.; Sugnaux, C.; Tugulu, S.; Klok, H.-A. *Chem. Rev.* **2009,** *109*, 5437-5527.
(4) Braunecker, W. A.; Matyjaszewski, K. *Prog. Polym. Sci.* **2007,** *32*, 93-146.
(5) Georges, M. K.; Veregin, R. P. N.; Kazmaier, P. M.; Hamer, G. K. *Macromolecules* **1993,** *26*, 2987-2988.
(6) Matyjaszewski, K.; Xia, J. *Chem. Rev.* **2001,** *101*, 2921-2990.
(7) Moad, G.; Rizzardo, E.; Thang, S. H. *Polymer* **2008,** *49*, 1079-1131.
(8) Buback, M.; Frauendorf, H.; Gunzler, F.; Vana, P. *J. Polym. Sci., Part A: Polym. Chem.* **2007,** *45*, 2453-2467.

(9) Song, J.; van Velde, J. W.; Vertommen, L. L. T.; van der Ven, L. G. J.; Heeren, R. M. A.; van den Brink, O. F. *Macromolecules* **2010,** *43*, 7082-7089.
(10) Subrahmanyam, B.; Baruah, S. D.; Rahman, M.; Baruah, J. N.; Dass, N. N. *J. Polym. Sci., Part A: Polym. Chem.* **1992,** *30*, 2531-2549.
(11) van Herk, A. M. *Macromol. Rapid Commun.* **2001,** *22*, 687-689.
(12) Quan, C.; Soroush, M.; Grady, M. C.; Hansen, J. E.; Simonsick, W. J. *Macromolecules* **2005,** *38*, 7619-7628.
(13) Junkers, T.; Koo, S. P. S.; Davis, T. P.; Stenzel, M. H.; Barner-Kowollik, C. *Macromolecules* **2007,** *40*, 8906-8912.
(14) Junkers, T.; Barner-Kowollik, C. *J. Polym. Sci., Part A: Polym. Chem.* **2008,** *46*, 7585-7605.
(15) Jovanovic, R.; Dubé, M. A. *J. Appl. Polym. Sci.* **2001,** *82*, 2958-2977.
(16) Jovanovic, R.; Dubé, M. A. *J. Appl. Polym. Sci.* **2004,** *94*, 871-876.
(17) Mckenna, T. F.; Villanueva, A.; Santos, A. M. *J. Polym. Sci., Part A: Polym. Chem.* **1999,** *37*, 571-588.
(18) Falkenhagen, J.; Much, H.; Stauf, W.; Muller, A. H. E. *Macromolecules* **2000,** *33*, 3687-3693.
(19) Jiang, X.; Lima, V.; Schoenmakers, P. J. *J. Chromatogr., A* **2003,** *1018*, 19-27.
(20) Jiang, X.; Schoenmakers, P. J.; Lou, X.; Lima, V.; van Dongen, J. L. J.; Brokken-Zijp, J. *J. Chromatogr., A* **2004,** *1055*, 123-133.
(21) Whitehouse, C. M.; Dreyer, R. N.; Yamashita, M.; Fenn, J. B. *Anal. Chem.* **1985,** *57*, 675-679.
(22) Fenn, J. B.; Mann, M.; Meng, C. K.; Wong, S. F.; Whitehouse, C. M. *Science* **1989,** *246*, 64-71.
(23) Crecelius, A. C.; Baumgaertel, A.; Schubert, U. S. *J. Mass Spectrom.* **2009,** *44*, 1277-1286.
(24) Montaudo, M. S.; Montaudo, G. *Macromolecules* **1999,** *32*, 7015-7022.
(25) Gruendling, T.; Guilhaus, M.; Barner-Kowollik, C. *Macromolecules* **2009,** *42*, 6366-6374.
(26) Falkenhagen, J.; Weidner, S. *Anal. Chem.* **2008,** *81*, 282-287.
(27) Stülten, D.; Lamshöfta, M.; Zühlkea, S.; Spiteller, M. *J. Pharm. Biomed. Anal.* **2008,** *47*, 371-376.
(28) Hilton, G. R.; Jackson, A. T.; Thalassinos, K.; Scrivens, J. H. *Anal. Chem.* **2008,** *80*, 9720-9725.
(29) Trimpin, S.; Plasencia, M.; Isailovic, D.; Clemmer, D. E. *Anal. Chem.* **2007,** *79*, 7965-7974.
(30) Staal, W. J. Gradient Polymer Elution Chromatography - A qualitative study on the prediction of retention times using could-points and solubility parameters. PhD. thesis, Technische Universiteit Eindhoven, 1996.
(31) van Rooij, G. J.; Duursma, M. C.; Heeren, R. M. A.; Boon, J. J.; de Koster, C. G. *J. Am. Soc. Mass Spectrom.* **1996,** *7*, 449-457.
(32) Cools, P. J. C. H.; Herk, A. M. v.; German, A. L.; Staal, W. *J. Liq. Chromatogr.* **1994,** *17*, 3133-3143.
(33) Philipsen, H. J. A.; Klumperman, B.; van Herk, A. M.; German, A. L. *J. Chromatogr., A* **1996,** *727*, 13-25.

6

High-resolution Ion Mobility Spectrometry-Mass Spectrometry on Poly (Methyl Methacrylate)

This chapter is based on, Junkan Song, Christian H. Grün, Ron M.A. Heeren, Hans-Gerd Janssen and Oscar F. van den Brink, *Angewandte Chemie,* **DOI: 10.1002/anie.201005225.**

Recent developments in ion mobility spectrometry (IMS)-mass spectrometry (IMS-MS) show promising potential for structure elucidation of synthetic polymers. The technique offers an extra dimension of separation based on size and conformation of the molecules in addition to *m/z* separation of mass spectrometry. Although extensive study has been done in IMS-MS of biomolecules, studies of applying this technique on complex synthetic polymer systems are still limited. In this chapter, detailed endgroup mapping of poly(metyl methacrylate) polymerised via free radical polymerisation using peroxide initiator was achieved without the need of a preceding time-consuming LC separation. While neither drift time nor mass-to-charge separation alone is capable of fully differentiating isobaric materials in a limited mass range, the combination of both offers an effective approach in identifying individual compounds in extremely complex mixtures covering a relatively large molecular weight distribution. The 2D and 3D visualisation of the data enhances the extraction of structural information reflecting differences in mass, and size and/or conformation of the molecules. This example shows the power and prospect of utilising IMS-MS on complex synthetic polymer systems as an analytical tool in itself and, potentially, in combination with separation techniques such as HPLC.

6.1 Introduction

Increasingly complex synthetic polymeric structures have been developed to provide desirable properties and functions.[1] The performance of these products depends on many factors such as endgroup composition, molecular weight distribution and 3D conformation.[2, 3] Various analytical methods have been developed to obtain the information. Conventional analytical techniques to study polymer systems include gel-permeation chromatography (GPC),[4] Fourier-transform infrared spectroscopy (FTIR),[5] nuclear magnetic resonance spectroscopy (NMR),[6] and differential scanning calorimetry (DSC).[7]

The development of "soft" ionisation methods such as elecrospray ionisation (ESI)[8, 9] and matrix-assisted laser desorption/ionisation (MALDI)[10, 11] allowed mass spectrometry (MS) to become one of the most promising analytical methods for the analysis of polymeric systems. MS has the ability to characterise a dispersed polymer containing oligomers with different structures such as isomers or isobaric molecular weights. The combination of liquid chromatography (LC) and MS reduces the effects of ion suppression that may occur in an infusion MS analysis and provides an extra dimension of separation.[12, 13] However, a relatively long separation time (>30 minutes for HPLC, around 10 minutes for UPLC) is needed and a complex elution system using a variety of solvents has to be developed to suit a specific polymeric system.

The combination of ion mobility spectrometry (IMS) and ESI-MS has been developed to analyse biomolecules and biopolymers.[14-16] Ion mobility describes how fast an ion in the gas phase moves through a drift cell that is filled with a carrier buffer gas under the influence of an electric field. More compact ions with a smaller collision cross section will drift more quickly than expanded ions. The time scale for separations in IMS is 100 μs to 10 ms, which is ideally suited for interfacing with an MS instrument. The extra dimension of separation based on drift time (t_D) provided by IMS is also highly complementary to the information obtained by MS. Although some studies on IMS-MS measurements of blends of disperse macromolecules, e.g. poly(ethylene glycol) (PEG), have been reported, studies using IMS-MS on complex synthetic polymer systems are still limited.[17-21]

In this chapter, high resolution IMS-MS is applied to study a poly(methyl methacrylate) (PMMA) synthesised via radical polymerisation using peroxide initiator (tert-butyl peroxy-

3,5,5-trimethylhexanoate) in solvent (butyl acetate). Comprehensive study on acrylic polymer produced by radical polymerisation using MS has been done in the past decade.[22-27] It has been proven that high-resolution MS can discriminate between the effects of various polymerisation mechanisms such as beta-scission, chain transfer to solvent and radical transfer to solvent from the initiator, etc.[22-27] A system with complex endgroup combinations is expected since various initiation and termination reactions may occur. In the current chapter, by using the IMS-MS combination, detailed endgroup information and discrimination of molecules with same nominal masses were achieved without the need of a preceding time-consuming LC separation.

6.2 Experimental Section

The PMMA polymer was prepared by radical polymerization in butyl acetate as solvent under relatively high temperature (160 ^{o}C) using tert-butyl peroxy-3,5,5-trimethylhexanoate as initiator. It was diluted to 10 µgml-1 in methanol for direct infusion experiments on a Waters Synapt G2 HDMS mass spectrometer. The system was used in positive ionization electrospray mode with 'resolution' set to 20 kDa. The *m/z* was calibrated using sodium formate. A solution of leucine-enkephaline at 2 ng/ml was used for the lock mass signal. Reference scans were taken every 10 s. Source parameters as well as mobility settings were optimized using the sample solution of PMMA. The most relevant parameters were the following: Capillary voltage: 3.7 kV; cone voltage: 60 V; source temperature: 100 °C; desolvation gas flow: 500 l/min; desolvation temperature: 350 °C; helium cell gas flow: 180 ml/min; IMS gas flow: 85 ml/min; IMS wave velocity: 600 ms; IMS wave height: 40 V. Nitrogen was used as carrier buffer gas. Data were obtained and processed using Waters MassLynx 4.1 SCN 779 and DriftScope 2.1 software. The scan time was 1 s with an inter-scan delay of 24 ms. A total of 100 scans taken in the range *m/z* 50-2000 were averaged for data processing.

6.3 Results and Discussion

Figure 6.1 shows the results of a typical IMS-MS experiment with a 2D analysis of the PMMA polymer, drift time along the x-axis and mass-to-charge along the y-axis. Clear distributions of sodium cation adducts of PMMA according to the size and shape of individual components with up to triply charged ion peaks were observed. The triply charged ion peaks ranging from *m/z* 1000 to *m/z* 2000 demonstrate the presence of PMMAs with molecular weights of up to 6000 Da, which is consistent with our GPC data (M_n of 3340 Da, data not shown). Although the abundance of the high molecular weight components in the PMMA is relatively low, IMS-MS is still capable of the analysis. Compared to the LC-MS work on poly(n–butyl acrylate)s (PBAs) of comparable average molecular weight (M_n of 3760 Da) in **Chapter 4**, in which components were only observed up to 2000 Da, IMS-MS is capable to determine the entire molecular weight distribution of the PMMA sample.

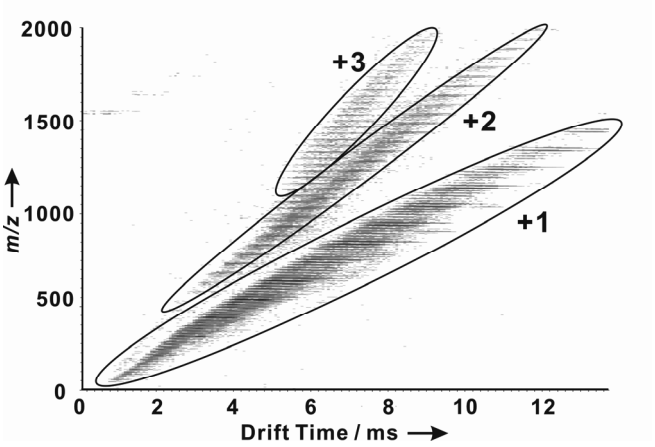

Figure 6.1. *m/z* vs. t_D plot of PMMA polymerised via free radical polymerisation on IMS-MS. Sodiated species with charge states up to +3 series were observed.

Averaged IMS-MS spectra of PMMA are presented in Figure 6.2(a). Several series of peaks start at *m/z* 339 continuing to greater than 1339 with a separation of 100 Da between each group. The 100-Da mass difference is attributed to the mass of MMA (C5H8O2;

theoretical exact mass 100.0524 Da). Figure 6.2(b) is an expanded averaged spectrum showing one monomeric mass range (*m/z* 700-800).

The elemental compositions of the endgroups appearing in the polymer series were identified using a linear regression method.[28] The naming system used here is similar to that used in previous reports[22, 27] and **Chapter 4** and **5**, i.e. the series are named after their endgroup composition. (See Figure 6.2. [-H] indicating an unsaturated endgroup resulting from disproportionation.) The most intense series of peaks sh (or mh, which is one degree of polymerisation higher than sh, but has the same elemental composition and therefore has the same molecular weight as sh), *m/z* 439 + (n–3)*100, contains a butyl acetate endgroup (or methyl) at one end of the chain and is terminated with an H-abstracted end group at the other end. The monomer mass calculated from the accurate mass data was 100.0523 Da (Δ = 0.0001 Da) and the residual mass of this series is 139.0770 Da (Δ = 0.0039 Da). The correlation coefficient (R2) of the calculation is 1.0000. Details of the procedure are presented in the Appendix. Although the results obtained by IMS-MS are not as accurate as those obtained from an FTICR MS or Orbitrap MS, which have higher resolution and mass accuracy, the accuracy of the results still allows determination of the endgroup elemental compositions.

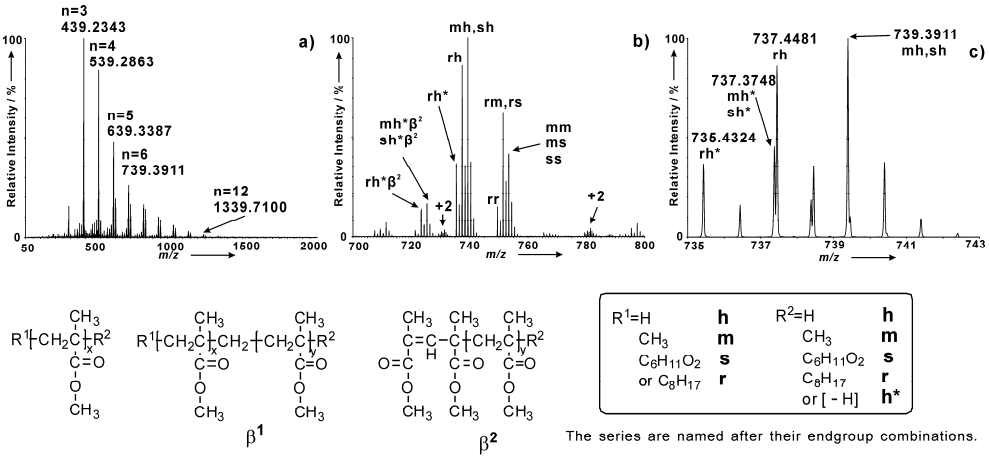

Figure 6.2. Averaged mass spectra of PMMA, a) the entire scan range *m/z* 50-2000, b) expanded (*m/z* 700-800) mass spectra with series assignment and c) further expanded (*m/z* 735-743) mass spectra with series assignment. Differences of ~72 mDa are clearly shown.

Further expanded mass spectra (*m/z* 735-743) are presented in Figure 6.2(c). Two resolved peaks with 0.0733 Da difference, *m/z* 737.3748 ($C_{38}H_{66}O_{12}$) and *m/z* 737.4481 ($C_{36}H_{58}O_{14}$), are observed in the spectra. This mass difference is attributed to the difference in elemental composition of two end groups, exchanging C2H8 for O2 (the theoretical mass difference is 0.0728 Da). The first peak (*m/z* 737.3748) is attributed to sh* or mh* and the second peak (*m/z* 737.4481) is attributed to rh. It is very likely that both mh* and sh* are present because both endgroups were observed by LC-Orbitrap MS in a PBA sample that was prepared under similar polymerisation conditions[27] in **Chapter 4**. This small exact mass difference would not be detected in a low resolution mass spectrometer, resulting in a single, unresolved peak with *m/z* 737.4.

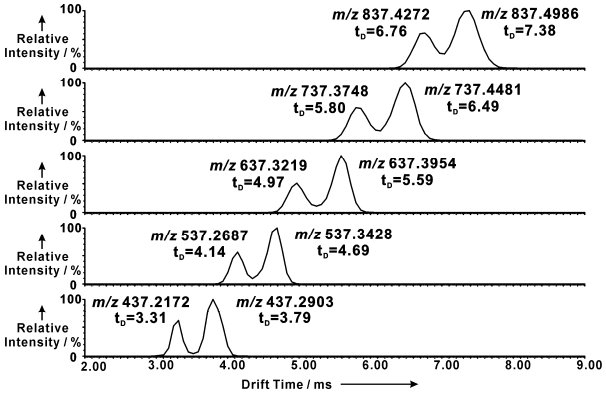

Figure 6.3. Extracted (extraction window=0.2000 Da) ion mobilogram of (sh* or mh*) and rh PMMA oligomers. The *m/z* difference between (sh* or mh*) and rh peaks is 0.0728 (±0.0014) Da.

Within this subset of the IMS-MS data, the aforementioned substances can also be differentiated by their different drift times. Figure 6.3 presents the ion mobilograms of the peaks in the two series (sh* or mh* and rh) described above (with 0.0728 Da difference). Within the same degree of polymerisation, molecules in series sh* and mh* have shorter drift times than the molecules in series rh. This demonstrates that although the backbones of the molecules in the two series are the same, the subtle differences in endgroups determine the size and space conformation differences which can be discriminated in IMS-MS. An explanation for this observation may be that the molecules in series rh have a more

extended octyl endgroup from the initiator than the methyl or butyl acetate endgroup (endgroup structure resulting from the termination raction makes it very similar to the backbone structure). Therefore molecules in series rh have a longer drift time. To confirm this hypothesis, modelling of the gas-phase molecular structures would be required.

Well-resolved *m/z* peaks of the two series (sh* or mh* and rh) were obtained in this IMS-MS study even up to a nominal mass of *m/z* 1037. Peaks at higher *m/z* were not very well resolved; a higher resolving power would be required. Drift time separation alone could not resolve the differences of the two peaks at higher masses either. A combination of drift time and mass-to-charge separation, however, allowed the discrimination of these peaks at higher degrees of polymerisation. Figure 6.4 is a 3D representation of the partial data set of the same IMS-MS experiment on PMMA. The drift time range displayed is 8.5-11.5 ms and the *m/z* range is 1137-1138. The inserts represent projections on a) the drift-time axis and b) the mass axis.

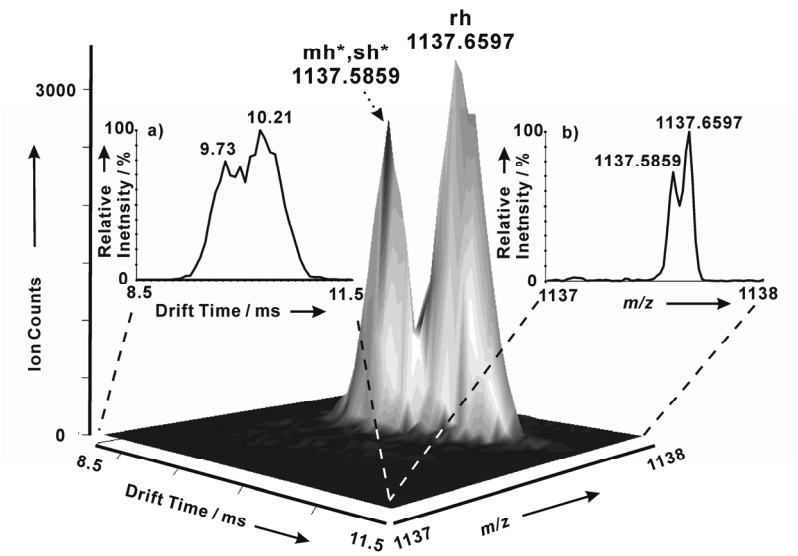

Figure 6.4. 3D representation of the IMS-MS data obtained on the PMMA sample; selected tD range 8.5-11.5 ms; selected *m/z* range 1137-1138. Inserts represent projections of a) the average ion mobiligram and b) the average mass spectrum.

At this degree of polymerisation neither the drift time separation nor the mass spectrum alone allowed the separation of the two peaks. In the 3D display however, two well separated peaks are observed. The 3D representation avoids the congestion of the data on either dimension. The extra dimension of separation brought by IMS in addition to the mass-to-charge information generated by MS increases the Euclidean distance between the peaks in the dataset and thereby facilitates the discrimination of nominal isobars.

Figure 6.5 shows a 3D representation of a part of the data of the same IMS-MS experiment on PMMA. The drift time range displayed is 6-7.5 ms and the *m/z* range displayed is 730-760. All the series were well separated based on their t_D and *m/z*.

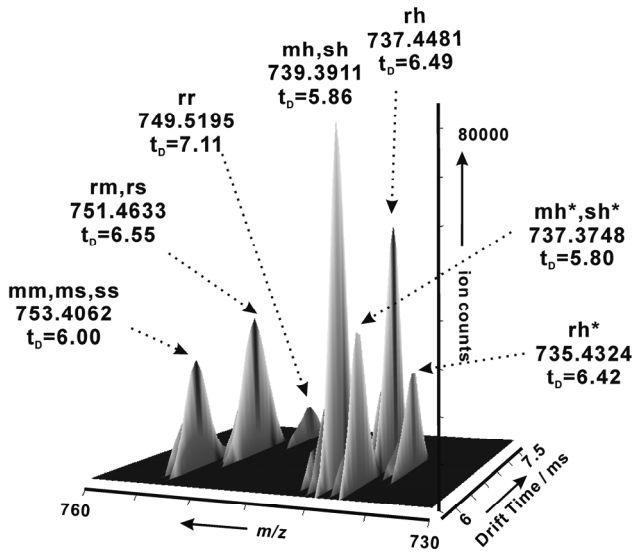

Figure 6.5. 3D representation of a typical IMS-MS experiment output with assignment of accurate masses, series and drift times.

Interestingly, some products with larger molecular weight were observed to have shorter drift times. For example, the peak at *m/z*753.4062 in series mm (or ms or ss) has a drift time of 6.00 ms. A lighter pseudomolecular ion at *m/z* 735.4324 from series rh* has a longer drift time of 6.42 ms. The cause of this phenomenon can be attributed to the different compositions of their endgroups. The lighter molecule, belonging to the series rh*

has a more extended endgroup, octyl, originating from the radical initiator. The heavier molecule, on the contrary, has a more compact methyl end group. This results in different drift times. It also proves that IMS does not only offer separation based on molecular weight but also on size and conformation of PMMAs. Similar observations have been made in IMS-MS of biomolecules,[14-16] but they have not yet been reported on a complex synthetic polymer sample with detailed mapping of end groups and to further allow confirmation or elucidation of polymerisation mechanisms.

6.4 Conclusions

In the very short time span of the experiment, in the tens of milliseconds range, IMS-MS offers full separation and identification of the components of the very complex PMMA system studied here across its molecular weight distribution. A similar result can be achieved using HPLC-MS or UPLC-MS technique but with a much longer experimental time. (See **Chapter 5** for HPLC-MS on PMMA, one-hour separation is normally needed for the HPLC-MS experiment.) These chromatographic techniques require that either a gradient or isocratic elution system is available or developed for every specific polymer system.

The development of multidimensional IMS-MS strategies is likely to aid the characterisation of more complex polymer systems such as copolymers. As subtle structural differences can be noticed by applying IMS-MS, a separation of isomers would be achieved by LC-IMS-MS or IMS-MS/MS. The 2D and 3D visualisation of the data facilitates extraction of structural information reflecting differences in mass and size, and/or conformation of the molecules. Furthermore, information such as branching in polymers which normally cannot be acquired by MS study alone can be investigated using IMS-MS[29].

References

(1) Ober, C. K. *Science* **2000,** *288*, 448-449.
(2) Frechet, J. M. *Science* **1994,** *263*, 1710-1715.
(3) Forrest, S. R. *Nature* **2004,** *428*, 911-918.
(4) Hammond, J. M.; Hooper, J. F.; Stutchbury, J. E. *Journal of Polymer Science: Polymer Symposia* **1975,** *49*, 117-125.
(5) Zou, H.; Wu, S.; Shen, J. *Chem. Rev.* **2008,** *108*, 3893-3957.
(6) Cheng, H. N.; Early, T. A. *Macromol. Symp.* **1994,** *86*, 1-14.
(7) Taniguchi, S.-i.; Takeshita, H.; Arimoto, M.; Miya, M.; Takenaka, K.; Shiomi, T. *Polymer* **2008,** *49*, 4889-4898.
(8) Whitehouse, C. M.; Dreyer, R. N.; Yamashita, M.; Fenn, J. B. *Anal. Chem.* **1985,** *57*, 675-679.
(9) Fenn, J. B.; Mann, M.; Meng, C. K.; Wong, S. F.; Whitehouse, C. M. *Science* **1989,** *246*, 64-71.
(10) Karas, M.; Bachmann, D.; Bahr, U.; Hillenkamp, F. *Int. J. Mass Spectrom. Ion Processes* **1987,** *78*, 53-68.
(11) Karas, M.; Hillenkamp, F. *Anal. Chem.* **1988,** *60*, 2299-2301.
(12) Nielen, M. W. F. *Mass Spectrom. Rev.* **1999,** *18*, 309-344.
(13) Nielen, M. W. F.; Buijtenhuijs, F. A. *Anal. Chem.* **1999,** *71*, 1809-1814.
(14) Bohrer, B. C.; Merenbloom, S. I.; Koeniger, S. L.; Hilderbrand, A. E.; Clemmer, D. E. *Annu. Rev. Anal. Chem.* **2008,** *1*, 293-327.
(15) Fenn, L. S.; McLean, J. A. *Anal. Bioanal. Chem.* **2008,** *391*, 905-909.
(16) Kanu, A. B.; Dwivedi, P.; Tam, M.; Matz, L.; Hill, H. H. *J. Mass Spectrom.* **2008,** *43*, 1-22.
(17) Trimpin, S.; Plasencia, M.; Isailovic, D.; Clemmer, D. E. *Anal. Chem.* **2007,** *79*, 7965-7974.
(18) Bagal, D.; Zhang, H.; Schnier, P. D. *Anal. Chem.* **2008,** *80*, 2408-2418.
(19) Trimpin, S.; Clemmer, D. E. *Anal. Chem.* **2008,** *80*, 9073-9083.
(20) Hilton, G. R.; Jackson, A. T.; Thalassinos, K.; Scrivens, J. H. *Anal. Chem.* **2008,** *80*, 9720-9725.
(21) Chan, Y.-T.; Li, X.; Soler, M.; Wang, J.-L.; Wesdemiotis, C.; Newkome, G. R. *J. Am. Chem. Soc.* **2009,** *131*, 16395-16397.
(22) Buback, M.; Frauendorf, H.; Gunzler, F.; Vana, P. *J. Polym. Sci., Part A: Polym. Chem.* **2007,** *45*, 2453-2467.
(23) Junkers, T.; Koo, S. P. S.; Davis, T. P.; Stenzel, M. H.; Barner-Kowollik, C. *Macromolecules* **2007,** *40*, 8906-8912.
(24) Junkers, T.; Barner-Kowollik, C. *J. Polym. Sci., Part A: Polym. Chem.* **2008,** *46*, 7585-7605.
(25) Koo, S. P. S.; Junkers, T.; Barner-Kowollik, C. *Macromolecules* **2009,** *42*, 62-69.
(26) Gruendling, T.; Guilhaus, M.; Barner-Kowollik, C. *Macromolecules* **2009,** *42*, 6366-6374.
(27) Song, J.; van Velde, J. W.; Vertommen, L. L. T.; van der Ven, L. G. J.; Heeren, R. M. A.; van den Brink, O. F. *Macromolecules* **2010,** *43*, 7082-7089.
(28) van Rooij, G. J.; Duursma, M. C.; Heeren, R. M. A.; Boon, J. J.; de Koster, C. G. *J. Am. Soc. Mass Spectrom.* **1996,** *7*, 449-457.
(29) Gies, A. P.; Kliman, M.; McLean, J. A.; Hercules, D. M. *Macromolecules* **2008,** *41*, 8299-8301.

7

Characterisation of Poly(Butylene Adipate-*co*-Butylene Terephthalate) and Its Partial Degradation Products by LC-MS^n

This chapter is based on, Junkan Song, Alena Šišková, Marcel G. Simons, Wiltod J. Kowalski, Marek M. Kowalczuk and Oscar F. van den Brink, **Submitted.**

The partial degradation of the poly(butylene adipate-co-butylene terephthalate) co-polyester was carried out under alkaline conditions at two different temperatures. Various characterisation techniques were used to obtain detailed structural information of both the original material and partial degradation products. The techniques used include gel permeation chromatography (GPC), NMR and liquid chromatography online coupled with multistage electrospray ionisation mass spectrometry (LC-ESI MS^n). The original material was converted to a mixture of oligomers at lower molecular mass (500 - 3000 g/mol) as determined by GPC. The occurrence of methanol transesterification in the degradation process was elucidated by both NMR and LC-MS^n. Furthermore, LC-MS^n confirmed the existence of cyclic structures in the original samples that disappear completely during the degradation. MS^2 on the first isotope peak helped to determine the elemental composition of the fragments and lead to end group determination. It can be used to provide an alternative for high mass accuracy MS^2 experiments. LC-MS^n was employed to reveal sequence information of certain copolymeric structures.

7.1 Introduction

Traditional plastic materials such as polyethylene, polypropylene or polystyrene are very resistant to environmental influences. The growing public and scientific concern on plastic waste in the last two decades have stimulated the development of many controlled biologically degradable polymers.

Polyesters, one specific class of the biodegradable polymers, play an important role due to their intensive industrial utilisation. They are broadly applied in specialty fibers, plastics, packaging, films and engineering materials.

Within the class of polyesters, aliphatic polyesters are considered important biodegradable polymers. The properties of commercialised biodegradable polymeric materials, such as melting point or mechanical properties, are usually rather poor and below the requirements for many applications. In order to improve the material characteristics, aromatic monomers are introduced into the polyester structure. Aromatic polyesters possess outstanding mechanical and processing properties. They are however not biodegradable. The biodegradability of aliphatic-aromatic co-polyesters decreases with the increase of the aromatic part in the chain.[1-5]

Ecoflex® is the trade name for thermoplastic co-polyester produced by BASF and represents an interesting group of biodegradable co-polyesters. The co-polyester (abbreviated as BTA) is composed of terephthalic acid (T), adipic acid (A), and 1, 4-butanediol (B) monomers. The biodegradability has been intensively evaluated by many authors.[1-3, 6, 7] The thermal properties of the polymer composition have been studied by means of DSC,[4] and the general structures and composition information have been investigated by using NMR and GC-MS.[7-9]

Over the last decades, the development of 'soft' ionisation methods such as electrospray ionisation (ESI)[10, 11] and matrix-assisted laser desorption/ionisation (MALDI)[12, 13] allowed mass spectrometry to become an important tool for the characterisation of synthetic polymers.[14-16] Adamus *et al.*[5, 17] have demonstrated that the copolyester structure (random or block) can be investigated using multistage mass spectrometry (MS^n) with various soft ionisation techniques. ESI generates multiply charged ions allowing the detection and subsequent characterisation of synthetic polymers of relatively high molecular weight.

Information such as average molecular weight and dispersity may be obtained.[18] Multistage mass spectrometry (MS^n) has been employed to many synthetic polymer systems for structural analysis. Many instruments for multistage mass spectrometry have been developed which perform MS/MS; tandem quadrupole-time-of-flight[19-21] is the example of a method of performing MS/MS in space. Ion trap[22-26] instruments allow MS/MS data to be generated in time and therefore also facilitate MS^n ($n>2$).

The combination of liquid chromatography with mass spectrometry (LC-MS) is often applied to polymer characterisation in order to avoid effects such as ion suppression that lead to mass discrimination in the detection of higher-mass portions of the material. The online connection of gradient polymer elution chromatography (GPEC) to MS separates the polymer distribution according to its molecular weight on the column used.

In this chapter, a combination of characterisation techniques was used to study the structure of BTA oligomers by partial degradation under alkaline conditions. The molecular weight distribution was determined by GPC. Qualitative and quantitative results were obtained by various NMR techniques (including ^1H, ^{13}C, DEPT, Correlation). A comprehensive study using LC-ESI MS^n was performed to get detailed structural information on both the original BTA and its partially degraded products. Although the original BTA has a relatively large molecular weight, studying its low molecular weight oligomers will provide important information on the general structure. On the other hand, the degradation products which mostly have low molecular weights fit in the detection range of multistage mass spectrometry. Hence, the majority of the degradation products could be studied using LC-MS^n.

7.2 Experimental Section

7.2.1 Sample degradation

Poly[(tetramethylene terephthalate)-co-(tetramethylene adipate)], BTA, was kindly supplied by BASF Ludwigshafen. The BTA partial degradation was carried out under

alkaline conditions, similar to the method described by Adamus *et al.*.[5] The starting BTA sample, in the form of granulate, was dissolved in chloroform ($CHCl_3$) (POCH, Gliwice, Poland). Degradation was performed in the mixture (1:5 v/v) of 1.5 mol/L aqueous solution of tetrabutylammonium hydroxide (TBA OH) (Sigma-Aldrich Chemie GmbH, Steinheim, Germany) and methanol (POCH, Gliwice, Poland). The procedure was performed at 35 or 75 ^oC.

7.2.2 Characterisation Methods

7.2.2.1 Gel Permeation Chromatography

The dispersity of the polymers was evaluated by gel permeation chromatography (GPC). The experiments were performed in $CHCl_3$ at 35^oC, at a flow rate of 1mL/min using a Viscotek VE 1122 solvent delivery system with 2xPLgel 5 μm Mixed-C columns (300x7.5mm ID) in series. A Shodex SE 61 refractive index detector was used as for detection of the eluate. A volume of 100 μL of the sample solution in $CHCl_3$ (in concentration 3mg/mL) was injected. OmniSec 4.1 software was used to compute the average molar masses of the samples. Low dispersity polystyrene standards were used to generate a calibration curve. The weight average molecular weights of the calibration samples were from 580 – 3,000,000.

7.2.2.2 Nuclear Magnetic Resonance Spectroscopy

All NMR spectra were recorded on a Bruker Avance III 600 MHz spectrometer (resonance frequencies 600.13 MHz for ^1H and 150.90 MHz for ^{13}C) equipped with a 5 mm broadband probe head with z-gradients and using standard Bruker pulse programs.

The sample concentration was typically between 10 and 15% m/m in deuterated chloroform containing 0.03 % v/v TMS. Chemical shifts are given in values of ppm, referenced to tetramethylsilane (TMS) at 0 ppm for ^1H and to the residual solvent signal at 77.1 ppm for ^{13}C in $CDCl_3$.

^{1}H-NMR data were collected with 64k complex data points and were apodised with an Exponential window function (lb = 0.3) prior to Fourier transformation. The spectral width was 20 ppm and the relaxation delay (d1) was 3s.

^{13}C and DEPT135 spectra with WALTZ16 ^{1}H decoupling were acquired using 64k complex data points and were apodised with an Exponential window function (lb = 3) prior to Fourier transformation. The spectral width was 240 ppm and the relaxation delay (d1) was 2s.

gs-HMBC spectra are recorded with a 8192 x 128 matrix with 2 or 8 transients (scans) per t1 increment and were apodised in both dimensions with a shifted sine squared function (QSINE, SSB=0). The spectral width was 12 ppm for the 1H dimension and 250 ppm for the ^{13}C dimension and the relaxation delay (d1) was 1.5s.

7.2.2.3 Liquid Chromatography – Mass Spectrometry

Samples with a concentration of 3 mg/mL in THF were prepared. The LC system used for separation was Agilent 1100 series LC binary pump with DAD detector. The LC column in the LC-ESI-MS setup was an Alltech Kromasil C18 (150 mm * 4.6 mm). During analysis, the column was maintained at 30 °C. A gradient of 10% tetrahydrofuran (THF) (Sigma-Aldrich) / 90% H_2O (from Millipore Direct-Q) to 100% tetrahydrofuran (THF) was used as mobile phase. 0.1% formic acid (FA) (Fluka) was added to both mobile phases. The running time of the gradient was 40 minutes. In most of the cases, sodium iodide (NaI) was added post-column using a Cole-Parmer 74900 series syringe pump at 0.6 ml/h. It was dissolved in THF (Sigma-Aldrich) at an approximate concentration of 1 μg/mL. The mass spectrometer used in this study was a Bruker Esquire 3000plus. The nebuliser pressure of this instrument was set to 60.0 psi, the drying gas flow to 11.0 L/min and the drying gas temperature to 360 ^{o}C. The maximum accumulation time was 50.0 ms. Data were processed and analysed using Bruker DataAnalysis 3.3.

7.3 Results and Discussion

7.3.1 Gel-permeation Chromatography

As a first level of observation of the effect of degradation on the BTA, GPC was applied to investigate the changes in the molecular weight distribution. The GPC traces of the original BTA sample (BTA-O) (a), the partial degradation products from the 35 ^oC process (BTA-35) after 2 hrs (b) and from the 75 ^oC process (BTA-75) after 2 hrs (c) are displayed in the Figure 7.1. The RI detector was used for detection. The molecular mass and dispersity data based on calibration with polystyrene standards are listed in Table 7.1.

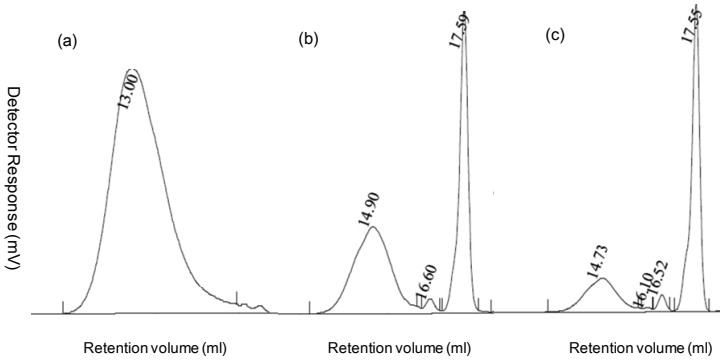

Figure 7.1. (a) GPC traces of the original BTA sample (BTA-O), (b) the degradation product from the 35 ^oC process (BTA-35) after 2 hrs and(c) the degradation product from the 75 ^oC process (BTA-75) after 2 hrs

A substantial decrease in molecular weight and increase in dispersity of the degradation product mixture were observed. The GPC trace of the sample from the 35 ^oC process indicated a trimodal molecular weight distribution, the first peak of which represented some degradation products with M_n of 3900 and M_w of 5600. The last and the most intense peak obviously had a very low molecular weight (M_n and M_w were calibrated against polystyrene). This indicates that the majority of the original BTA has been degraded to small molecules although the process is not 100% completed. Similarly, the GPC of the sample from the 75 ^oC process also had a trimodal molecular weight distribution. The molecules having number average molecular weight of 5500 was observed while the M_n of

most of the products was in the range of 170 – 600 Da. Compared to the partial degradation at 35 ^{o}C, it has less high molecular weight fractions left. The reaction in the higher temperature is more progressed although the structures of the degraded products in both temperatures are similar (explained in NMR and LC-MS^{n} section). The increased kinetics due to the increasing of temperature is a possible cause of this effect.

Table 7.1. The weight average molecular weight mass (M_w), number average molecular weight (M_n) and dispersity of the untreated and degraded BTA samples.[a]

Sample	Number average molecular weight (M_n) [Da]	Weight average molecular weight (M_w)[Da]	Dispersity ($Đ$)
BTA-O	$1.6x10^4$	$3.8x10^4$	2.3
BTA-35	320	3000	9.4
BTA-75	230	760	3.3

[a] Low dispersity polystyrene standards were used to generate a calibration curve.

7.3.2 Nuclear Magnetic Resonance Spectroscopy

Analysis by ^{1}H NMR spectroscopy determined that the proportions of the monomers in the original sample were 23.5 mol% of terephthalic acid, 26.6 mol% of adipic acid and 49.9 mol% of 1, 4-butanediol. The result agrees well with the estimation in several other studies.[3, 6, 8] Figure 7.2 shows the ^{13}C and DEPT NMR spectra of BTA-O and BTA-75. Scheme 7.1 shows the corresponding structures for the assignment of the carbon signals in Figure 7.2. BTA-35 has very similar ^{13}C spectra to BTA-75.

Comparing the degraded BTA to the original sample, several characteristic peaks appeared. The DEPT spectrum of the degraded sample indicates that peaks 12, 29, 39 and 42 are either primary or tertiary carbons. The long range J_{C-H} couplings in HMBC spectra show the coupling from the hydrogens of carbons 12, 39 and 42 to carbonyl carbons. In proton NMR, the peaks 12, 39 and 42 are all singlet so they have no coupling neighbors. Combined with their peak positions (between 3.5 ppm and 4.0 ppm), they are all assigned to methyl esters which are the methyl end groups appearing in the degradation process. The possible cause of the appearance of CH_3 end groups is the methanol transesterification taking place at the conditions of partial alkaline degradation in the presence of water/methanol system. Peak 29, on the other hand, was assigned to the methyl group of

the tetrabutyl ammonium ion due to its peak position in carbon NMR and triplet presence in proton NMR.

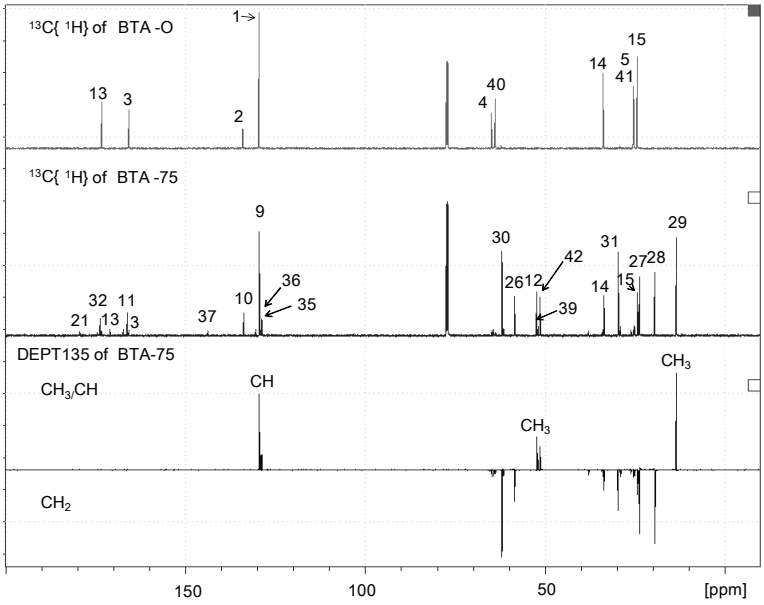

Figure 7.2. ^{13}C NMR spectrum of BTA-O, ^{13}C and DEPT NMR spectra of BTA-75.

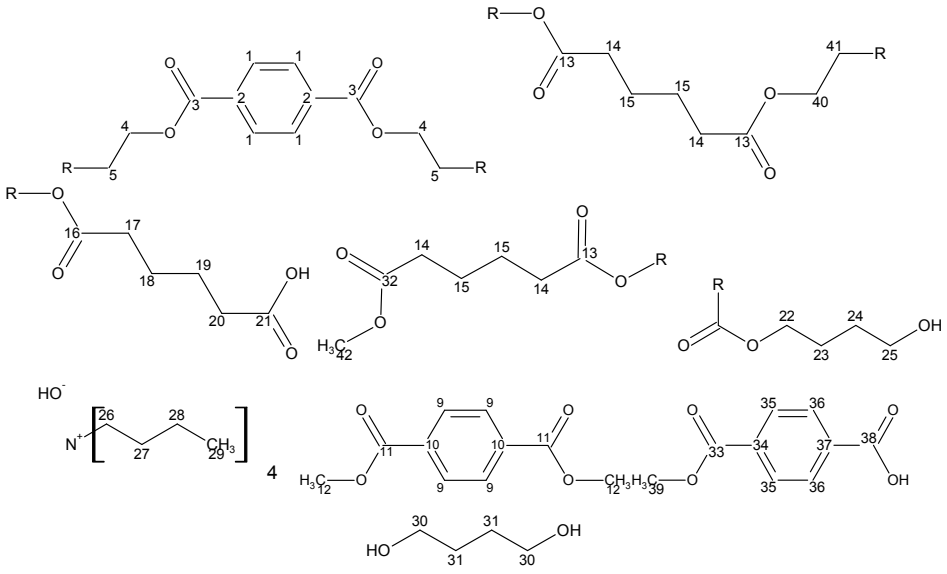

Scheme 7.1. Structures corresponding to the assignment of peaks in Figure 7.2.

The CH_2 peaks 30 and 31 were assigned to the CH_2 in the backbone of free 1, 4-butanediol, based on the ^2J coupling of C31-H30, ^2J coupling of C31-H31 and ^1J coupling of C30-H30 in the HMBC experiment, shown in Figure 7.3. ^2J coupling of C30-H31 and ^1J coupling of C31-H31 were also observed but are not denoted in the spectrum because of peak overlap.

The structural assignment above indicates the abundance of methyl end groups in comparison to the polymer / oligomer backbones in the partially degraded samples. The existence of free 1, 4-butanediol in the degraded samples also proved the partial degradation was a relatively complete reaction.

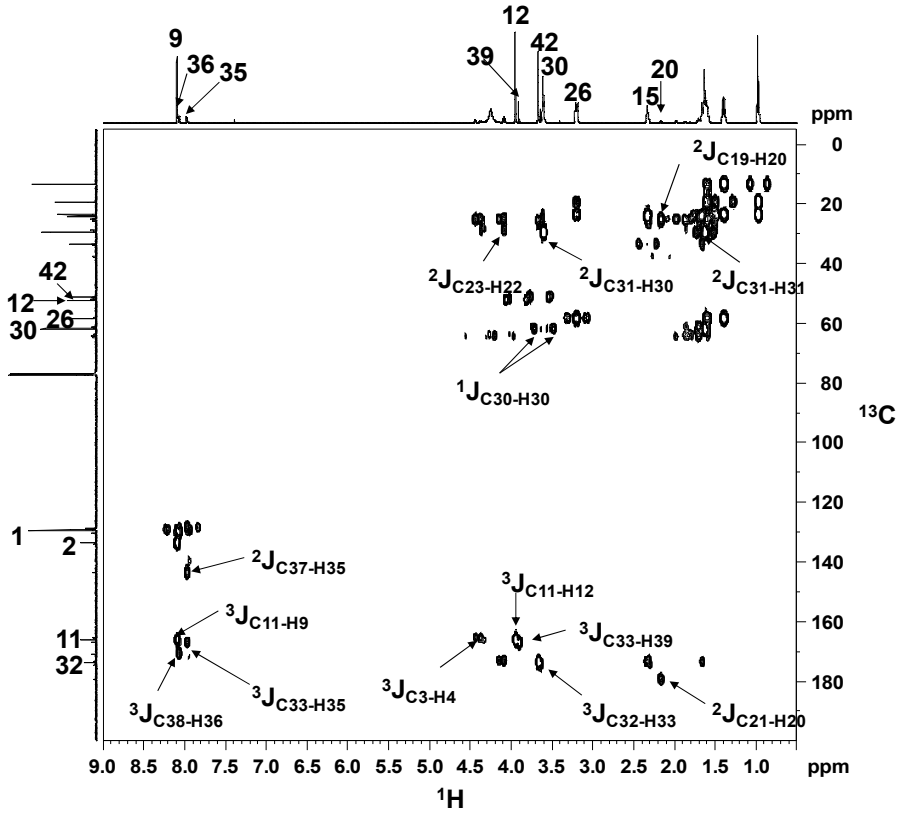

Figure 7.3. HMBC spectra of BTA-75 with assignment of J couplings.

7.3.3 Liquid Chromatography – Multistage Mass Spectrometry

Figure 7.4(a) shows LC-MS data showing log abundance of $[M-H]^-$ (data point weight) versus *m/z* (as y-axis) versus chromatographic elution time (as x-axis). Figure 7.4(b) shows the abundance of the BTA molecules with positive adduct ions versus *m/z* (as y-axis) versus chromatographic elution time (as x-axis). Summation of the data shown in Figure 7.4 over the elution time from 15 to 32 minutes resulted in the mass spectra shown in Figure 7.5(a) and 7.5(b). The detection range of the MS data covers part of the first two peaks in the GPC data shown above. The products in the last GPC peak have very low molecular weight and are therefore not observed in MS.

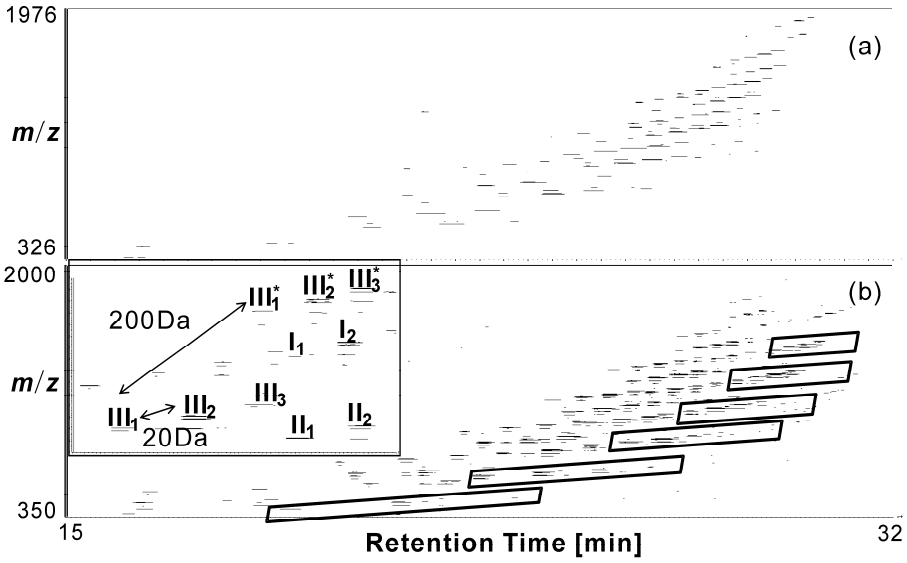

Figure 7.4. (a) LC-MS data obtained on sample BTA-O showing log abundance of $[M-H]^-$ (line weight) versus *m/z* (as y-axis) versus chromatographic elution time (as x-axis). (b) The abundance of the BTA molecules with adduct ions versus *m/z* (as y-axis) versus chromatographic elution time (as x-axis). The insert is the expanded region of (b) with *m/z* 800 – 1100 (y-axis) and elution time from 23 – 27 mins (x-axis).

The *m/z* differences between the peaks in Figure 7.4(a) and 7.4(b) is 24, which is observed in the corresponding spectra 7.5(c) and 7.5(d), e.g. , I_1 in 7.5(c) (*m/z* 945.7) and 7.5(d) (*m/z* 969.5). The cause of the mass shift is that the mass of the $[M+Na]^+$ is *m/z* 24

greater than that of the corresponding $[M-H]^-$ ion. The corresponding peaks surrounded by boxes in 7.4(b) are not seen in 7.4(a). Expanded spectra (*m/z* 800 – 1100) of 7.5(a) and 7.5(b) are shown in 7.5(c) and 7.5(d). The most intense series of peak in $[M+Na]^+$ spectrum 7.5(b), labeled as II, has no corresponding series (*m/z* 24 less) in the negative ion mode. We assigned these peaks to those molecules with cyclic structures. The cyclic polyester structures were

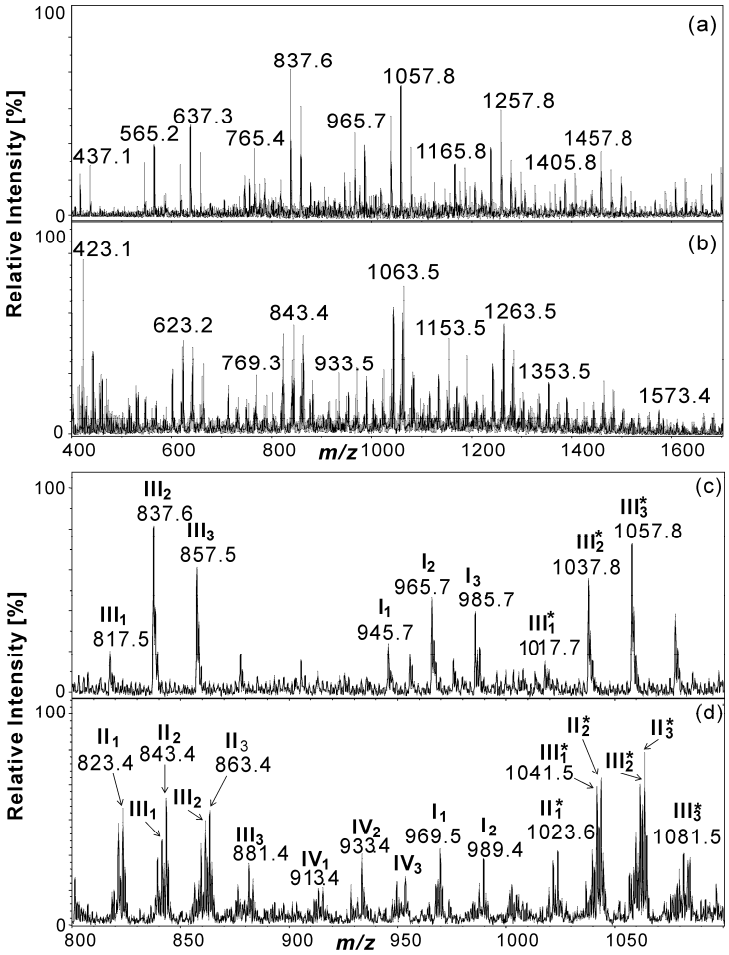

Figure 7.5. The summation (15' -32') LC-MS spectra of BTA-O: (a), (b) the corresponding spectra to Figures 7.4(a) (negative ion mode) and 7.4(b) (positive ion mode), respectively, (c) the expanded (*m/z* 800-1100) version of Figure 7.5(a) and (d) the expanded (*m/z* 800-1100) version of Figure 7.5(b).

not ionised in negative scan mode, due to absence of an acidic (easily abstractable) proton, but with adduct ions in positive mode, they are easily ionised and observed. The mass-to-charge ratios of the cyclic copolyesters agree well with the structure assignment. Further LC-MS^n results also support this interpretation, which will be shown later in this chapter. Similarly, Series IV were assigned to the copolyesters without an acid end group (only have alcohol end groups). They were also observed in positive scan mode but not in negative scan mode which is dominated by carboxyl end group ions.

The inset in the three-dimensional plot (Figure 7.4(b)) and Figure 7.5(b) clearly demonstrate the presence of a difference of *m/z* 20 between eluting oligomers (such as III_1, III_2 and III_3). The mass difference corresponds to the difference between the molecular weight of a butylene adipate (BA, molecular weight: 200 Da) and a butylene terephthalate (BT, molecular weight: 220 Da) unit. A homologous series with peak-to-peak mass increments of 200 Da, such as between III_1 and III_1*, is also observed. This mass increment exactly equals the mass of the repeating unit of BA. In addition, different combinations of B, A and T result in different compositions. The corresponding mass increments were 72 Da (one extra B) and 128 Da (one extra A) which were also observed in the spectra. Series III were observed in both negative and positive ion scan spectra with *m/z* 24 mass differences (mass differences of the $[M+Na]^+$ and the corresponding $[M-H]^-$ ion). Furthermore, the corresponding positive and negative ions also have the same LC elution time, for example, III_1 at 24.4 mins. This confirmed that the ions with 24 mass differences in the two scan modes have the same structure.

Using these mass differences the assignments of homologous combinations of the polymer building blocks, 1, 4-butanediol (B), terephthalic acid (T) and adipic acid (A) (all three are without H_2O in the structure, hence as residue) listed in Table 7.2 could be made in the *m/z* 663-1009 mass range of the positive ion spectra. These results indicate that the polymers present in the original sample can both be linear and cyclic. The cyclic molecules detected all contain a number of B monomers that equals the sum of the number of T and A monomers, which is in line with the structural requirements of cyclic co-polyesters. The linear molecules all have net water (H_2O) end groups but in three different ways, *viz.* (1) with one alcohol end groups at both ends, (2) one alcohol and one acid end group and (3) one acid end groups at both ends.

Table 7.2. Monomer composition assignments of the spectrum in Figure 7.5(b).

Mass (*m/z*)	Structure Assignments ($-Na^+$)	Mass (*m/z*)	Structure Assignments ($-Na^+$)	Label in Figure 7.5(d)
641	$H(AB)_3OH$	841	$H(AB)_4OH$	III_1
661	$H(AB)_2(TB)OH$	861	$H(AB)_3(TB)OH$	III_2
681	$H(AB)(TB)_2OH$	881	$H(AB)_2(TB)_2OH$	III_3
713	$HB(AB)_3OH$	913	$HB(AB)_4OH$	IV_1
733	$HB(AB)_2(TB)OH$	933	$HB(AB)_3(TB)OH$	IV_2
753	$HB(AB)(TB)_2OH$	953	$HB(AB)_2(TB)_2OH$	IV_3
769	$H(AB)_3AOH$	969	$H(AB)_4AOH$	I_1
789	$H(AB)_3TOH$	989	$H(AB)_4TOH$	I_2
809	$H(AB)_2(TB)TOH$	1009	$H(AB)_3(TB)TOH$	
623	Cyclic $(AB)_3$	823	Cyclic $(AB)_4$	II_1
643	Cyclic $(AB)_2(TB)$	843	Cyclic $(AB)_3(TB)$	II_2
663	Cyclic $(AB)(TB)_2$	863	Cyclic $(AB)_2(TB)_2$	II_3

LC-MS^n spectra of the cyclic structures are very different to those of the linear structures. Figure 7.6 shows the MS^2 and MS^3 spectra of the cyclic structure $[(AB)_3+Na]^+$ (elemental composition $[C_{30}H_{48}O_{12}Na]^+$) detected at *m/z* 623. The first neutral loss (*m/z* 54) is only observed in the MS^2 spectra of cyclic but not in the tandem mass spectra of the linear structures. Peaks *m/z* 495.3 and *m/z* 477.3 are observed in the MS^2 spectra of *m/z* 623.4 but not in the MS^3 spectra of *m/z* 569. Therefore, the formation of these two peaks is attributed to direct neutral losses of 128 and 146, respectively. The other peaks in the MS^2 spectrum can all be attributed to neutral losses amounting to combinations of 54, 72, 128 and 146.

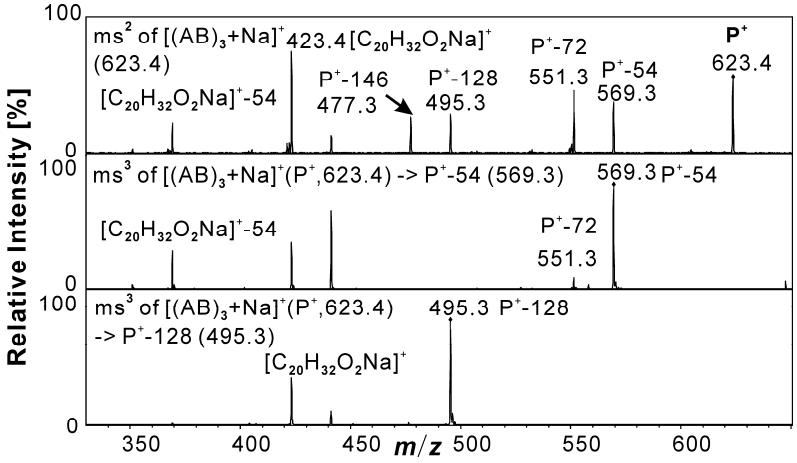

Figure 7.6. The MS^2 and MS^3 spectra of the cyclic structure $[(AB)_3+Na]^+$ ($[C_{30}H_{48}O_{12}Na]^+$) detected at *m/z* 623 in BTA-O.

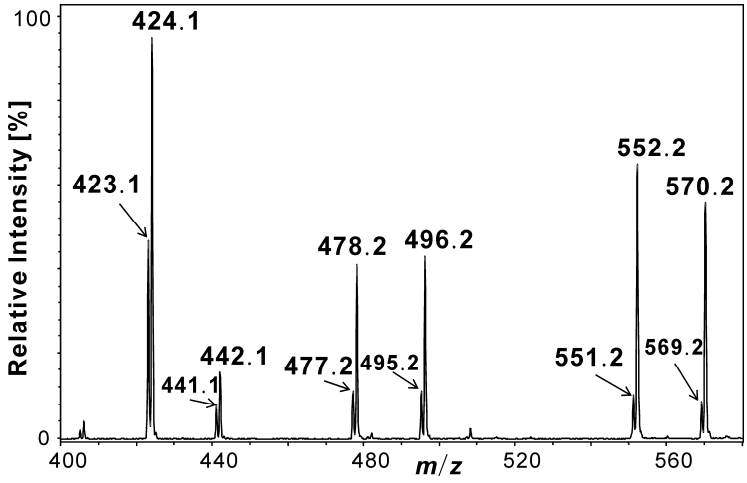

Figure 7.7. The MS^2 spectrum of first ^{13}C isotope peak m/z 624 (precursor peak not shown) in BTA-O.

The possible elemental composition of the first neutral loss (*m/z* 54) could be C_3H_2O or C_4H_6 (based on the raw materials used in the reaction and the isotope pattern of the parent ion suggesting that it only contains C, H and O). An alternative approach, using MS^2 on the first ^{13}C isotope peak, was developed to identify the elemental composition of the neutral loss so that high accuracy MS^2 instrument is not needed. *m/z* 624, the first ^{13}C isotope peak of *m/z* 623, contains one ^{13}C and twenty nine ^{12}C. Theoretically, MS^2 on *m/z* 624 will generate two peaks, at *m/z* 570 and 569. If the neutral loss contains three carbons, the ratio of the peak intensities of *m/z* 570 and 569 should be 27:3, *viz.* 9. On the other hand, the ratio of the four carbons' case would be 26:4, *viz.* 6.5.

Table 7.3 shows the average peak intensity of several peaks in the MS^2 spectra of *m/z* 624. The spectrum is shown in Figure 7.7. The data were generated in three experiments using the same instrumental setting. Relatively long acquisition times were used to minimise the experimental errors. The fragmentation amplitude used was 0.35 V to achieve 50% surviving yield[27] of the precursor ion at *m/z* 624.

The peak intensity ratio of *m/z* 570 and 569 is 6.4. The standard deviation of the intensity ratio is 0.03. Therefore, the *m/z* 54 loss contains four carbons and the elemental composition is assigned as C_4H_6. Likewise, the elemental compositions of the loss of 72,

was assigned to C_4H_8O (B-residue), the aforementioned attributions of neutral losses 128 (A-residue, $C_6H_8O_3$), 146 (adipic acid, $C_6H_{10}O_4$), 182 (128 A-residue, $C_6H_8O_3$ + 54 B-residue, C_4H_6) and 200 (AB, $C_{10}H_{16}O_4$) were confirmed. The standard deviations of the experiments were 0.04, 0.00(1), 0.08, 0.02 and 0.09, respectively. The calculated ratios are all lower than the theoretical values. The underestimation of the first fragment peak resulting from the peak integration algorithm used could be the cause.

All the elemental compositions of the fragments in the following spectra were determined using the same method (MS^2 on the first ^{13}C isotope peak of the parent ion followed by comparison of the intensity ratio of the fragment peak pairs with the theoretical isotope ratios of proposed elemental compositions) as described above.

Table 7.3. Intensities and ratios of the peaks generated in the MS2 of first ^{13}C isotope peak m/z 624 in the mass spectrum of BTA-O.

P+	m/z: 624	Theoretical	Exp.1	Exp.2	Exp.3	Average	Standard Deviation
Frag 1	570	26	2515	2812	2798		
Frag 1*	569	4	396	435	439		
ratio 1:1*		6.50	6.35	6.46	6.37	6.40	0.03
Frag 2	552	26	2896	3220	3245		
Frag 2*	551	4	474	518	516		
ratio 2:2*		6.50	6.11	6.22	6.29	6.20	0.04
Frag 3	496	24	2041	2147	2165		
Frag 3*	495	6	523	559	562		
ratio 3:3*		4.00	3.90	3.84	3.85	3.87	0.00(1)
Frag 4	478	24	1908	2070	2054		
Frag 4*	477	6	488	567	562		
ratio 4:4*		4.00	3.91	3.65	3.65	3.74	0.08
Frag 5	442	20	733	806	787		
Frag 5*	441	10	373	407	403		
ratio 5:5*		2.00	1.97	1.98	1.96	1.97	0.02
Frag 6	424	20	4286	4774	4747		
Frag 6*	423	10	2290	2362	2351		
ratio 6:6*		2.00	1.87	2.02	2.02	1.97	0.09

In the MS^2 spectra of the linear structure $[HB(AB)_4OH+Na]^+$ at *m/z* 913, Figure 7.8, there is no *m/z* 54 loss (C_4H_6) as observed in the spectra of cyclic structures. Basically, three kinds of losses were observed. The loss of *m/z* 72 (C_4H_8O) is from monomeric unit B, *m/z* 128 ($C_6H_8O_3$) is from monomeric unit A and *m/z* 166 ($C_8H_6O_4$) is from monomeric unit

T. All the fragments mentioned above can be explained by ester bond cleavages of the precursor ions. The consecutive losses of two *m/z* 72 (C_4H_8O) from *m/z* 913 indicates B residues are present at both ends of the chain.

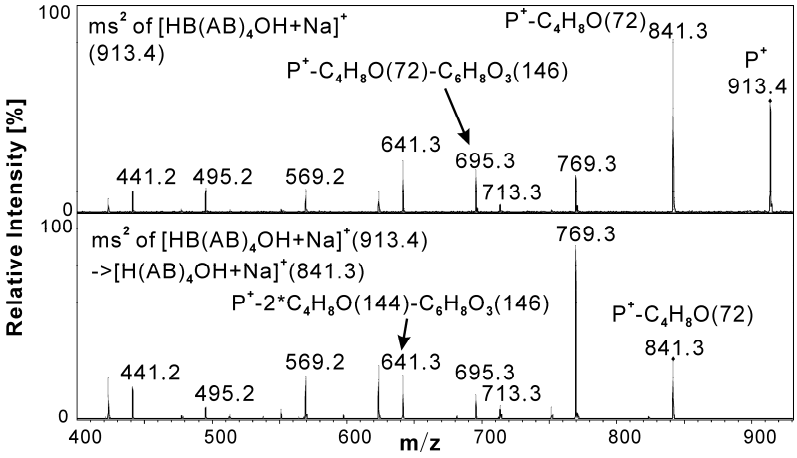

Figure 7.8. The MS^2 and MS^3 spectra of linear structure $[HB(AB)_4OH+Na]^+$ at *m/z* 913 in of BTA-O.

By studying the different fragmentation patterns of the structural isomers, the sequence of the monomeric unit in certain structures could be revealed. For example, $[H(AB)_2(TB)OH+Na]^+$ (*m/z* 661) has three different structural (monomer sequence) isomers, shown in Scheme 7.2.

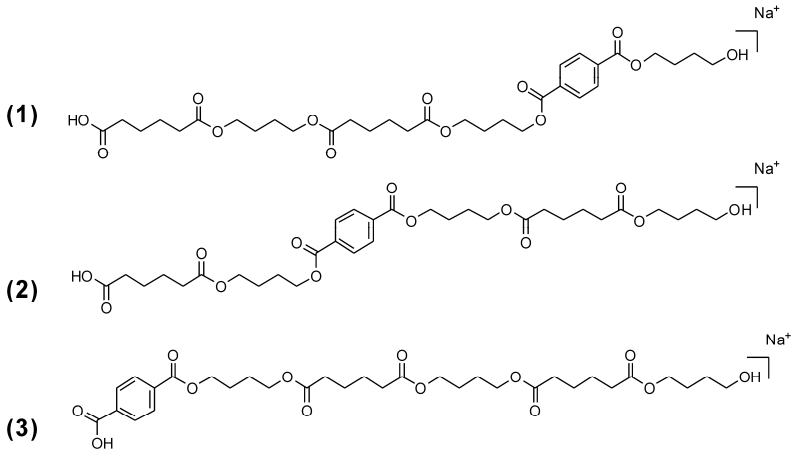

Scheme 7.2. Possible sequences of $[H(AB)_2(TB)OH+Na]^+$ (m/z 661 detected in BTA-O).

Figure 7.9(a) is the extracted ion chromatogram of *m/z* 661 in an LC-MS^2 experiment. Two peaks in the chromatogram indicate that at least two different structural isomers are present. Figure 7.9(b) shows the MS^2 spectra of *m/z* 661 at the two retention times corresponding to the two peaks in the chromatogram. Clearly, the two spectra are different, indicating different fragmentation pathways and structures. A neutral loss of 72 (C_4H_8O) observed in both spectra confirms that a B residue is present at the end of the chain. This is in line with the monomer composition (i.e. the number of B residues being equal to the sum of the T and A residues). However, in the mass spectrum of the first chromatographic peak a neutral loss of 128 ($C_6H_8O_3$) corresponding with the mass of an A residue is observed, that is not observed in the mass spectrum of the second chromatographic peak. Therefore monomeric unit A must form an endgroup of the chain. On the other hand, the occurrence of the loss of *m/z* 166 ($C_8H_6O_4$, terephthalic acid) in the mass spectrum of the second chromatographic peak indicates that the substance eluting there has a terephthalic monoester as end group of the structure.

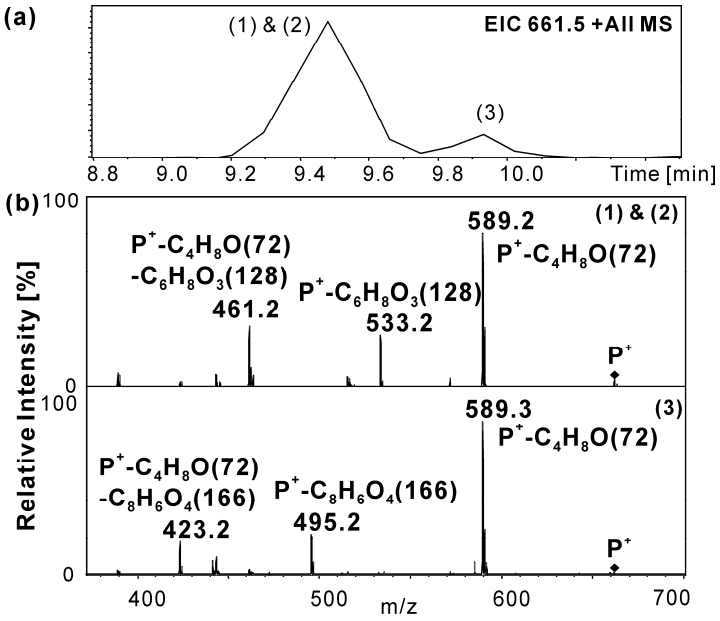

Figure 7.9. (a) The extracted ion chromatograms of $[H(AB)_2(TB)OH+Na]^+$ (m/z 661) in LC-MS^2 of BTA-O. (b) The MS^2 spectra of $[H(AB)_2(TB)OH+Na]^+$ (m/z 661) at two retention times corresponding to the two peaks in the extracted ion chromatogram.

Therefore, the structures in the Scheme 7.2 were assigned to the chromatogram and the spectra as indicated by the labels in Figure 7.9. The first peak in the EIC and the corresponding spectrum were generated by structure (1) and (2) and the second peak and its spectrum were from structure (3).

The LC-MS spectra of BTA-35 and BTA-75 showed no difference in either peaks or their intensity. The very early elution time of TBA OH in the chromatography of the degraded samples avoids interference of the usually dominant TBA OH signal with the mass spectra of the degraded products in LC-MS. The summation (5' - 32') LC-MS spectrum of BTA-75 is shown in Figure 7.10. Clearly, changes of mass were observed in the spectrum of BTA-75 compared to the spectrum of BTA-O. The peak from cyclic structures are not observed in the spectra anymore; apparently they were converted to linear structures during the hydrolysis / degradation process and went through methanol transesterification to form methyl end groups.

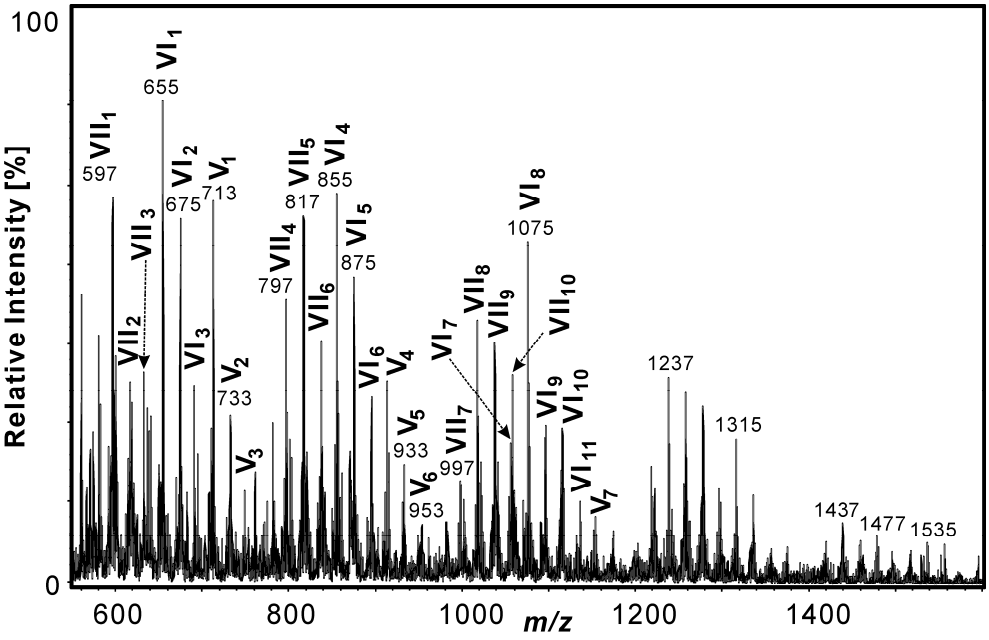

Figure 7.10. The summation (5' - 32') LC-MS spectrum of BTA-75.

Peaks with different residual masses were labeled as such, 3 as series V, 5 as series VI and 7 as series VII and assigned to three end groups. Series V are those BTA with alcohol

end groups at both ends. They were not transesterified by methanol in the hydrolysis / degradation process. Therefore the end groups remained the same. The unchanged MS^n spectra of these peaks also confirmed this point. Series VI are the BTAs with one alcohol end group at one end and an acid end group at the other. For these molecules the methanol transesterification that took place in the hydrolysis / degradation process resulted in a net change of *m/z* 14 in the end group, which is attributed to a methyl end group (CH_3) instead of hydrogen (H). Series VII are those BTAs with a methyl end group at each end.

Figure 7.11 is the MS^2 spectrum of *m/z* 797.5 from series VII. A unique loss of *m/z* 160 is observed in peaks from series VII that is not observed in the other series. Two consecutive losses of *m/z* 160 from 797.5 to 637.3 and then to 477.2 are observed in the spectrum, which indicates the loss of same end groups on both sides of the structure. MS^2 on the first ^{13}C isotope peak of the parent ion indicated that the elemental composition of the m/z 160 is $C_7H_{12}O_4$ and indicates the presence of adipic acid methyl ester end groups.

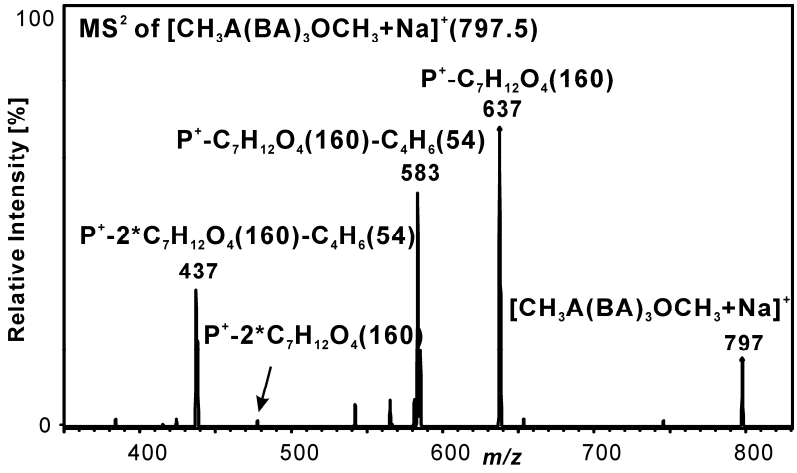

Figure 7.11. The MS^2 spectra of $[CH_3A(BA)_3OCH_3+Na]+$ (m/z 797.5) from series VII detected in sample BTA-75.

The components determined in the degraded BTAs by using $LC\text{-}MS^n$ are slightly different than those proposed from NMR data. The NMR data show the existence of free 1, 4-butanediol in the degraded samples of BTA but MS did not detect noticeable concentration of 1, 4-butanediol. The molecular weight of 1, 4-butanediol is quite low (m/z

90) which does not fall in the optimised detection range of the mass spectrometer. Traces of acidic endgroups that were not transesterified were also found in NMR spectra. In the MS data of the degraded BTA no ions with hydroxyl endgroup were observed. The possible causes are either the molecules with such structures having very low molecular weight or the abundance being too low.

7.4 Conclusions

The results of this chapter revealed that molecular level structure of BTA copolyester and its partial degraded products could be determined by the LC-MS^n analysis. The partial degradation of this aliphatic – aromatic copolyester was successfully carried out under alkaline conditions in 35 ^oC and 75 ^oC, respectively, using water/methanol system. The GPC results showed that the process at 75 ^oC is a more drastic one and leads to a more progressed reaction than the process at 35 ^oC. The number (M_n) and weight (M_w) average molecular weight decreased significantly and the dispersity increased in both cases.

NMR confirmed the presence of -$COOCH_3$ end group in the degraded samples. It proved the occurrence of methanol transesterification during the partial degradation. The existence of free 1, 4-butanediol confirmed the partial degradation under alkaline was a very progressed reaction.

Degraded samples from both temperatures showed very much the same spectra both in NMR and LC-MS or LC-MS^n. It is therefore concluded that temperature influences the extent but not the nature of the degradation reaction.

Detailed endgroup structures of both original and partially degraded samples were assigned by using LC-MS and LC-MS^n. The cyclic structures, that were not clearly identified using NMR, were discovered in the original sample (but not in the degraded ones). The transesterification by methanol was confirmed. The MS^2 experiment on the first ^{13}C isotope peak helped to confirm the elemental composition of the fragments. It may be used to provide an alternative for high mass accuracy MS^2 experiments, when such an

instrument is not available in the lab. LC-MS^n also revealed sequence information of certain copolymeric structures.

References

(1) Witt, U.; Müller, R. J.; Deckwer, W. D. *Macromol. Chem. Phys.* **1996,** *197*, 1525-1535.
(2) Witt, U.; Müller, R. J.; Deckwer, W. D. *J. Polym. Environ.* **1997,** *5*, 81-89.
(3) Marten, E.; Müller, R. J.; Deckwer, W. D. *Polym. Degrad. Stab.* **2005,** *88*, 371-381.
(4) Dacko, P.; Kowalczuk, M.; Janeczek, H.; Sobota, M. *Macromol. Symp.* **2006,** *239*, 209-216.
(5) Adamus, G.; Sikorska, W.; Kowalczuk, M.; Montaudo, M.; Scandola, M. *Macromolecules* **2000,** *33*, 5797-5802.
(6) Witt, U.; Yamamoto, M.; Seeliger, U.; Müller, R.-J.; Warzelhan, V. *Angew. Chem., Int. Ed.* **1999,** *38*, 1438-1442.
(7) Rychter, P.; Kawalec, M.; Sobota, M.; Kurcok, P.; Kowalczuk, M. *Biomacromolecules* **2010,** *11*, 839-847.
(8) Witt, U.; Einig, T.; Yamamoto, M.; Kleeberg, I.; Deckwer, W. D.; Müller, R. J. *Chemosphere* **2001,** *44*, 289-299.
(9) Gan, Z.; Kuwabara, K.; Yamamoto, M.; Abe, H.; Doi, Y. *Polym. Degrad. Stab.* **2004,** *83*, 289-300.
(10) Whitehouse, C. M.; Dreyer, R. N.; Yamashita, M.; Fenn, J. B. *Anal. Chem.* **1985,** *57*, 675-679.
(11) Fenn, J. B.; Mann, M.; Meng, C. K.; Wong, S. F.; Whitehouse, C. M. *Science* **1989,** *246*, 64-71.
(12) Karas, M.; Bachmann, D.; Bahr, U.; Hillenkamp, F. *Int. J. Mass Spectrom. Ion Processes* **1987,** *78*, 53-68.
(13) Karas, M.; Hillenkamp, F. *Anal. Chem.* **1988,** *60*, 2299-2301.
(14) Hanton, S. D. *Chem. Rev.* **2001,** *101*, 527-570.
(15) McEwen, C. N.; Peacock, P. M. *Anal. Chem.* **2002,** *74*, 2743-2748.
(16) Peacock, P. M.; McEwen, C. N. *Anal. Chem.* **2004,** *76*, 3417-3428.
(17) Adamus, G. *Macromolecules* **2009,** *42*, 4547-4557.
(18) Kallos, G. J.; Tomalia, D. A.; Hedstrand, D. M.; Lewis, S.; Zhou, J. *Rapid Commun. Mass Spectrom.* **1991,** *5*, 383-386.
(19) Jackson, A. T.; Scrivens, J. H.; Williams, J. P.; Baker, E. S.; Gidden, J.; Bowers, M. T. *Int. J. Mass Spectrom.* **2004,** *238*, 287-297.
(20) Jackson, A. T.; Slade, S. E.; Scrivens, J. H. *Int. J. Mass Spectrom.* **2004,** *238*, 265-277.
(21) Jackson, A. T.; Slade, S. E.; Thalassinos, K.; Scrivens, J. H. *Anal. Bioanal. Chem.* **2008,** *392*, 643-650.
(22) Chen, R.; Li, L. *J. Am. Soc. Mass Spectrom.* **2001,** *12*, 832-839.
(23) Chen, R.; Yu, X.; Li, L. *J. Am. Soc. Mass Spectrom.* **2002,** *13*, 888-897.
(24) Arnould, M. A.; Wesdemiotis, C.; Geiger, R. J.; Park, M. E.; Buehner, R. W.; Vanderorst, D. *Prog. Org. Coat.* **2002,** *45*, 305-312.
(25) Wollyung, K. M.; Wesdemiotis, C.; Nagy, A.; Kennedy, J. P. *J. Polym. Sci., Part A: Polym. Chem.* **2005,** *43*, 946-958.
(26) Cerda, B. A.; Horn, D. M.; Breuker, K.; McLafferty, F. W. *J. Am. Chem. Soc.* **2002,** *124*, 9287-9291.
(27) Heeren, R. M. A.; Vékey, K. *Rapid Commun. Mass Spectrom.* **1998,** *12*, 1175-1181.

Appendix 1

Structure illustration of the series resulting from the possible combinations of initiation and termination mechanisms in the radical polymerisation of PBA(A-C).

Series	Initiation	Termination	Structure
β^{2b}	N/A	β-scission pathway β2b then H-abstration	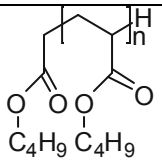
β^{1b}	N/A	β-scission pathway β1b	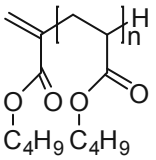
r	Octyl radical from the initiator	H-abstraction or disproportionation 1 / β-scission pathway β1a then H-abstraction or disproportionation 1	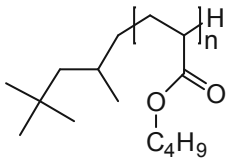
m	Methyl radical from the initiator	H-abstraction or disproportionation 1 / β-scission pathway β1a then H-abstraction or disproportionation 1	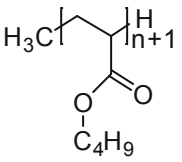
β^{2a}r	Octyl radical from the initiator	β-scission pathway β2a	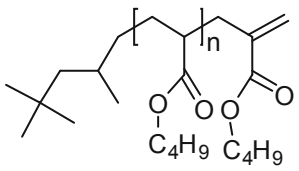
β^{2a}m	Methyl radical from the initiator	β-scission pathway β2a	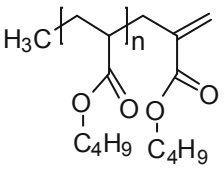

(continue on next page)

Series	Initiation	Termination	Structure
s^1	Solvent radical from xylene / chain transfer to solvent	H-abstraction or disproportionation 1 / β-scission pathway β1a then H-abstraction or disproportionation 1	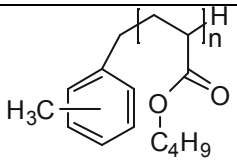
s^2	Solvent radical from pentyl propionate / chain transfer to solvent	H-abstraction or disproportionation 1 / β-scission pathway β1a then H-abstraction or disproportionation 1	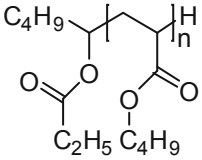
s^3	Solvent radical from butyl acetate / chain transfer to solvent	H-abstraction or disproportionation 1 / β-scission pathway β1a then H-abstraction or disproportionation 1	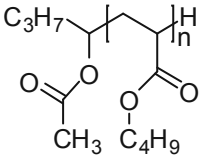
$\beta^{2a}s^1$	Solvent radical from xylene / chain transfer to solvent	β-scission pathway β2a	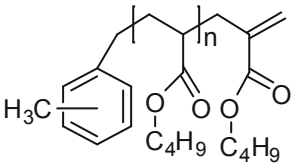
$\beta^{2a}s^2$	Solvent radical from pentyl propionate / chain transfer to solvent	β-scission pathway β2a	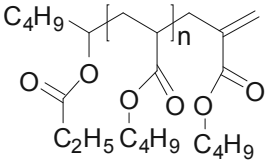
$\beta^{2a}s^3$	Solvent radical from butyl acetate / chain transfer to solvent	β-scission pathway β2a	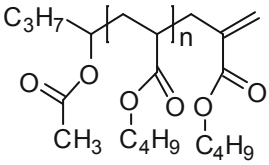

Appendix 2

Identification of elemental compositions of the endgroups appearing in the polymer series using a linear regression method, FTICR MS data.

In the spectra of PMMA, one of the very intense sets of peaks are those from series rh*, *m/z* 335+100*(n-2). The mass-to-charge ratios of seven peaks from this series were plotted against the number of MMA units, as shown in Figure A1.

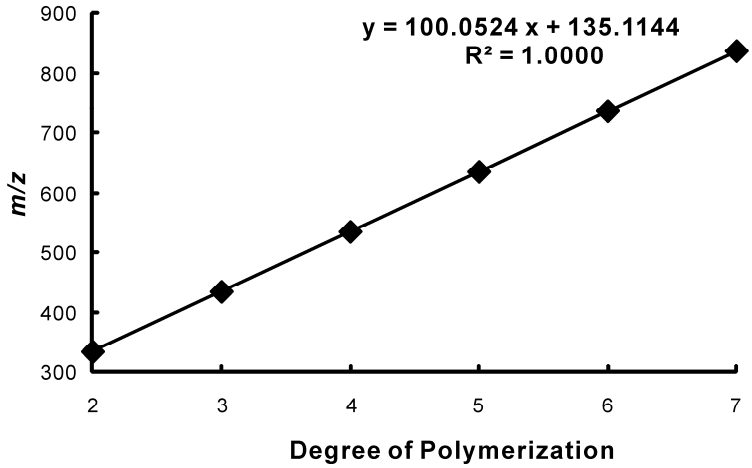

Figure A1. Linear regression of *m/z* peaks of series rh* from PMMA. (m/z 400 - 1200, degree of polymerization 4-10)

The residual mass of the series was 139.1144 Da, as calculated using linear regression. The monomer mass calculated was 100.0524 (the theoretical mass of an MMA monomer is 100.0524, $\Delta < 0.0001$ Da) and its standard deviation was 0.0001. The chemical composition of the combined mass of the end groups is assigned as $[C_8H_{16}+Na]^+$ (the theoretical mass is 139.1144, $\Delta < 0.0001$ Da). The comparison of experimental and theoretical data is presented in Table A1.

Table A1 Comparison of experimental and theoretical data of the peaks series m/z 335+(n–2)*100

Degree of Polymerization	$Mass_{exp}$ (*m/z*)	$Mass_{theo}$ (*m/z*)	Δ (Da)
2	335.2192	335.2193	0.0001
3	435.2716	435.2717	0.0001
4	535.3242	535.3241	0.0001
5	635.3764	635.3766	0.0002
6	735.4290	735.4290	<0.0001
7	835.4812	835.4814	0.0002

The elemental composition of the combined endgroups is attributed to an octyl end group at one end of the chain and and a terminally unsaturated end group at the other end. The structures within this series are resulted from octyl radical initiation and terminated by an unsaturated end group formed by disproportionation.

A similar procedure was also applied to the other series of peaks.

Appendix 3

Identification of elemental compositions of the endgroups appearing in the polymer series using a linear regression method, Orbitrap data.

In the spectra of PMMA, the most intense set of peaks are those from series sh (or mh), *m/z* 439 + (n–3)*100. The mass-to-charge ratios of seven peaks from this series were plotted against the number of MMA units, as shown in Figure S1.

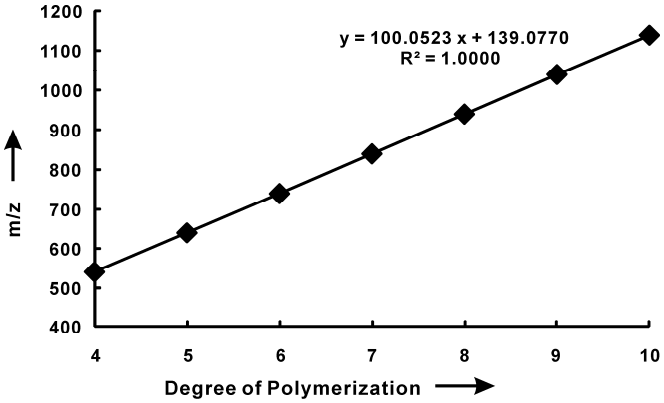

Figure A2. Linear regression of *m/z* peaks of series sh or (mh) from PMMA. (*m/z* 400 - 1200, degree of polymerisation 4-10)

The residual mass of the series was 139.0770 Da, as calculated using linear regression. The monomer mass calculated was 100.0523 (the theoretical mass of an MMA monomer is 100.0524, Δ = 0.0001 Da) and its standard deviation was 0.0008. The chemical composition of the combined mass of the end groups is assigned as $[C_6H_{12}O_2+Na]^+$ (the theoretical mass is 139.0809, Δ = 0.0039 Da). The comparison of experimental and theoretical data is presented in Table A2.

Table A2 Comparison of experimental and theoretical data of the peaks series *m/z* 439+(n–3)*100

Degree of Polymerisation	$Mass_{exp}$ (*m/z*)	$Mass_{theo}$ (*m/z*)	Δ (Da)
4	539.2863	539.2827	0.0036
5	639.3387	639.3351	0.0036
6	739.3911	739.3875	0.0036
7	839.4417	839.4400	0.0017
8	939.4942	939.4923	0.0018
9	1039.5480	1039.5448	0.0032
10	1139.6003	1139.5972	0.0031

The elemental composition of the combined endgroups is attributed to a butyl acetate endgroup (or methyl) at one end of the chain and and an H-abstracted end group at the other end (hence, mh or sh).

A similar procedure was also applied to the other series of peaks.

Glossary of Symbols and Abbreviations

A	Adipic acid
ACN	Acetonitrile
ATRP	Atom transfer radical polymerisation
B	1,4-butanediol
BTA	Butylene adipate and butylene terephthalate copolyester
CAD	Collision-activated dissociation
CID	Collision-induced dissociation
CRP	Controlled/living radical polymerisation
$Đ$	dispersity
DEPT	Distortionless enhancement by polarisation transfer
DSC	Differential scanning calorimetry
ECD	Electron-capture dissociation
EI	Electron impact ionisation
ESI	Electrospray ionisation
ETD	Electron-transfer dissociation
FA	Formic acid
FAB	Fast atom bombardment
FD	Field desorption
FTICR	Fourier transform ion cyclotron resonance
FTIR	Fourier transform spectroscopy
GPC	Gel-permeation chromatography
GPEC	Gradient polymer elution chromatography
HMBC	Heteronuclear multiple quantum coherence
IMS	Ion mobility spectrometry
IRMPD	Infrared multiphoton dissociation
IT	Ion trap
LAC	Liquid adsorption chromatography
LC	Liquid chromatography
LCCC	Liquid chromatography at critical condition
m/z	Mass-to-charge ratio
m_{cation}	Mass of the cation
$m_{endgroup}$	Mass of the end group
m_{exp}	Experimental mass
$m_{monomer}$	Mass of the monomer
M_n	Number average molecular weight
M_v	Viscosity average molecular weight
M_w	Weight average molecular weight
M_z	z-average molecular weight
MALDI	Matrix assisted laser desorption/ionisation
MS	Mass spectrometry
MS/MS	Tandem mass spectrometry
MS^n	Multistage mass spectrometry to n
MWD	Molecular weight distribution

n	Degree of polymerisation
NaI	Sodium iodide
NMR	Nuclear Magnetic resonance
P(MMA-*r*-BA)	Methyl methacrylate and *n*-butyl acrylate random copolymer
PBA	Poly(*n*-butyl acrylate)
PEG	Poly(ethylene glycol)
PMMA	Poly(methyl methacrylate)
PSD	Post-source decay
RAFT	Reversible addition-fragmentation chain transfer radical polymerisation
RF	Radio frequency
RI	Refractive index
SEC	Size exclusion chromatography
SFRP	Stable free radical polymerisation
SIMS	Secondary ion mass spectrometry
SY	Survival yield
T	Terephthalic acid
t_D	Drift time
THF	Tetrahydrofuran
TOF	Time-of-flight
Trigonox 42S	*tert*-butyl peroxy-3,5,5-trimethylhexanoate

Summary

Synthetic polymers and polymer-based materials are essential and indispensable in almost every aspect of our life. An increasing demand of new materials has led to an extraordinary range of polymers with tailor-made properties. To this end, numerous characterisation techniques have been developed to understand the properties of the synthetic polymer. However, most of the methods only produce results on an average over the entire molecular weight distribution of the polymer. The combination of multimodal separations and mass spectrometry (MS) allows the study of polymer system not only over the whole distribution but also of individual polymer molecules. Therefore, it has its particular value for the characterisation of synthetic polymers. MS has the ability of identifying the elemental composition of individual molecules in the polymer mixtures. Coupled with separation techniques specifically developed for applications in polymer research, MS provides more capabilities to obtain detailed information on polymers.

Chapter 2 gives a general introduction of the polymer properties, MS and liquid chromatography (LC) and their combined use (LC-MS). Polymers are complex large molecules with diverse functions and structures. A synthetic polymer has a molecular weight distribution rather than an exact molecular weight. The properties of polymers are largely influenced by their end groups. Polymers also have various intramolecular arrangements, such as monomer sequence. New polymerisation methods have been invented to control the properties and structures of polymers. Mass spectrometry is capable of studying almost all the properties listed above together with the polymerisation mechanisms. The most important ionisation methods for polymer analysis are electrospray ionisation and matrix-assisted laser desorption/ionisation. The fragments generated by multistage MS offer additional structural information. Modern mass spectrometers have been developed to achieve high accuracy and resolution MS study. Instruments mentioned in the chapter include quadrupole ion trap, Orbitrap and Fourier Transform Ion Cyclotron Resonance (FTICR) MS and Ion Mobility Spectrometry-MS. Three LC separation methods of polymers provide additional capabilities to MS in polymer characterisation studies. Chapter 2 introduces these methods and some important parameters that may influence the performance of LC-MS analysis.

In **Chapter 3**, a fundamental aspect of mass spectrometry of synthetic polymers, *viz.* the effect of the charge bearing cation on MS/MS, is studied. The chapter demonstrates that changing the size of the adduct ion can be used to increase the degree of fragmentation of polymers in tandem mass spectrometry. Tandem MS spectra of PBA oligomers ionised with Li^+ and Na^+ provide more structural information than those of PBA oligomers ionised with larger cations. By performing a size-dependence analysis using breakdown diagrams with at least two different cations, the catalytic influence of the cation on the fragmentation processes observed can be investigated. A procedure for determination of the presence of an effect of the cation on the fragmentation (charge-catalysed or charge-independent) has also been delineated. This procedure should also be generally applicable to homopolymers (or alternating copolymers). The limitation is however that there should be more than one product ion. The applicability of the method to tandem MS experiments that produce more than two different product ions should be investigated. A particularly interesting subject of research would be fragmentations in which the backbone of the polymer is cleaved in two ways, producing a multitude of product ions that can be grouped as two types.

C**hapter 4** shows the power of coupling LC to high resolution and high accuracy MS/MS instrument on homopolymer characterisation. LC-ESI MS^2 of the three PBA samples identified many initiation and termination reactions that occur during the polymerisation, including peroxide initiator initiation, solvent radical initiation or chain transfer to solvent, a multitude of four different β-scission pathways, H-abstraction, disproportionation and termination by combination. The combination of these mechanisms generated a great variety of end groups which were all identified by using high resolution LC-MS. Multistage MS showed different fragmentations for peaks that had identical exact mass but different elution times (*i.e.* isomers). Isomers were observed that originated from different initiation mechanisms. The high accuracy and resolution MS spectra obtained using the Orbitrap allowed discrimination of two isobars with 0.072 Da mass difference which could easily be overlooked in normal low mass accuracy and resolution MS. The comprehensive attribution of the peaks in the LC-MS data allowed the end group distribution in a semi-quantitative way to be addressed for one of the polymers studied. Although the data do not allow semi-quantitative comparison of the various initiation and

termination mechanisms in all three PBAs, the results clearly show that the solvent used for polymerisation strongly influences the polymer composition.

Copolymer structure determination is discussed in **Chapter 5**. Separation of the homopolymer PMMA based on the end groups and subsequent detection/identification has been achieved by the combination of gradient elution LC with MS. By using high-resolution and high-accuracy MS and MS^2, elemental compositions of the molecules were obtained. End groups could therefore be determined. Isobaric materials with subtle structure differences were easily identified by applying different isolation windows in MS^2 experiments. The same analytical strategy was then applied to the copolymer. However, the complex copolymer system presented more difficulties to fully identify all the end groups for peaks with relatively low intensity. The isocratic elution LC-MS allowed identification of copolymer with different end groups in a shorter analysis time. It was applied to the system to reduce the complexity of the spectra. A near critical condition was achieved on PMMA using isocratic elution LC-MS. PMMA was separated based on its end-group functionality without the influence of the molecular weight distribution. When applying the same isocratic elution condition to the P(MMA-r-BA) polymer, the effect of MMA fraction on elution was minimized to almost none. The elution therefore is purely based on the molecular distribution of BA and the total end-group functionality. The resulting MS spectra were therefore simplified. Combining the results obtained under both elution conditions online coupled with MS, it can be concluded that the relatively reactive solvent has influences in the compositions of PMMA and P(MMA-*r*-BA). The effect of β-scission during polymerisation on the copolymer composition appeared to be very dominant.

A further step of using ion mobility spectrometry (IMS)-mass spectrometry (IMS-MS) to study the complex synthetic polymer system is demonstrated in **Chapter 6**. The developments in IMS-MS show a promising potential for structure elucidation of synthetic polymers. In this chapter, detailed endgroup mapping of PMMA with complex end group combinations was achieved without the need of a preceding time-consuming LC separation. In the very short time span of the experiment, in the tens of milliseconds range, IMS-MS offers full separation and identification of the components of the very complex PMMA system studied here across its entire molecular weight distribution. A similar result can be achieved using HPLC-MS or UPLC-MS but with a much longer experimental time. The

combination of drift time and *m/z* separation offers an effective approach for the identification of individual compounds in this extremely complex mixture, while covering a relatively large molecular weight distribution. The development of multidimensional IMS-MS strategies is likely to aid the characterisation of more complex polymer systems such as copolymers. As subtle structural differences can be noticed by applying IMS-MS, LC-IMS-MS or IMS-MS/MS will probably allow discrimination of components of even more complex mixtures of isomers. The 2D and 3D visualisation of the data facilitates extraction of structural information reflecting differences in mass, size, and/or conformation of the molecules. Furthermore, information such as branching in polymers which normally cannot be acquired by MS study alone can be investigated using IMS-MS.

Finally **Chapter 7** shows an example of using a combination of analysis techniques for the characterisation of a complex polymer system and its degradation process. The partial degradation of this BTA (aliphatic–aromatic) copolyester was successfully carried out under alkaline conditions at 35^{o}C and 75^{o}C, respectively, using a water/methanol solvent system. The GPC results showed that the process at 75^{o}C is a more drastic one and leads to a more progressed reaction than the process at 35^{o}C. The M_n and M_w decreased significantly and the dispersity increased in both cases. NMR confirmed the presence of -$COOCH_3$ end group in the degraded samples. It proved the occurrence of methanol transesterification during the partial degradation. The presence of free 1,4-butanediol confirmed that the partial degradation under alkaline was a very progressed reaction. Degraded samples from both temperatures showed very much the same spectra both in NMR and LC-MS or LC-MS^n. It is therefore concluded that temperature influences the extent but not the nature of the degradation reaction. Detailed endgroup structures of both original and partially degraded samples were assigned by using LC-MS and LC-MS^n. The cyclic structures, that were not identified using NMR, were discovered in the original sample (but not in the degraded ones). The transesterification by methanol was confirmed. The MS^2 experiment on the first ^{13}C isotope peak helped to assign the elemental composition of the fragments. The applied method may be used to provide an alternative for high mass accuracy MS^2 experiments, when such an instrument is not available in the lab. This example demonstrated the applicability of the many techniques and methodologies discussed in this thesis.

Samenvatting

Synthetische polymeren en materialen die polymeren bevatten zijn niet meer weg te denken uit het dagelijkse leven. Een toenemende behoefte aan nieuwe materialen heeft geleid tot een buitengewoon grote variëteit aan polymeren met specifiek ontwikkelde eigenschappen. Er is een groot aantal ontwikkeld om de relatie tussen structuur en eigenschap van polymeren te bestuderen. De meeste polymeerkarakteriseringsmethoden leveren echter slechts informatie over de gehele moleculair-gewichtsverdeling (*MWD*) van het materiaal. De combinatie van multimodale scheiding en (meervoudige) massaspectrometrie ($MS^{(n)}$) is van bijzondere betekenis voor de karakterisering van polymeren; zij maakt het mogelijk om niet alleen de gehele MWD maar ook individuele moleculen uit die MWD te onderzoeken. Massaspectrometrie (MS) kan de elementaire samenstelling van individuele polymeermoleculen bepalen. De koppeling van speciaal voor polymeeronderzoek ontwikkelde scheidingsmethoden met MS vergroot de mogelijkheden om gedetailleerde informatie over polymeren te verkrijgen.

Hoofdstuk 2 van dit proefschrift is een algemene inleiding op polymeereigenschappen, massaspectrometrie, vloeistofchromatografie (*LC*) en de combinatie van de laatste twee (*LC-MS*). Polymeren zijn complexe grote moleculen met verschillende functies en structuren. Een synthetisch polymeer heeft een moleculair-gewichtsverdeling in plaats van een exact moleculair gewicht. De eigenschappen van polymeren worden sterk beïnvloed door hun eindgroepen. Polymeren hebben verschillende intramoleculaire rangschikkingen zoals monomeervolgorde. Moderne polymerisatiemethoden zijn ontwikkeld om de eigenschappen en structuren van polymeren te kunnen beheersen. Met behulp van massaspectrometrie kunnen bijna alle bovengenoemde eigenschappen bestudeerd worden, tezamen met de polymerisatiemechanismen. De belangrijkste ionisatiemethoden voor polymeeranalyse zijn electrospray-ionisatie en matrix-geassisteerde laserdesorptie/-ionisatie (MALDI). De fragmenten die gevormd worden in meervoudige massaspectrometrie geven extra structuurinfomatie. Moderne massaspectrometers zijn ontwikkeld om data met hoge nauwkeurigheid en hoge resolutie te kunnen verkrijgen. In dit hoofdstuk komen quadrupool ionenvalmassaspectrometrie, Orbitrapmassaspectrometrie en Fouriertransformatie-ionencyclotronresonantiemassaspectrometrie (FTICR-MS) en ionenmobiliteitspectrometrie-massaspectrometrie (IMS-MS) aan de orde. Drie LC scheidingsmethoden van polymeren verschaffen extra mogelijkheden voor MS in polymeerkarakteriseringsstudies. Hoofdstuk 2 geeft een inleiding op deze technieken tezamen met enkele parameters die de resultaten van LC-MS beïnvloeden.

In **Hoofdstuk 3** komt een specifiek fundamenteel aspect van tandem-massaspectrometrie van synthetische polymeren aan de orde, namelijk het effect van het ladingsdragende cation op de fragmentatie. Het hoofdstuk laat zien dat verandering van het adduct-ion gebruikt kan worden om de mate van fragmentatie van polymeren in tandem-MS te beïnvloeden. MS/MS spectra van polybutylacrylaat (PBA) oligomeren die geïoniseerd zijn met Li^+ en Na^+ bevatten meer informatie dan die van PBA oligomeren die geïoniseerd zijn met grotere kationen. De invloed van het kation op de fragmentatieprocessen kan onderzocht worden met behulp van breakdowndiagrammen van soortgelijke ionen die uitsluitend verschillen in polymerisatiegraad (polymerisatiehomologen) en kation. Het hoofdstuk beschrijft een methode om onderscheid te maken tussen ladingsgekatalyseerde en ladingsonafhankelijke fragmentatieprocessen in tandem-MS van polymeren. Deze methode is waarschijnlijk algemeen toepasbaar op homopolymeren (en alternerende copolymeren). Zij is echter beperkt tot systemen die meer dan een fragment produceren. De toepasbaarheid van de methode voor MS/MS experimenten die meer dan twee verschillende fragmenten produceren moet nog onderzocht worden. Systemen die twee verschillende fragmentatiemechanismen van de ruggengraat van het polymeer laten zien zouden een bijzonder interessant onderwerp van studie kunnen zijn.

Hoofdstuk 4 laat zien hoe krachtig de koppeling van LC met hoge resolutie- en hoge nauwkeurigheids-MS/MS is. Met behulp van LC-ESI-MS^2 analyse zijn veel initiatie- en terminatiereacties die plaatsvinden tijdens de polymerisatie van polybutylacrylaat (PBA) geïdentificeerd. Hieronder bevinden zich peroxide-initiatie, initiatie door oplosmiddelradicalen of ketenoverdracht op oplosmiddel, vier verschillende verschijningsvormen van β-scission, H-abstractie, disproportionering en terminatie door combinatie. De combinatie van deze mechanismen genereerde een grote variëteit aan eindgroepen die alle met behulp van hoge-resolutie LC-MS geïdentificeerd zijn. Moleculen die dezelfde exacte massa hadden maar op verschillende momenten elueerden (isomeren) konden met behulp van meervoudige massaspectrometrie onderscheiden worden. Zo werden isomeren geïdentificeerd die hun oorsprong vonden in verschillende initiatiemechanismen. De hoge nauwkeurigheid en resolutie van de massaspectra die met behulp van de Orbitrap verkregen waren, maakte het mogelijk om twee isobaren die slechts 0.072Da in massa verschilden te onderscheiden. Zulke kleine verschillen kunnen met gewone massaspectrometrie (met lagere nauwkeurigheid en resolutie) gemakkelijk over het hoofd gezien worden. Door de volledige toekenning van de pieken in de LC-MS data kon voor een van de onderzochte polymeren de eindgroepverdeling semikwantitatief bepaald worden. Hoewel op basis van de data een semikwantitatieve

vergelijking van de initiatie en terminatiemechanismen in alle drie de onderzochte PBA systemen niet mogelijk was, was duidelijk te zien dat het gebruikte oplosmiddel een grote invloed heeft op de polymeersamenstelling.

Structuurbepaling van copolymeren wordt behandeld in **Hoofdstuk 5**. Een combinatie van gradiëntelutie LC met MS maakte het mogelijk om een PMMA homopolymeer te scheiden op basis van de eindgroepsamenstelling en vervolgens te identificeren. Hoge resolutie- en hoge nauwkeurigheidsmassaspectrometrie gaven de elementaire samenstelling van de moleculen. Hierdoor konden de eindgroepen bepaald worden. Isobare ionen met subtiele structuurverschillen werden op eenvoudige wijze geïdentificeerd door verschillende isolatiebereiken in MS/MS toe te passen. Dezelfde analytische strategie is toegepast op het copolymeer. De complexiteit van het copolymeer stond de volledige identificatie van alle eindgroepen in pieken met relatief lage intensiteit in de weg. Isocratische elutie LC-MS maakte het mogelijk om coploymeer met verschillende eindgroepen te identificeren in een kortere analysetijd. Door toepassing van deze methode werd de complexiteit van de spectra gereduceerd. Met isocratische elutie LC-MS werd een bijna-critische conditie voor PMMA gerealiseerd. PMMA kon hierdoor gescheiden worden op basis van eindgroepsamenstelling onafhankelijk van het molgewicht van het polymeer. Door toepassing van deze condities op het P(MMA-*r*-BA) polymeer kon het effect van de MMA-fractie bijna volledig teruggedrongen worden. Zo werd de elutie geheel bepaald door de eindgroepen en de moleculaire distributie van BA. Hierdoor werden de massaspectra ook eenvoudiger. Combinatie van de LC-MS resultaten verkregen onder beide condities leidt tot de conclusie dat het relatief reactieve oplosmiddel dat in de polymerisatie gebruikt is invloed heeft op de samenstelling van de PMMA en P(MMA-*r*-BA) polymeren. Het effect van β-scission op de polymeersamenstelling bleek zeer dominant te zijn.

Een volgende stap, het gebruik van ionenmobiliteitsspectrometrie-massaspectrometrie (IMS-MS) voor onderzoek van complexe synthetische polymeren, wordt gepresenteerd in **Hoofdstuk 6**. De ontwikkelingen in IMS-MS zijn veelbelovend voor de structuuropheldering van synthetische polymeren. Dit hoofdstuk laat zien dat het mogelijk is om zonder tijdrovende LC scheiding de eindgroepverdeling van een monster van PMMA met complexe eindgroepen in kaart te brengen. In de korte tijd van het experiment, slechts enkele tientallen milliseconden, biedt IMS-MS een volledige scheiding en identificatie van de componenten van het zeer complexe PMMA polymeer over de gehele MWD. Een vergelijkbaar resultaat kan verkregen worden met HPLC-MS en UPLC-MS, maar dan met een veel langere analysetijd. De combinatie van scheiding op basis van drifttijd en massa-ladingsverhouding (*m/z*) biedt een doeltreffende

benadering voor de identificatie van individuele componenten van dit extreem complexe mengsel, terwijl de relatief brede moleculair-gewichtsverdeling afgedekt wordt. De ontwikkeling van multidimensionale IMS-MS strategieën zal waarschijnlijk behulpzaam zijn bij de karaterisering van complexere systemen zoals copolymeren. Aangezien subtiele structuurverschillen met IMS-MS onderscheiden kunnen worden, zullen LC-IMS-MS en IMS-MS/MS waarschijnlijk nog complexere polymeersystemen zoals copolymeren kunnen onderscheiden. De 2D- en 3D-visualisatie van de data maakt het gemakkelijker om structuurinformatie te extraheren, omdat verschillen in massa, grootte en/of conformatie van moleculen uitvergroot worden. Daarnaast kan de vertakking van polymeren die normaliter niet geadresseerd kan worden met MS alleen wel bestudeerd worden met IMS-MS.

Tenslotte laat **Hoofdstuk 7** een voorbeeld zien van het gebruik van een combinatie van analysetechnieken voor de karakterisering van een complex polymeersysteem en zijn degradatieprocessen. In een water/methanol oplosmiddelsysteem en onder basische condities bij temperaturen van 35°C respectievelijk 75°C, kon een alifatisch-aromatische BTA copolymeer succesvol gedegradeerd worden. De GPC-resultaten lieten zien dat het proces bij 75°C drastischer verloopt en verder doorloopt dan bij 35°C. In beide gevallen dalen de M_n en M_w significant en neemt de dispersiteit toe. Met behulp van NMR werd de aanwezigheid van -$COOCH_3$ eindgroepen in de gedegradeerde monsters bevestigd. Hierdoor werd bewezen dat transesterificatie met methanol plaatsvindt gedurende de partiële degradatie. De aanwezigheid van 1,4-butanol bevestigde dat de partiële degradatie onder basische condities een vergevorderde reactie is. Monsters van degradatie bij beide temperaturen laten vergelijkbare spectra zien in NMR, LC-MS en LC-MS^n. Daarom wordt geconcludeerd dat de temperatuur wel invloed heeft op de progressie van de degradatiereactie maar niet op aard van de reactie. Gedetaillleerde eindgroepstructuren van zowel het originele als het partieel gedegradeerde materiaal werden toegekend met behulp van LC-MS en LC-MS^n. Cyclische structuren die niet geïdentificeerd werden met NMR zijn gevonden in het originele monster (maar niet in de gedegradeerde monsters). De transesterificatie met methanol werd bevestigd. Door MS^2 analyse van de eerste ^{13}C-isotooppiek was het mogelijk om de elementaire samenstelling van de fragmenten te bepalen. De toegepaste methode kan gebruikt worden als alternatief voor hoge nauwkeurigheids-MS/MS, bij gebrek aan een dergelijk instrument in het laboratorium. Het in dit hoofdstuk behandelde voorbeeld demonstreert de toepasbaarheid van de veelheid aan technieken en methodologieën die in dit proefschrift behandeld worden.

Acknowledgements

It has been a great journey with many ups and downs in the last four years. It all started from a phone call from the Netherlands in a mid-summer afternoon. I was probably having lunch with my mates from "Flat 2, Broad Lane" in Peace Garden, Sheffield. To be honest, I didn't expect to receive any answer from the project since it's highly EU citizen focused. After several rounds of interviews, including a surprising two-hour interview in London Heathrow airport, I finally became a Marie Curie Research Fellow and started working on this POLY-MS project.

Every bit of this thesis is not only my story but also the work of many people's efforts. At the very end of this book, I would love to express my sincere gratitude to everyone who helped me in the past four years. This thesis would not have been possible without these people.

First of all, my grateful thanks to my promoter, Ron Heeren. Ron is a very intelligent person with positive attitude, great enthusiasm and endless energy. I was deeply impressed by his working style from the very first time when we met. I remember vividly that we had some problems with the FT until he came in with a little tweaking, the instrument magically started working. In every publication of mine, Ron always has genius ideas to make it even better. It's a great privilege to work with a scientist like Ron.

I spent most of my time working in AkzoNobel during my PhD. research. My copromoter, Oscar van den Brink, is the group head of spectroscopy and process analysis group and as well the POLY-MS project leader. Oscar hired me for the project and guided me throughout the whole process. I wouldn't be who I am today without Oscar. He is not only a manager but also a good friend.

EC POLY-MS project funded most part of this work. This also makes the project more multi-national. In these four years, I worked with researchers from many countries. All the supervisors involved in the project, Károly Vékey, Marek Kowalczuk, László Drahos and Wiltod Kowalski, offered me enormous help and guidance. I was also well taken care of during my several visits to their labs and my three-month secondment in Poland. Thank you all for keeping the project running as well as making me progress.

Within this POLY-MS project, there are other four Marie Curie Fellows, Andreas Nasioudis, Antoine Membeouf, Alena Šišková and Christian Peptu. We worked closely in the whole project, especially Andreas. We two started at almost the same time in the same location. Our sub-projects are somehow similar but ended up in different routes. This really shows the charm and versatility of scientific research. Andreas is passionate, careful and always ready to help. He has amazing language ability that enables him speaking Greek, German, English, French and Dutch fluently. I also learned a lot from him on theoretical part of the mass spectrometry. Antoine and I worked on a theoretical research sub-project and produced a publication together. Because of the different education background he has, which is physics, he can see the research from a different angle and make it more complete. Alena helped me on my daily life in my secondment in Poland as well as a sub-project. Although I didn't really work with Christian on the same topic, I did receive many good suggestions from him. Of course, some are on drinking and enjoying life rather than scientific research. I really enjoyed working with all four of you. My thanks for the past years and best wishes for your future, too.

The IMS work is one of the most important parts of this thesis. Christian Grün and Professor Hans-Gerd Janssen helped me to obtain access to Synapt G2 and secured many working hours on the instrument. Christian also worked on the instrument with me. It was truly a pleasant and fruitful experience. Thank you and hope we can work together again in near future.

In terms of polymer chemistry, Luc Vertommen is the person I turned to most frequently in my project. Luc has extensive knowledge in not only analytical chemistry but also polymer area. We couldn't have had those papers published without his contribution. Luc is also a very charismatic and pleasant person to work with.

Ab Buijtenhuis is probably one of the most-experienced chromatography specialists in the world. He is like an encyclopaedia that every time you want to check something on chromatography, you can just turn to him. He would point out exactly what column, solvent and condition to use. I had many intriguing discussions with him on the separation system used in this thesis. I'm very thankful I could even drag him from home to the lab after his retirement.

Jan van Velde was my office-mate till October 2010. He has been working on mass spectrometry for many years (longer than all my study years apparently). I learned basic mass spectrometer operation from him. We also had frequent discussion on my research results, most of which are very constructive. He also taught me invaluable lessons on Dutch and life. I greatly appreciate it that I could have an office-mate like Jan.

Marcel Simons did great NMR work for this thesis although not all the results are shown. Henk-Jan van Manen guided me through the publication submission process such as writing cover letter, working on replies to the referees. Former CAP department head Cees Groeneboom advised and inspired me since I joined the department. All the ECG-MAS colleagues, more or less helped me in the whole research process. Thank you all and I'm sure we will still work closely in future. Special thanks to the running gang, Carina, Koen, Raymond, Rob and Wiljam. Sorry I couldn't join you for a very long time but I promise I will run more with you guys from now on. Tony Jackson is the newly-established ECG-MAS leader. He also partly helped me to secure the position for the last-year research in AkzoNobel. The research would not be possible without the last-year input. I also need to thank Leo G.J. van der Ven, Marco Koenraadt and Ber Yebio from AkzoNobel Car Refinishes for the preparation of the acrylic resins studied in this thesis. No results would have been obtained without these complex samples.

In these four years, I also spent some good time in AMOLF. I really love the atmosphere in AMOLF, not only because of the research but also the people. Marc, Ioana, Don helped me to work on the FT; Andras, Andry, Erika, Florian, Kamila, Lara, Lennaert, Luke and Sander all had good discussion with me at certain point (and of course some drinking and parties). Thank you all for the kindness.

My bond with this country started from a conversation with a visiting professor, Jacques Joosten, to Fudan University during my undergraduate study. During that conversation, I was asked if I had considered doing my graduate study in the Netherlands. At that moment, I didn't realise that I would end up doing a whole PhD study here. In 2007, I visited Jacques in Eindhoven (for the first time in this country). It was almost three years after our conversation in Shanghai. After then, we made the meeting once every year. Jacques opened my eyes to look outside of China. He helped me through many stages of the

research and gave me valuable career suggestions. I am truly lucky to have a wise and experienced mentor to point out my way.

Life without friends is dull and meaningless. I'm lucky to have made many good friends here. I'd like to say thanks to Alexandra, Alicia, Amélie and Rémi, Andre, Ariadna and Peter, Ewout, Eva and Steve, Jasmijn and Jony, Luo Xiaolei (especially her ideas on cover design inspired me) and Cui Xiaoyu, Manuel, Marion, Marjolein and Arjan, Martin, Matthieu, Nadjana and Bob, Paula and Gilles, Sheila and Lars, Sigismund and also my tennis partners like Marjolein and Henry, and Richard. It's you made my life so colourful and never boring. Moreover, my thanks to my friends back in China, UK, USA and many corners of this world. I'm grateful wherever I go that I can find a place to stay and a guide to bring me to the best food and the most beautiful scenery. You guys rock!

In Arnhem, I rent a room from a lovely family in a fantastic neighbourhood. They offered me not only a shelter but also a home. Tinenke and Johan, Roxana and Akko, and de liefst Odette en Giselle, thank you all for the love and tolerance.

After all, I am still a very traditional Chinese deep inside myself. Having a big family is considered to be the biggest fortune for Chinese. I rejoice in this good fortune. My uncles, aunts, cousins, nephews and nieces gave me so much sweet memory and joy. Having no siblings, my cousins are just like brothers and sisters. They are always my firmest support.

My dearest grandpa passed away in 2009. It was certainly the most painful and powerless moment of my life. Thousand miles away, I could do nothing. Forgive me that I could not be with you for the last part of your life. You are always in my heart.

Lastly, I need to express my deepest gratitude to my parents. It is my parents who brought me to this world, educated me from the very beginning and taught me the basic to be a decent citizen. They morally and financially supported every decision I made. I know it is hard for them not to have the only child beside them. I am so sorry that this will still be the case for the coming years. From the bottom of my heart, I wish them good health and every happiness.

Curriculum Vitae

Junkan Song was born on 30th January 1983 in Shanghai, China.

He received his high school degree at Shanghai Yan'an High School in 2001 and achieved excellent grades to enter Fudan University, Shanghai, China. His undergraduate major was Macromolecular Science and Engineering. During the four-year undergraduate study, he worked on research projects in the Key Laboratory of Molecular Engineering of Polymers, Ministry of Education, China. Projects he worked on include 'Synthesis of PS(HEA)-DVB diblock copolymer through Atom Transfer Radical Polymerisation' (Summer 2004) and 'Tribology of thermosets and thermoplastics' (September 2004 – July 2005).

In September 2005, after obtained his BSc. Degree in Fudan University, he went on pursuing an MSc. Degree in the department of Engineering Materials in University of Sheffield, UK. He finished his thesis project 'Synthesis, characterisation and evaluation of a novel ABA triblock copolymer gelator by Atom Transfer Radical Polymerisation' in Prof. Steve Armes's group. In November 2006, he obtained his MSc. Degree on Polymer and Polymer Composites Science and Engineering with first-class honours with distinction.

In the end of 2006, he received Marie Curie early stage research fellowship and started his PhD research on structure analysis of synthetic polymers with multistage mass spectrometry in POLY-MS project under the supervision of Prof. dr. Ron Heeren from AMOLF and Universiteit Utrecht, the Netherlands and Dr. Oscar van den Brink from AkzoNobel. The major results of this PhD project are presented in this thesis.

作者簡歷

宋駿侃於一九八三年一月三十日出生於中國上海。

二零零一年，他從上海市延安中學以優異成績畢業並考入復旦大學高分子科學系。在本科四年的學習中，他參與了幾個國家聚合物材料工程重點實驗室的研究項目。項目有"通過自由基活性聚合合成 PS(HEA)-DVB 兩段共聚物"和"熱塑性聚合物-熱固性聚合物間摩擦學性能的研究"。

二零零五年九月，他在獲得學士學位之後到英國謝菲爾德大學的工程材料系繼續深造，學習碩士學位的課程。他在 Steve Armes 教授的課題組完成了論文"合成、表征和評價通過自由基活性聚合合成的新型 ABA 三段共聚膠體"。二零零六年十一月，他以壹等特優成績取得高分子及高分子合成材料科學和工程碩士。

二零零六年底，他獲得了歐盟居裏夫人早期研究獎學金並開始了他的博士學位研究。他的博士學位研究方向是利用多階質譜學習和表征合成高分子材料的結構。他博士研究的導師是來自荷蘭原子和分子物理學研究所和烏德勒支大學的 Ron Heeren 教授和阿克蘇諾貝爾的 Oscar van den Brink 博士。這本論文冊包含了他博士研究的主要成果。

List of Publications

Publications

Chapter 3 is based on, *Discrimination between Charge-Catalyzed and Charge-Independent Fragmentation Processes of Cationized Poly (n-Butyl Acrylate),* Junkan Song, Antony Memboeuf, Ron M.A. Heeren, Károly Vékey and Oscar F. van den Brink, *Rapid Communication in Mass Spectrometry* **2010**, *24*, 3214-3216.

Chapter 4 is based on, *Investigation of Polymerization Mechanisms of Poly (n-Butyl Acrylate)s Generated in Different Solvents by LC ESI-MS^2,* Junkan Song, Jan W. van Velde, Luc L.T. Vertommen, Leo G.J. van der Ven, Ron M.A. Heeren and Oscar F. van den Brink, *Macromolecules* **2010**, *43*, 7082-7089.

Chapter 5 is based on, *End-group Analysis of Acrylic (co)Polymers by LC-ESI-MS^2,* Junkan Song, Jan W. van Velde, Luc L.T. Vertommen, Donald F. Smith, Ron M.A. Heeren and Oscar F. van den Brink, Submitted.

Chapter 6 is based on, *High-resolution Ion Mobility Spectrometry-Mass Spectrometry on Poly (methyl methacrylate)*, Junkan Song, Christian H. Grün, Ron M.A. Heeren, Hans-Gerd Janssen and Oscar F. van den Brink, *Angewandte Chemie*, Article first published online: 29 November 2010, DOI: 10.1002/anie.201005225.

Chapter 7 is based on, *LC-Multistage Mass Spectrometry Characterization of Poly (Butylene Adipate-co-Butylene Terephthalate) and Its Partial Degradation Products*, Junkan Song, Alena Šišková, Marcel G. Simons, Wiltod J. Kowalski, Marek M. Kowalczuk and Oscar F. van den Brink, Submitted.

Presentations and Lectures

- *Presentation at American Society for Mass Spectrometry Annual Meeting*

'Structure Analysis of Acrylic Copolymers by LC/MS^n', June 2008, Denver, USA

'Characterization of Poly (*n*-Butyl Acrylate)s by LC/ESI-MS^n', June 2009, Philadelphia, USA (didn't make the trip due to visa delay, O.F. van den Brink gave the final presentation)

- *Presentation at De Nederland Vereniging voor Massaspectrometrie Annual Meeting*

'Polymer Analysis by LC-MS', PhD student flash presentation, November 2007, Haarlem, The Netherlands

'LC-MS^n Analysis of Polybutylacrylates - Elucidating Structures and Polymerisation Mechanisms', poster and flash presentation, March 2009, Rodulc, The Netherlands

- *Lecture at AkzoNobel Car Refinishes*

'Preliminary LC-MS results of Acrylic Resins', September 2008, Sassenheim, The Netherlands

'Liquid Chromatography – Multistage Mass Spectrometry of Synthetic Polymers', April 2010, Sassenheim, The Netherlands

- *Lecture at Hungarian Academy of Science*

'LC-MS^n Analysis of Acrylic Polymers--Structure Elucidation and Insight to Polymerisation Mechanism', February 2009, Budapest, Hungary

- *Lecture at Polish Academy of Sciences*

'Characterisation of Poly (n-Butyl Acrylate)s by LC/ESI-MS^n', September 2009, Centre of Polymer and Carbon Materials, Zabrze, Poland

- *Lecture at DSP (Discussiegroep Scheidingsmethoden van Polymeren) meeting*

'Liquid Chromatography – Multistage Mass Spectrometry of Synthetic Polymers', April 2010, Antwerpen, Belgium